

EUR 4234 e

EUROPEAN ATOMIC ENERGY COMMUNITY — EURATOM

**THE DETERMINATION OF INTRINSIC REACTIVITY
VARIATIONS OF THE LATINA REACTOR**

Final report

by

A. ARIEMMA, G. BELLIA, F. CALABRESI, G. GUALTIERI,
G. LESNONI LA PAROLA, T. MARZULLO, M. PAOLETTI GUALANDI and
B. ZEFFIRO (ENEL)

1969



Report prepared by ENEL
Ente Nazionale per l'Energia Elettrica, Rome (Italy)

Euratom Contract N° 050-65-1 TEGI

LEGAL NOTICE

This document was prepared under the sponsorship of the Commission of the European Communities.

Neither the Commission of the European Communities, its contractors nor any person acting on their behalf:

Make any warranty or representation, express or implied, with respect to the accuracy, completeness, or usefulness of the information contained in this document, or that the use of any information, apparatus, method, or process disclosed in this document may not infringe privately owned rights; or

Assume any liability with respect to the use of, or for damages resulting from the use of any information, apparatus, method or process disclosed in this document.

This report is on sale at the addresses listed on cover page 4

at the price of FF 15.—	FB 150.—	DM 12.—	Lit. 1870	Fl. 11.—
-------------------------	----------	---------	-----------	----------

When ordering, please quote the EUR number and the title, which are indicated on the cover of each report.

Printed by Van Muyswinkel
Brussels, April 1969

This document was reproduced on the basis of the best available copy.

EUR 4234 e

THE DETERMINATION OF INTRINSIC REACTIVITY VARIATIONS OF THE LATINA REACTOR — Final Report by A. ARIEMMA, G. BELLIA, F. CALABRESI, G. GUALTIERI, G. LESNONI LA PAROLA, T. MARZULLO, M. PAOLETTI GUALANDI and B. ZAFFIRO (ENEL)

European Atomic Energy Community — EURATOM

Report prepared by ENEL

Ente Nazionale per l'Energia Elettrica, Rome (Italy)

Euratom Contract No. 050-65-1 TEG1

Luxembourg, April 1969 — 108 Pages — 47 Figures — FB 150

The performance of a natural-uranium gas-graphite reactor is closely dependent, throughout the station lifetime, on a accurate fuel and absorber cycle programming. This programming entails the knowledge of the reactivity variation as a function of irradiation, and an accurate assessment of the reactivity controlled by various factors, namely absorbers, xenon, boron contained in the graphite, control rods and temperature effects.

EUR 4234 e

THE DETERMINATION OF INTRINSIC REACTIVITY VARIATIONS OF THE LATINA REACTOR — Final Report by A. ARIEMMA, G. BELLIA, F. CALABRESI, G. GUALTIERI, G. LESNONI LA PAROLA, T. MARZULLO, M. PAOLETTI GUALANDI and B. ZAFFIRO (ENEL)

European Atomic Energy Community — EURATOM

Report prepared by ENEL

Ente Nazionale per l'Energia Elettrica, Rome (Italy)

Euratom Contract No. 050-65-1 TEG1

Luxembourg, April 1969 — 108 Pages — 47 Figures — FB 150

The performance of a natural-uranium gas-graphite reactor is closely dependent, throughout the station lifetime, on a accurate fuel and absorber cycle programming. This programming entails the knowledge of the reactivity variation as a function of irradiation, and an accurate assessment of the reactivity controlled by various factors, namely absorbers, xenon, boron contained in the graphite, control rods and temperature effects.

EUR 4234 e

THE DETERMINATION OF INTRINSIC REACTIVITY VARIATIONS OF THE LATINA REACTOR — Final Report by A. ARIEMMA, G. BELLIA, F. CALABRESI, G. GUALTIERI, G. LESNONI LA PAROLA, T. MARZULLO, M. PAOLETTI GUALANDI and B. ZAFFIRO (ENEL)

European Atomic Energy Community — EURATOM

Report prepared by ENEL

Ente Nazionale per l'Energia Elettrica, Rome (Italy)

Euratom Contract No. 050-65-1 TEG1

Luxembourg, April 1969 — 108 Pages — 47 Figures — FB 150

The performance of a natural-uranium gas-graphite reactor is closely dependent, throughout the station lifetime, on a accurate fuel and absorber cycle programming. This programming entails the knowledge of the reactivity variation as a function of irradiation, and an accurate assessment of the reactivity controlled by various factors, namely absorbers, xenon, boron contained in the graphite, control rods and temperature effects.

For each general condition of core irradiation, the algebraic sum of the deviations of reactivity components controlled by the aforesaid factors from the reference values represents the intrinsic reactivity variation from the initial core conditions.

The execution of these reactivity balances, extended to the first four years of reactor operation, permitted the intrinsic reactivity variation of the Latina reactor to be known as a function of the energy generated.

The reactivity balances were performed on the basis of experimental data and calculation methods whose validity was verified by comparison with the results of measurements purposely taken.

The results obtained for the intrinsic reactivity variation are generally in good agreement with similar data relating to other reactors of the same type and provide a valid contribution to data availability.

For each general condition of core irradiation, the algebraic sum of the deviations of reactivity components controlled by the aforesaid factors from the reference values represents the intrinsic reactivity variation from the initial core conditions.

The execution of these reactivity balances, extended to the first four years of reactor operation, permitted the intrinsic reactivity variation of the Latina reactor to be known as a function of the energy generated.

The reactivity balances were performed on the basis of experimental data and calculation methods whose validity was verified by comparison with the results of measurements purposely taken.

The results obtained for the intrinsic reactivity variation are generally in good agreement with similar data relating to other reactors of the same type and provide a valid contribution to data availability.

For each general condition of core irradiation, the algebraic sum of the deviations of reactivity components controlled by the aforesaid factors from the reference values represents the intrinsic reactivity variation from the initial core conditions.

The execution of these reactivity balances, extended to the first four years of reactor operation, permitted the intrinsic reactivity variation of the Latina reactor to be known as a function of the energy generated.

The reactivity balances were performed on the basis of experimental data and calculation methods whose validity was verified by comparison with the results of measurements purposely taken.

The results obtained for the intrinsic reactivity variation are generally in good agreement with similar data relating to other reactors of the same type and provide a valid contribution to data availability.

EUR 4234 e

EUROPEAN ATOMIC ENERGY COMMUNITY — EURATOM

THE DETERMINATION OF INTRINSIC REACTIVITY VARIATIONS OF THE LATINA REACTOR

Final report

by

A. ARIEMMA, G. BELLIA, F. CALABRESI, G. GUALTIERI,
G. LESNONI LA PAROLA, T. MARZULLO, M. PAOLETTI GUALANDI and
B. ZEFFIRO (ENEL)

1969



Report prepared by ENEL
Ente Nazionale per l'Energia Elettrica, Rome (Italy)

Euratom Contract N° 050-65-1 TEGI

ABSTRACT

The performance of a natural-uranium gas-graphite reactor is closely dependent, throughout the station lifetime, on an accurate fuel and absorber cycle programming. This programming entails the knowledge of the reactivity variation as a function of irradiation, and an accurate assessment of the reactivity controlled by various factors, namely absorbers, xenon, boron contained in the graphite, control rods and temperature effects.

For each general condition of core irradiation, the algebraic sum of the deviations of reactivity components controlled by the aforesaid factors from the reference values represents the intrinsic reactivity variation from the initial core conditions.

The execution of these reactivity balances, extended to the first four years of reactor operation, permitted the intrinsic reactivity variation of the Latina reactor to be known as a function of the energy generated.

The reactivity balances were performed on the basis of experimental data and calculation methods whose validity was verified by comparison with the results of measurements purposely taken.

The results obtained for the intrinsic reactivity variation are generally in good agreement with similar data relating to other reactors of the same type and provide a valid contribution to data availability.

KEYWORDS

REACTIVITY
VARIATIONS
LATINA REACTOR
DETERMINATION

I N D E X

	page
1.0 PURPOSE OF THE RESEARCH PROGRAM	1
1.1 Reactivity balances	1
2.0 AVERAGE REACTOR AND ZONE IRRADIATIONS	3
2.1 Determination of the average reactor irradiation	3
2.2 Determination of zone irradiations	4
3.0 DETERMINATION OF ABSORBER WORTH	29
3.1 Experimental absorber calibrations	29
3.2 Calculation of absorber-controlled reactivity	29
3.3 Calculation of the reactivity controlled by the various absorber patterns	31
4.0 DESCRIPTION OF THE METHOD USED FOR ROD CALIBRATION UNDER REDUCED-TEMPERATURE ISOTHERMAL CONDITIONS	52
4.0.1 Processing of experimental data	52
4.0.2 Correlation between doubling times and reactivity	52
4.0.3 Determination of the calibration curves	53
4.1 Experimental measurements	54
4.1.1. Results of the experimental measurements	55
4.2 Description of the method followed for the theoretical calibration of the sector rods and related results	56
4.3 Comparison of calculated and experimental results in isothermal conditions	57
4.4 Criterion followed to obtain semi-empirical calibration curves under nominal operating conditions	58
5.0 DETERMINATION OF REACTIVITY ASSOCIATED WITH TEMPERATURE VARIATIONS	75
5.1 Description of the method used for the measurement of the combined temperature coefficient	76
5.2 Description of the method used for the measurement of the separate temperature coefficients	77
5.3 Experimental results	78

	page
6.0 DETERMINATION OF XENON-CONTROLLED REACTIVITY	82
7.0 DETERMINATION OF BORON-CONTROLLED REACTIVITY	83
8.0 REACTIVITY BALANCES	85
9.0 CONCLUSIONS	99
10.0 REFERENCES	101
APPENDIX I	108

1.0 PURPOSE OF THE RESEARCH PROGRAM (*)

The performance of a natural-uranium gas-graphite reactor is closely dependent on proper exploitation of the core throughout the station lifetime. It is indeed necessary to maintain reactor conditions such as will afford the maximum thermal output with the best utilization of the fuel. For this purpose an adequate neutron flux distribution must be maintained by programming the fuel and absorber cycles appropriately. This program entails the a priori knowledge of the reactivity variation as a function of fuel irradiation. In particular, by virtue of the considerable progress in metallurgy, the discharge limits used in programming the fuel cycle may be conditioned only on the available reactivity.

In 1965, that is, at the beginning of this research, the reactivity variation in gas-graphite reactors as a function of irradiation could not be closely estimated because of the uncertainties extant on some of the fundamental data. The experiments conducted at Latina under this contract considerably contributed to the elimination of these uncertainties. The measurement techniques used for the research program permitted very valuable information to be gathered, even though the measurements were taken on a commercial power reactor.

For the determination of the intrinsic reactivity variations, several measurements, described later, had to be taken periodically, and the fuel irradiation data had to be updated continuously by means of heat balances and power distribution measurements. In addition, a great deal of data had to be processed with the station computer (see Appendix I).

Since the Latina fuel cycle has an initial delay of one year, reactivity equilibrium conditions cannot be reached but after a long period of station operation. To obtain as much information as possible in the determination of the reactivity variation, the measurements scheduled in the research program were spread over a period of three years. To complete the picture, the data collected during station commissioning and first operation -- that is, before the execution of this contract -- were also processed.

1.1 Reactivity balances

The experimental determination of the intrinsic reactivity variation as a function of irradiation is based on reactivity balances. The variation in reactivity in any moment of the reactor life can be represented in the steady-state condition by the following formula:

$$\Delta \rho_{\text{rods}} + \Delta \rho_{\text{abs}} + \Delta \rho_{\text{T}} + \Delta \rho_{\text{Xe}} + \Delta \rho_{\text{boron}} = \Delta \rho_{\text{tot}}$$

where:

$\Delta \rho_{\text{rods}}$ = variation in rod-controlled reactivity as a function of temperature and irradiation as compared with the initial reference conditions

(*) Manuscript received on 11 December 1968.

- $\Delta \rho_{\text{abs}}$ = variation in absorber-controlled reactivity as a function of temperature and irradiation as compared with the reactivity controlled by the initial absorber distribution
- $\Delta \rho_{\text{T}}$ = variation in reactivity owing to temperature deviations from reference conditions
- $\Delta \rho_{\text{Xe}}$ = variation in reactivity owing to xenon deviations from reference conditions
- $\Delta \rho_{\text{boron}}$ = variation in reactivity owing to gradual depletion of the boron initially present in the graphite
- $\Delta \rho_{\text{tot}}$ = variation in intrinsic core reactivity as compared with the reference conditions.

The research program entailed the assessment of these terms as a function of irradiation according to the following procedure.

1. The term $\Delta \rho_{\text{rods}}$, which is essential for the determination of the reactivity balance, was obtained by extrapolating the control rod calibration curves measured periodically.
2. The term $\Delta \rho_{\text{abs}}$ was computed with a calculation program, the adequacy of which was verified by comparison with the results of measurements purposely taken.
3. The term $\Delta \rho_{\text{T}}$ was calculated from the reactivity temperature coefficients obtained experimentally.
4. The term $\Delta \rho_{\text{Xe}}$ was computed on a theoretical basis; it takes into account the reactor power variation from the reference conditions at the time of balance performance.
5. The term $\Delta \rho_{\text{boron}}$ was computed on a theoretical basis; it takes into account the boron content variation as compared with the reference conditions.
6. The term $\Delta \rho_{\text{tot}}$, obtained as the algebraic sum of the preceding terms, represents the intrinsic reactivity variation from the reference conditions and constitutes the final result of the work conducted under the research program.

The following chapters describe the calculation procedures used for the determination of the individual terms of the reactivity balance, and the measurements on which the calculations were based. Chapter 9 gives the experimental results and the conclusions.

Appendix I provides a summary description of the GEPAC 4050 computer and main calculation programs required for the processing of the experimental data. It is known that the parameters used for the execution of reactivity balances are representative of the core as a whole, so that it is necessary to make an ideal subdivision of the core in zones and to process the zone data by extremely painstaking calculation procedures, such as the ones described in ref. 7 for the calculation of the temperature coefficients.

2.0 AVERAGE REACTOR AND ZONE IRRADIATIONS

For the purpose of this research, it is essential to know the average irradiation to be correlated with the intrinsic reactivity variations, and the irradiations of the individual zones into which the core is ideally subdivided, to be used as the basic information in the calculation of absorber worth, control rod worth, etc.

2.1 Determination of the average reactor irradiation

The average irradiation of the fuel is defined as the ratio between the integral of the thermal reactor power over a given time interval and the tonnes of fuel which generated the related energy.

The thermal reactor power is determined by heat balances performed both on the steam side and on the gas side of the station (see ref. 48). In practice, since the heat balances on the steam side, though more accurate, are very tedious and more difficult to perform, for the determination of the reactor power use was more frequently made of the balances relating to the gas side, appropriately correlated by means of a normalization constant to the balances performed on the steam side from time to time as a cross-check.

To determine the power variations in the time lapse between two successive heat balances, use was made of the chart recording the electric power generated (recorded continuously and very accurately). The electric power was then converted into thermal power by means of the station efficiency factor, η , which does not vary appreciably within this time interval.

The thermal power chart thus obtained was then integrated to give the generated energy chart.

For the first part of the fuel cycle, the average core irradiation was obtained simply by dividing the cumulative energy generated by the tons of fuel present in the reactor.

When refuelling started, the energy produced by the discharged channels was deducted from cumulative energy generated by the reactor to obtain the average core irradiation. The energy generated by the discharged channels, and thus the corresponding discharge irradiations, were determined as accurately as possible on the basis of the average channel power in the zone from which the channels were discharged. The average channel power in the zone was obtained from the gas flow rates and temperatures at the outlet of the instrumented channels.

Figs. 2.1.I to IV give the average fuel irradiation as a function of the cumulative energy generated. Figs. 2.1.V to VII give the cumulative thermal energy as a function of time.

2.2 Determination of zone irradiations

In order to determine the actual zone irradiations to be used in the calculations, the reactor was ideally subdivided (Fig. 2.2.I) axially into four zones (each having the height of two fuel elements), and radially into seven concentric annular zones (containing respectively 8, 115, 384, 421, 444, 1092, 455 fuel channels).

On the basis of this core subdivision, the average irradiations of the individual radial zones was calculated, taking into account any fuel discharges. The results thus obtained were then multiplied by the respective axial shape factors, derived by averaging the shape factors determined experimentally every other week during operation (see refs. 5, 22, 33, 39, 47).

A detailed description of the method followed for the determination of the zone irradiations is provided in the report under ref. 22.

Tables 2.2.I to IX give the zone irradiations calculated at different dates. The linear interpolations between one date and the next (Figs. 2.2.II to VIII) are approximate because of the irregular manner in which the fuel was discharged because of operating requirements.

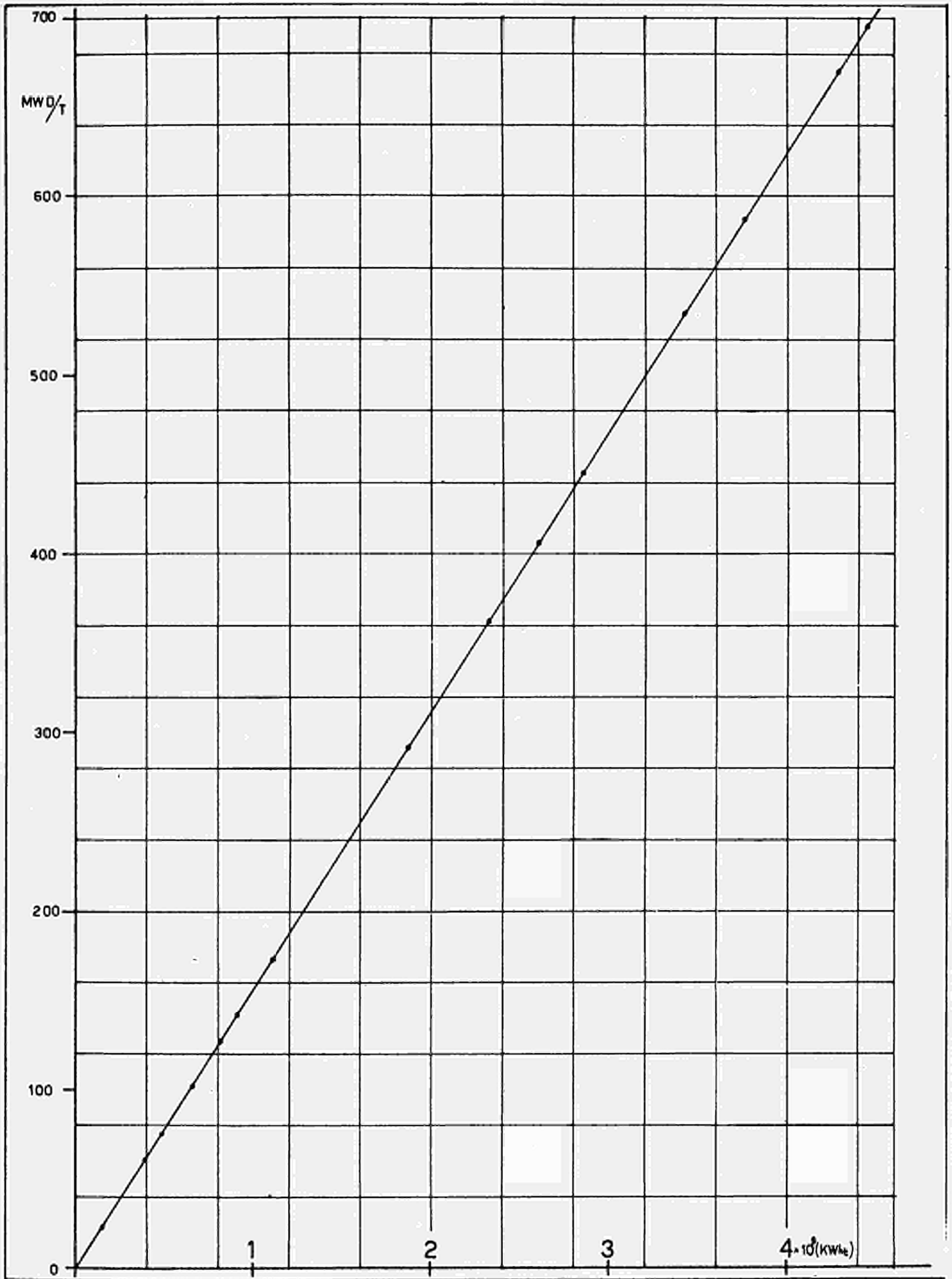


Fig 2.1,1 Average irradiation of the core as a function of the energy generated

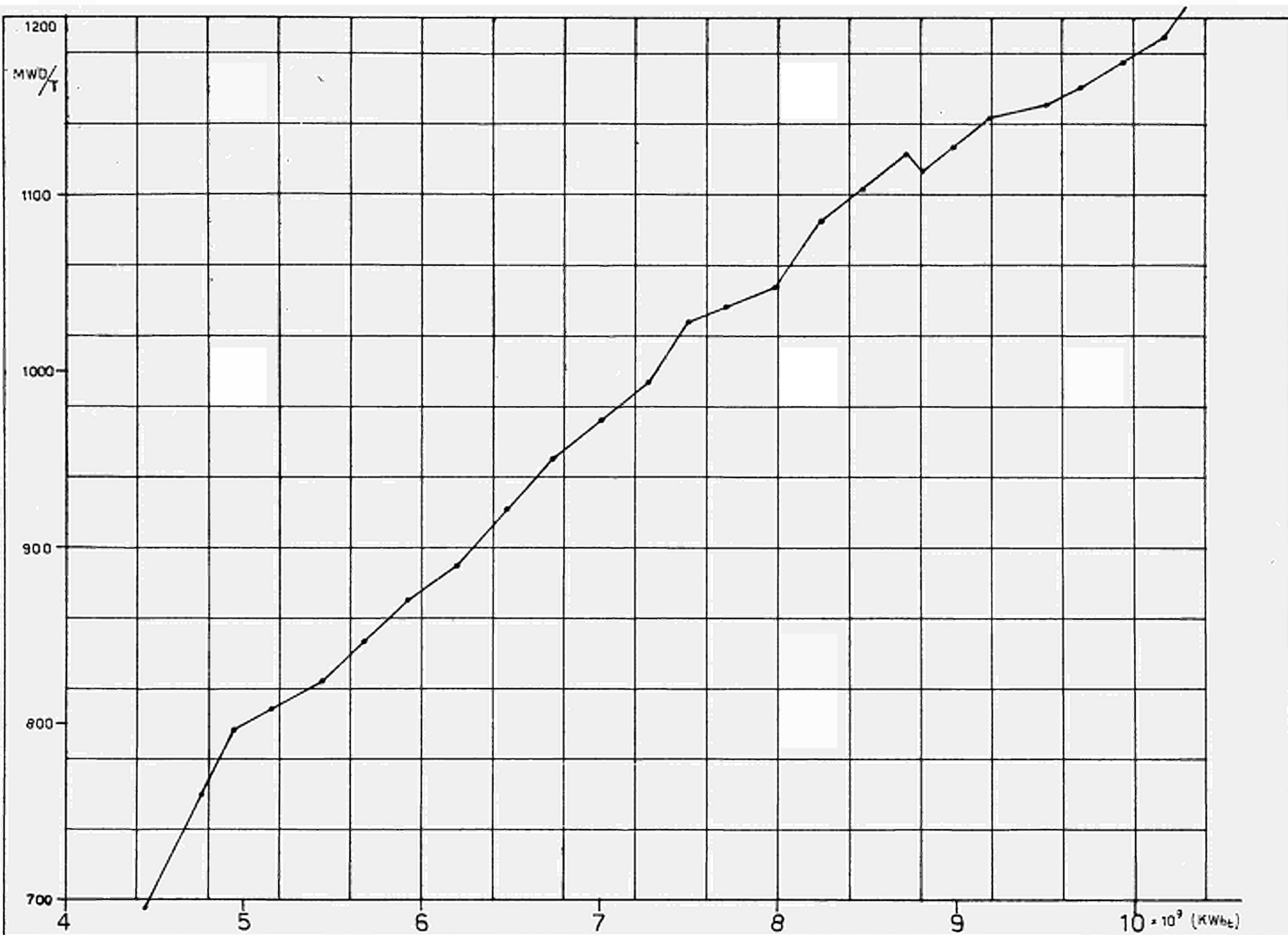


Fig. 2.1.11 Average irradiation of the core as a function of the energy generated



Fig.2.1,III Average irradiation of the core as a function of the energy generated

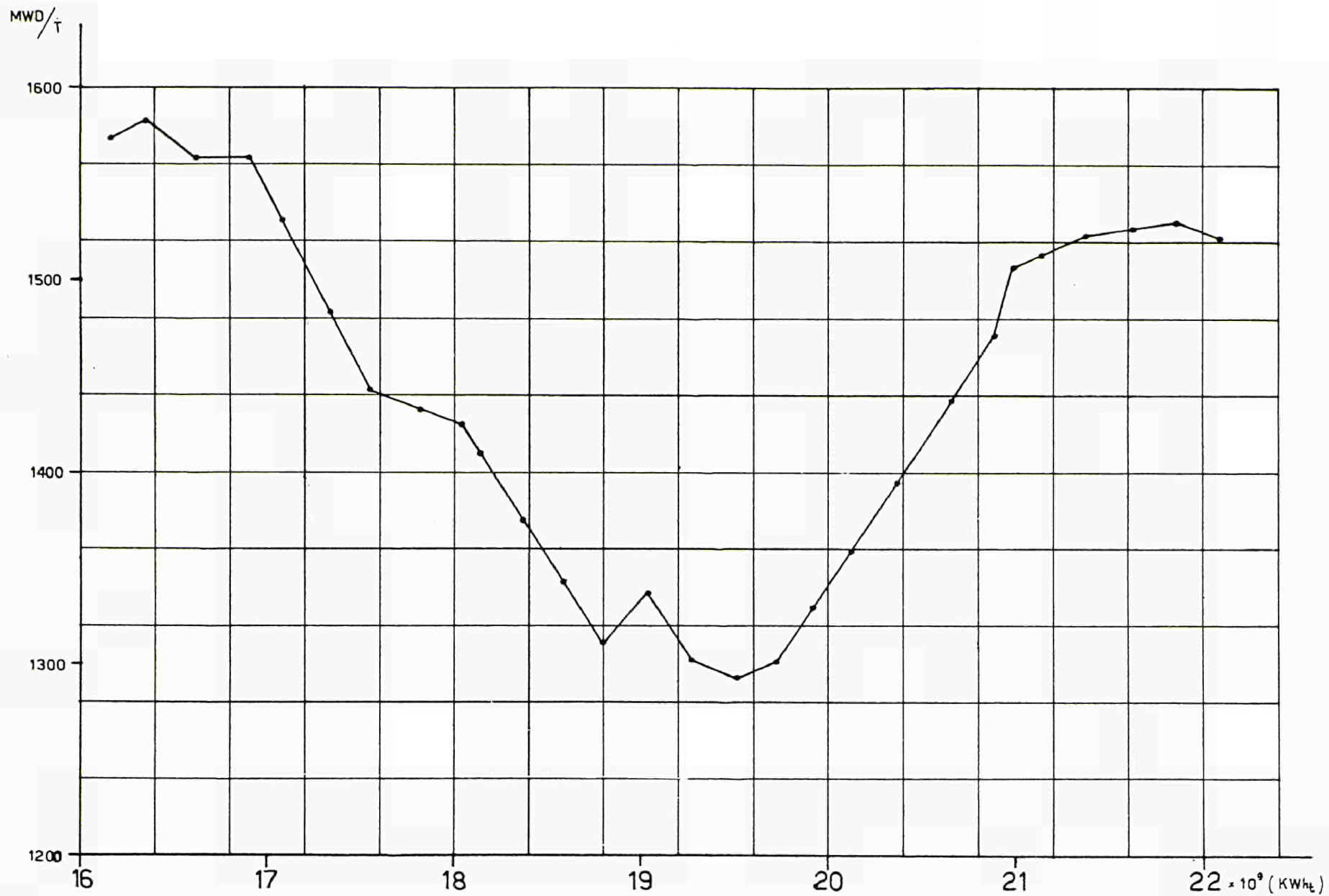


Fig.2.1, IV Average irradiation of the core as a function of the energy generated

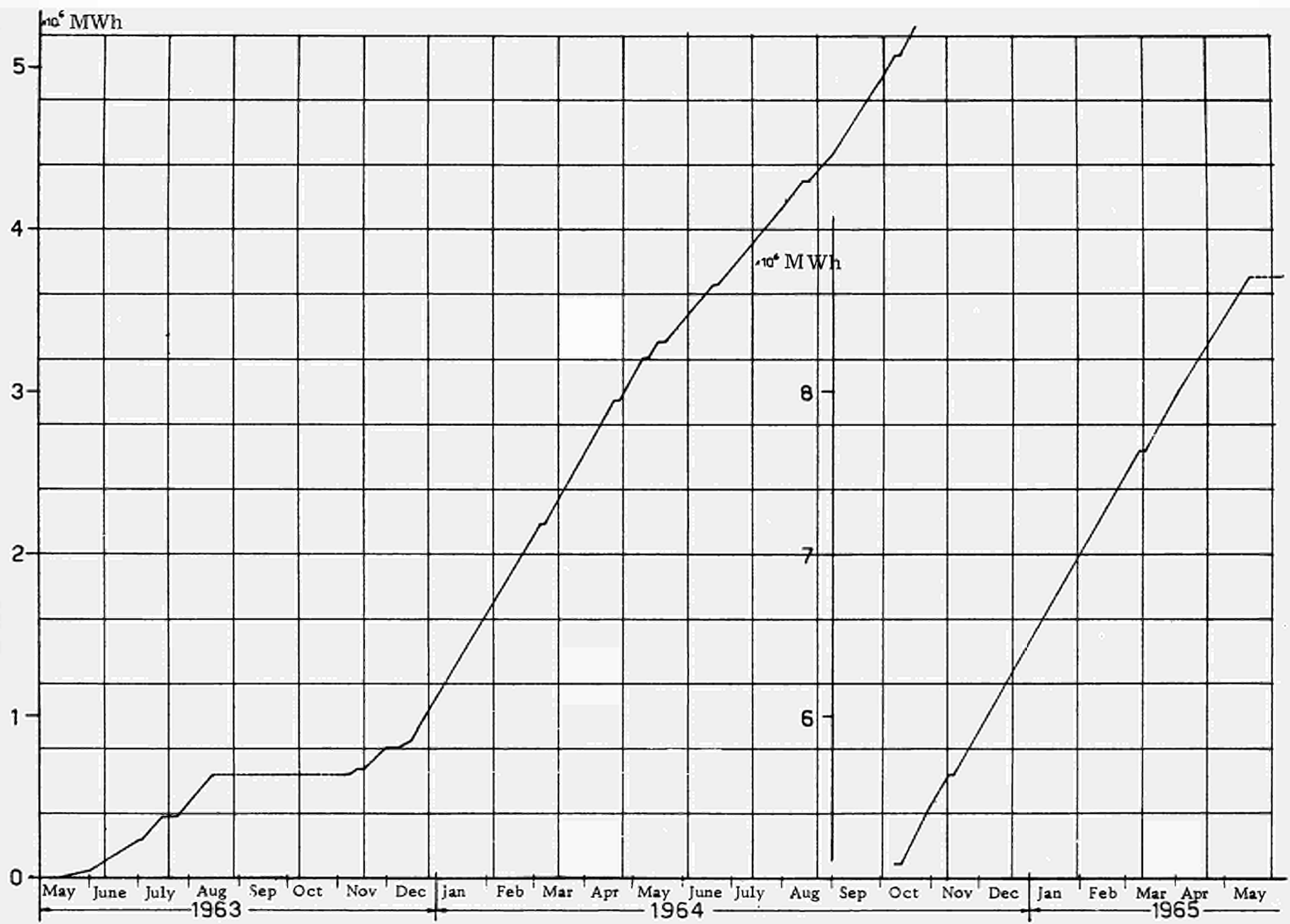


Fig.2.1,V Cumulative thermal energy generated by the core as a function of time.

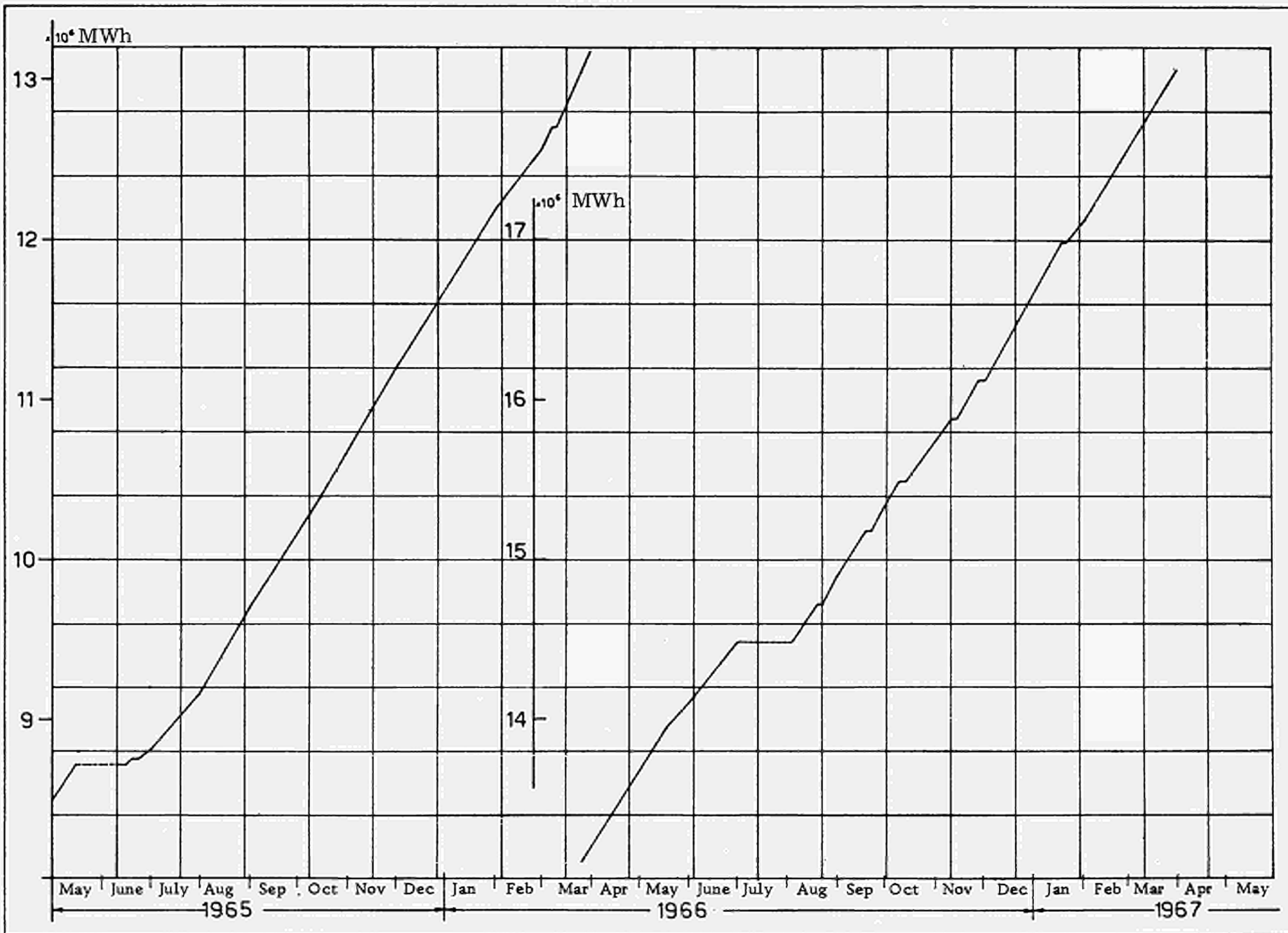


Fig. 2.1, VI Cumulative thermal energy generated by the core as a function of time

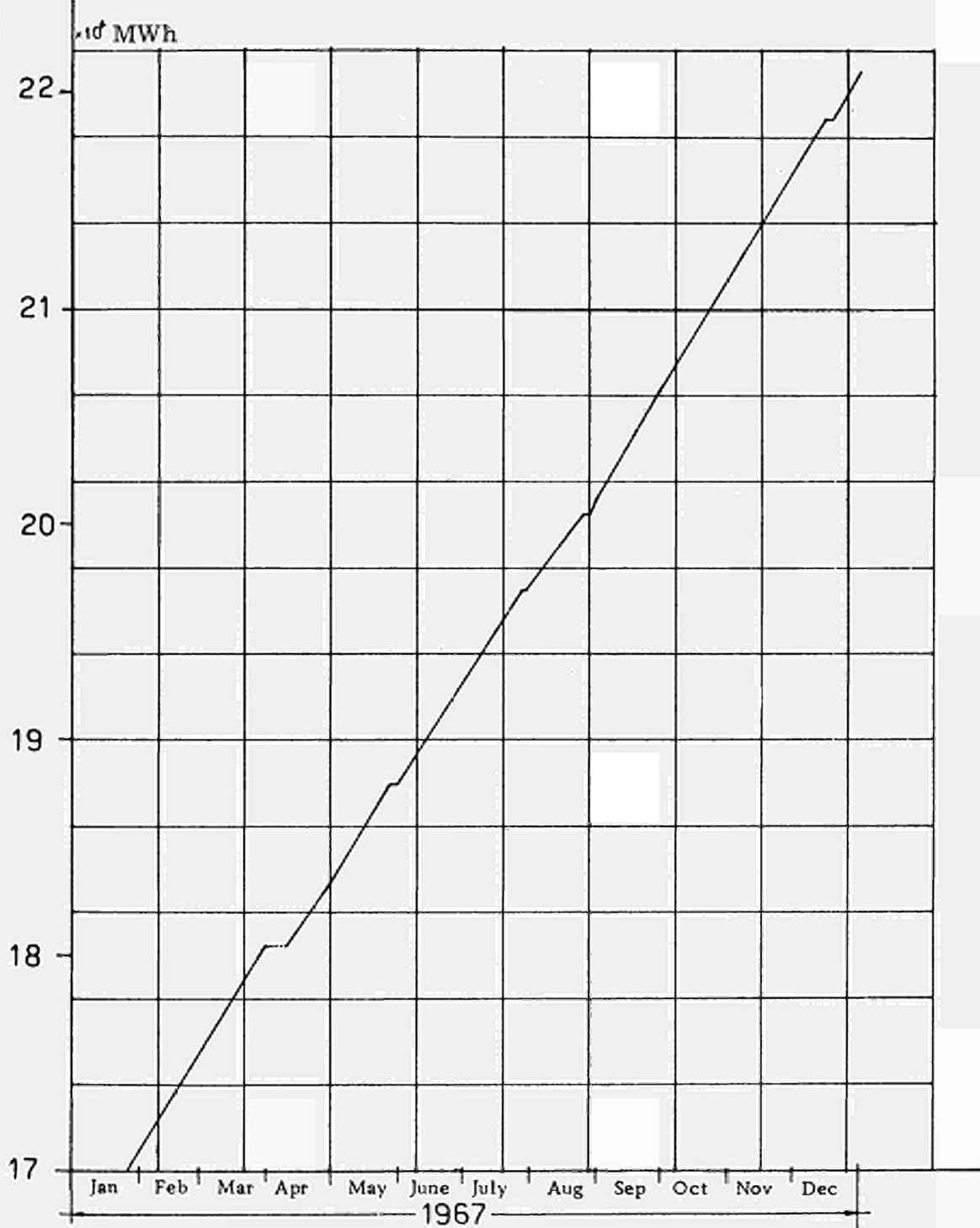


Fig. 2.1, VII Cumulative thermal energy generated by the core as a function of time

TABLE 2.2.I

THERMAL ENERGY = 675,000,000 kWh IRRADIATION AS OF 15.11.1963 AVERAGE CORE IRRADIATION = 105 MWD/T								THERMAL ENERGY = 1,860,000,000 kWh IRRADIATION AS OF 15.2.1964 AVERAGE CORE IRRADIATION = 290 MWD/T							
Rad. zone Ax. zone	1	2	3	4	5	6	7	Rad. zone Ax. zone	1	2	3	4	5	6	7
I	119	114	110	103	97	70	40	I	336	322	313	297	276	189	109
II	196	192	191	188	180	133	80	II	567	555	548	532	509	372	222
III	142	147	152	154	151	120	76	III	384	400	412	416	416	335	211
IV	68	70	73	76	73	57	37	IV	159	164	172	184	184	154	103
Rad. zone I	131	131	131	130	125	95	58	Rad. zone I	361	360	361	357	346	262	161

TABLE 2.2.II

THERMAL ENERGY = 3,310,000,000 kWh IRRADIATION AS OF 15.5.1964 AVERAGE CORE IRRADIATION = 516 MWD/T								THERMAL ENERGY = 3,940,000,000 kWh IRRADIATION AS OF 15.7.1964 AVERAGE CORE IRRADIATION = 614 MWD/T							
Rad. zone \ Ax. zone	1	2	3	4	5	6	7	Rad. zone \ Ax. zone	1	2	3	4	5	6	7
I	606	578	558	529	491	338	194	I	721	688	664	629	585	401	231
II	1018	996	984	952	914	669	396	II	1210	1186	1170	1134	1088	795	470
III	676	707	733	737	735	591	375	III	804	842	872	877	876	702	446
IV	272	284	299	322	320	267	183	IV	323	338	356	383	380	318	217
Rad. zone \bar{I}	643	641	643	635	615	466	287	Rad. zone \bar{I}	765	763	765	756	732	554	341

TABLE 2.2.III

THERMAL ENERGY = 4,450,000,000 kWh IRRADIATION AS OF 31.8.1964 AVERAGE CORE IRRADIATION = 694 MWD/T								THERMAL ENERGY = 8,720,000,000 kWh IRRADIATION AS OF 14.5.1965 AVERAGE CORE IRRADIATION = 1,100 MWD/T							
Rad. zone Ax. zone	1	2	3	4	5	6	7	Rad. zone Ax. zone	1	2	3	4	5	6	7
I	819	781	753	716	665	455	260	I	921	1208	1147	1066	993	712	424
II	1374	1346	1329	1297	1242	904	531	II	1623	2150	2081	1962	1880	1427	877
III	905	948	980	986	984	791	504	III	1143	1581	1604	1581	1561	1275	830
IV	357	373	393	418	417	354	246	IV	470	652	675	699	695	589	399
Rad. zone I	864	862	864	854	827	626	385	Rad. zone I	1039	1397	1376	1327	1282	1001	632

TABLE 2.2.IV

THERMAL ENERGY = 9,402,236,701 kWh IRRADIATION AS OF 13.8.1965 AVERAGE CORE IRRADIATION = 1,147 MWD/T								THERMAL ENERGY = 11,636,193,463 kWh IRRADIATION AS OF 28.12.1965 AVERAGE CORE IRRADIATION = 1,393 MWD/T							
Rad. zone Ax. zone	1	2	3	4	5	6	7	Rad. zone Ax. zone	1	2	3	4	5	6	7
I	1054	1273	1125	1134	999	755	473	I	1369	1509	1362	1377	1235	919	588
II	1856	2287	2051	2093	1900	1512	968	II	2463	2702	2469	2526	2333	1826	1206
III	1307	1711	1598	1675	1583	1363	911	III	1824	2039	1927	2039	1927	1627	1136
IV	529	696	664	732	696	621	437	IV	765	840	804	899	854	748	544
Rad. zone <u>I</u>	1186	1491	1359	1409	1294	1062	697	Rad. zone <u>I</u>	1605	1772	1640	1710	1587	1280	868

TABLE 2.2.V

THERMAL ENERGY = 12,935,276,728 kWh IRRADIATION AS OF 17.3.1966 AVERAGE CORE IRRADIATION = 1,490 MWD/T								THERMAL ENERGY = 13,432,188,378 kWh IRRADIATION AS OF 15.4.1966 AVERAGE CORE IRRADIATION = 1,542 MWD/T							
Rad. zone Ax. zone	1	2	3	4	5	6	7	Rad. zone Ax. zone	1	2	3	4	5	6	7
I	1070	1586	1445	1502	1229	977	644	I	1149	1663	1498	1518	1252	1017	672
II	1939	2852	2628	2803	2345	1950	1320	II	2085	2995	2732	2849	2399	2033	1379
III	1465	2209	2109	2279	1976	1761	1244	III	1579	2326	2198	2321	2028	1844	1303
IV	607	896	864	991	870	806	595	IV	656	942	898	1003	890	844	622
Rad. zone I	1270	1886	1761	1894	1605	1373	951	Rad. zone I	1367	1981	1831	1923	1642	1434	994

TABLE 2. 2. VI

THERMAL ENERGY = 14, 476, 642, 536 kWh IRRADIATION AS OF 21.7.1966 AVERAGE CORE IRRADIATION = 1, 462 MWD/T								THERMAL ENERGY = 15, 385, 641, 002 kWh IRRADIATION AS OF 4.10.1966 AVERAGE CORE IRRADIATION = 1, 557 MWD/T							
Rad. zone Ax. zone	1	2	3	4	5	6	7	Rad. zone Ax. zone	1	2	3	4	5	6	7
I	1342	1343	1385	1306	1217	1032	688	I	1481	1438	1466	1351	1287	1102	740
II	2435	2419	2529	2467	2328	2034	1394	II	2694	2599	2687	2551	2464	2168	1497
III	1828	1863	2019	2012	1958	1816	1303	III	2042	2024	2165	2097	2087	1949	1402
IV	744	753	825	855	857	834	618	IV	839	831	900	914	926	898	668
Rad. zone I	1587	1594	1689	1660	1590	1429	1001	Rad. zone I	1764	1723	1804	1728	1691	1529	1077

TABLE 2.2.VII

THERMAL ENERGY = 16,406,207,894 kWh IRRADIATION AS OF 18.12.1966 AVERAGE CORE IRRADIATION = 1,573 MWD/T								THERMAL ENERGY = 18,053,637,567 kWh IRRADIATION AS OF 31.3.1967 AVERAGE CORE IRRADIATION = 1,418 MWD/T							
Rad. zone \ Ax. zone	1	2	3	4	5	6	7	Rad. zone \ Ax. zone	1	2	3	4	5	6	7
I	1647	1510	1408	1388	1297	1117	757	I	1187	759	841	971	1140	1220	854
II	2984	2719	2569	2598	2462	2195	1528	II	2203	1415	1577	1860	2179	2399	1722
III	2273	2129	2077	2149	2095	1979	1440	III	1686	1091	1263	1532	1855	2179	1627
IV	946	888	878	961	942	917	691	IV	674	412	500	662	830	1018	783
Rad. zone I	1962	1811	1733	1774	1699	1552	1104	Rad. zone I	1437	919	1045	1256	1501	1704	1247

TABLE 2. 2. VIII

THERMAL ENERGY = 19,558,515,974 kWh IRRADIATION AS OF 18.7.1967 AVERAGE CORE IRRADIATION = 1,286 MWD/T								THERMAL ENERGY = 19,999,907,454 kWh IRRADIATION AS OF 21.8.1967 AVERAGE CORE IRRADIATION = 1,338 MWD/T							
Rad. zone Ax. zone	1	2	3	4	5	6	7	Rad. zone Ax. zone	1	2	3	4	5	6	7
I	1454	1007	1034	868	931	980	933	I	1528	1079	1080	936	993	1001	952
II	2651	1843	1911	1669	1786	1927	1877	II	2778	1967	1992	1790	1901	1968	1914
III	2020	1427	1532	1364	1500	1728	1774	III	2117	1527	1599	1465	1601	1766	1809
IV	829	565	623	571	652	797	853	IV	874	611	654	622	701	816	870
Rad. zone <u>I</u>	1739	1210	1275	1118	1217	1358	1359	Rad. zone <u>I</u>	1824	1296	1331	1203	1299	1387	1386

TABLE 2.2.IX

THERMAL ENERGY = 21,373,411,683 kWh IRRADIATION AS OF 15/11/1967 AVERAGE CORE IRRADIATION = 1,532 MWD/T							
Rad. zone Ax. zone	1	2	3	4	5	6	7
I	1756	1299	1281	1130	1159	1119	1033
II	3178	2359	2348	2130	2211	2206	2070
III	2417	1837	1893	1752	1876	1992	1954
IV	1013	753	789	759	835	925	942
Rad. zone - I	2091	1562	1578	1443	1520	1560	1500

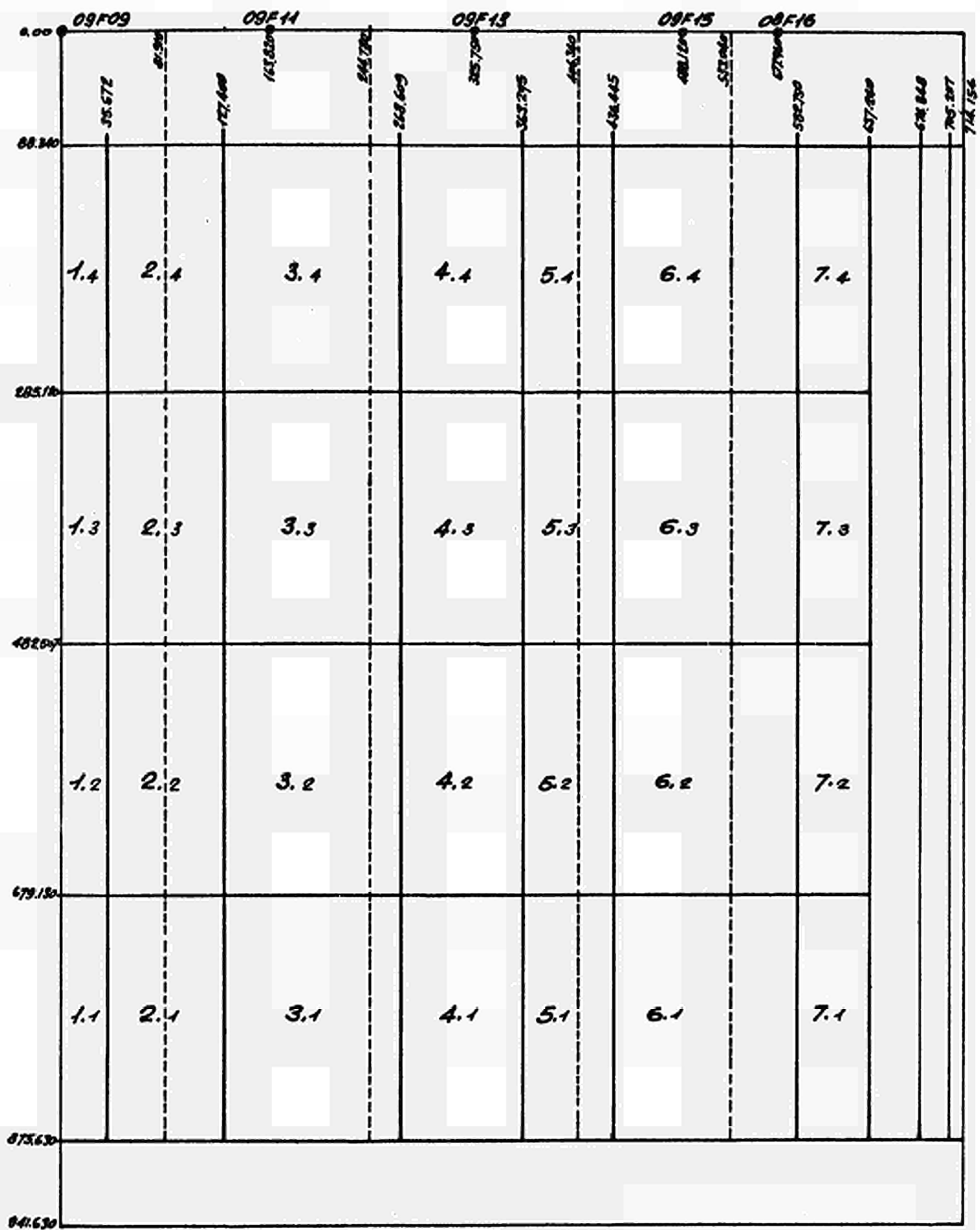


Fig. 2.2,1 Core subdivision adopted for zone irradiation calculations.

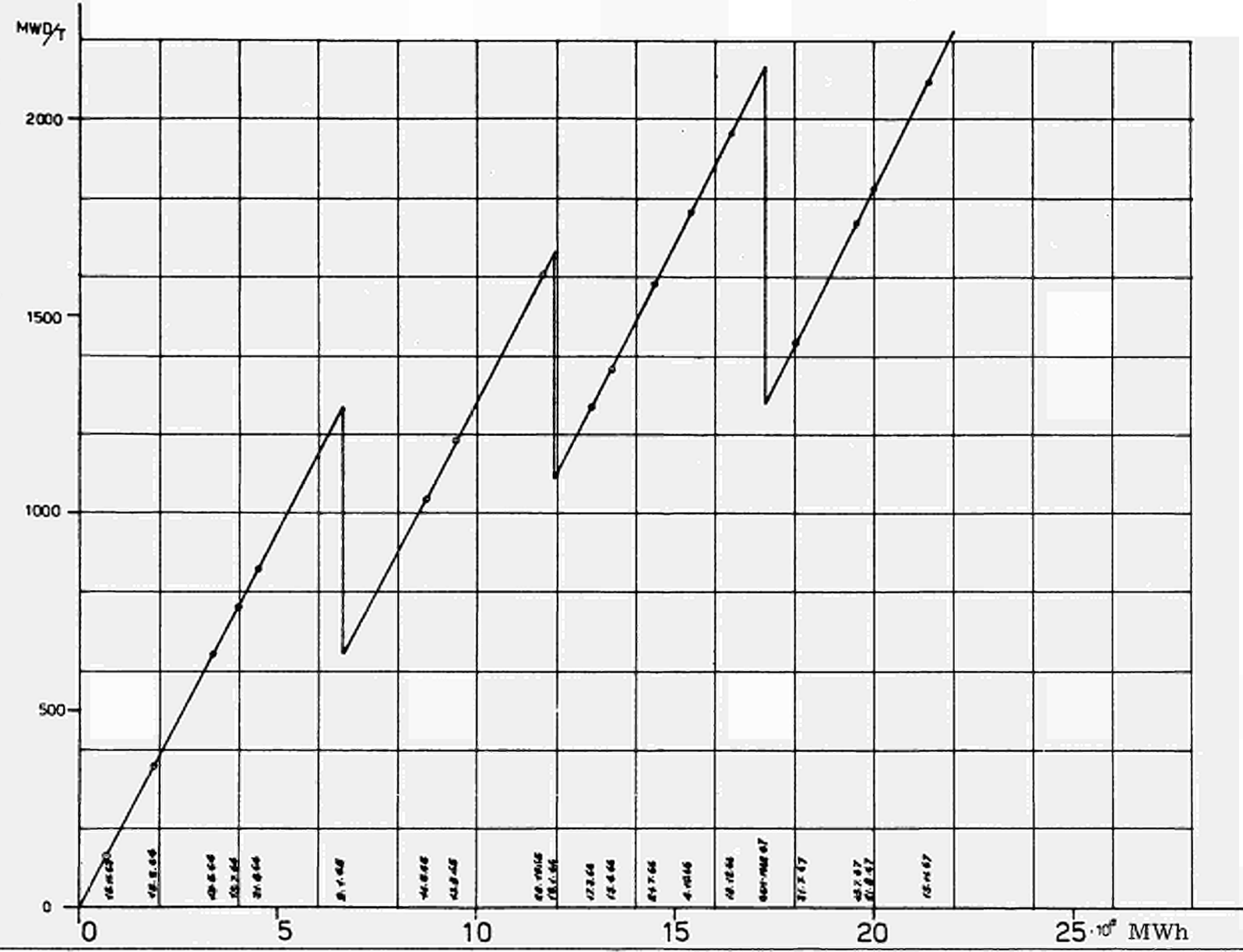


Fig. 2.2.11 Irradiation of radial zone No. 1 as a function of the energy generated by the core.

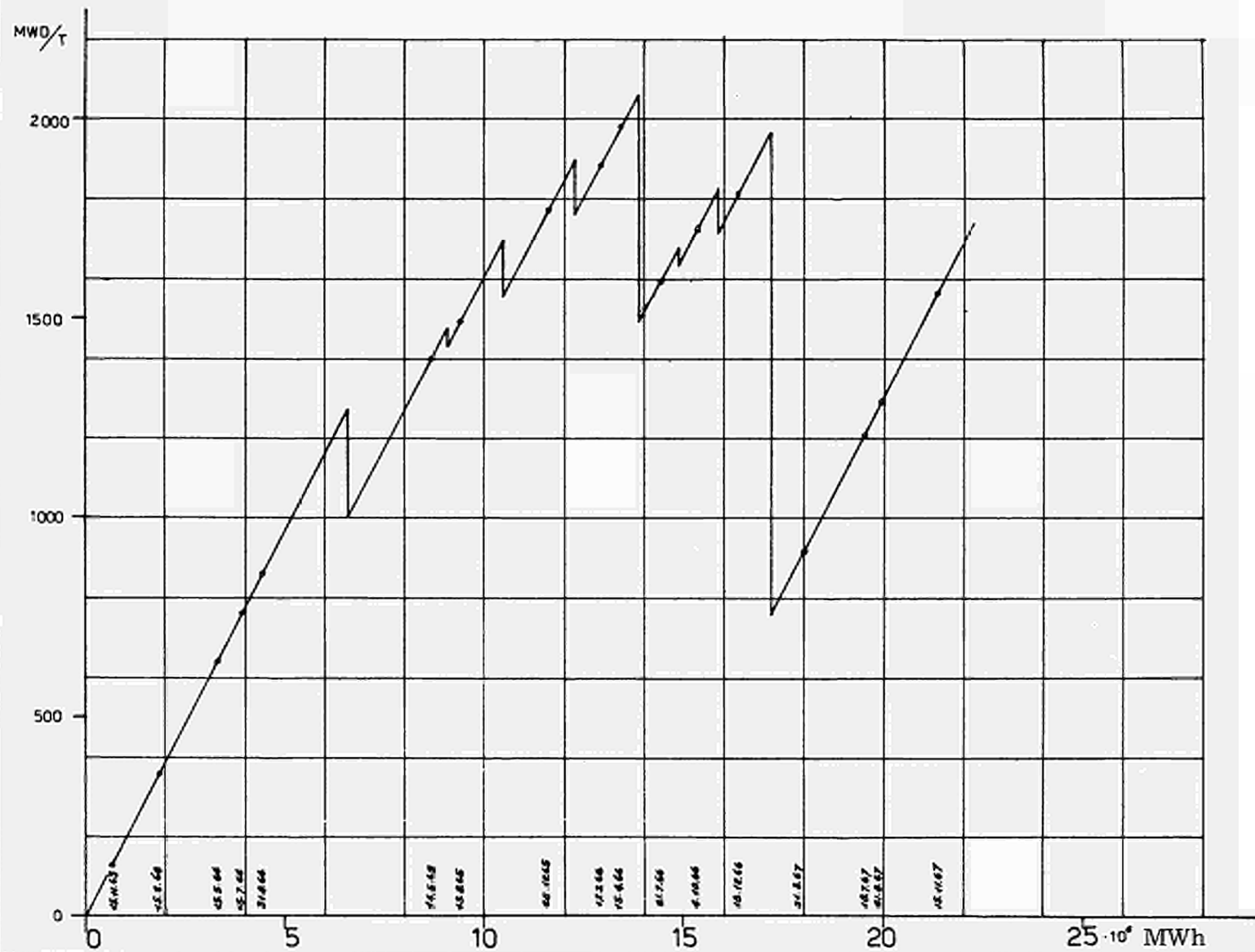


Fig. 2.2, III Average irradiation of radial zone 2 as a function of the energy generated by the core.

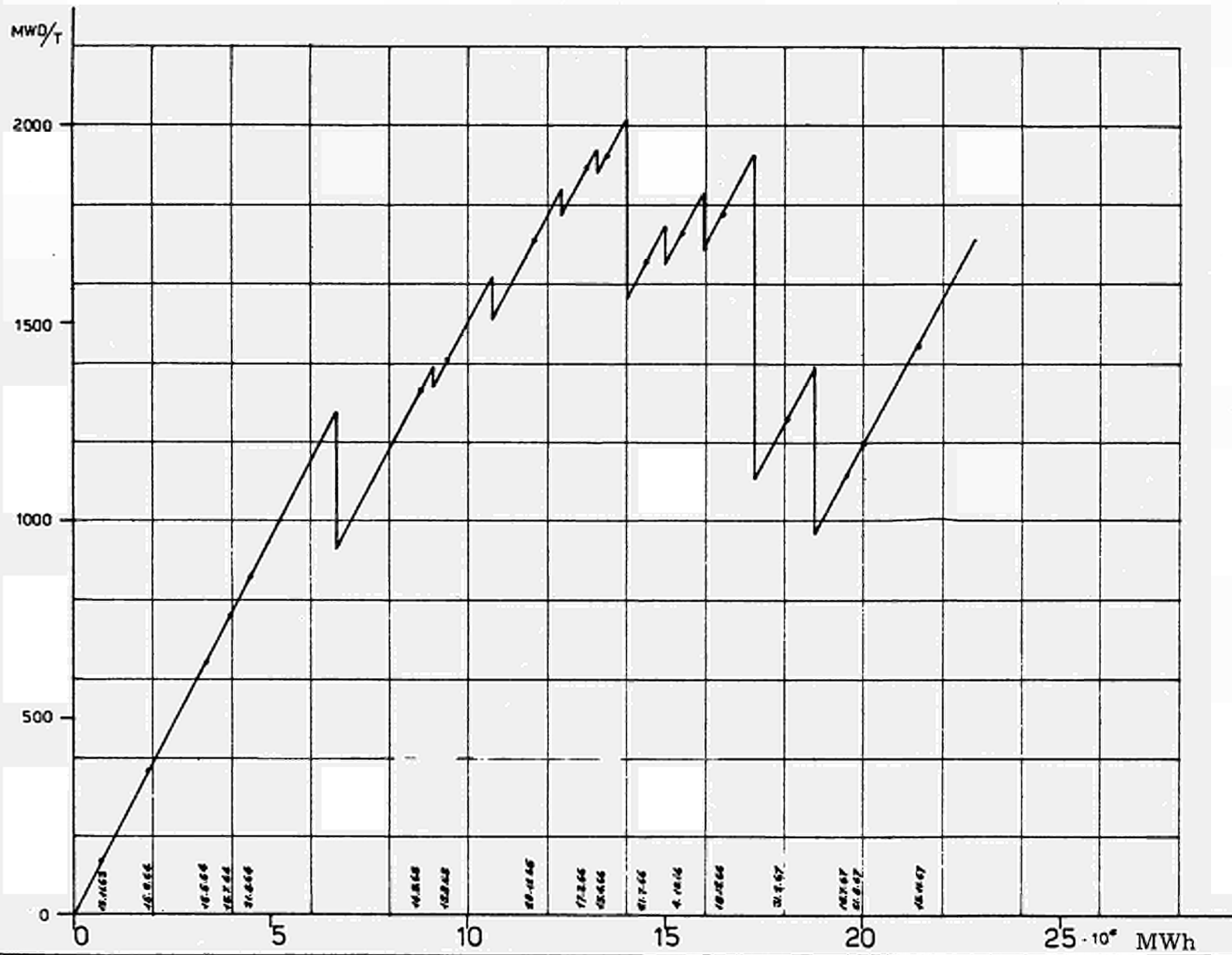


Fig. 2.2, V Average irradiation of radial zone 4 as a function of the energy generated by the core.

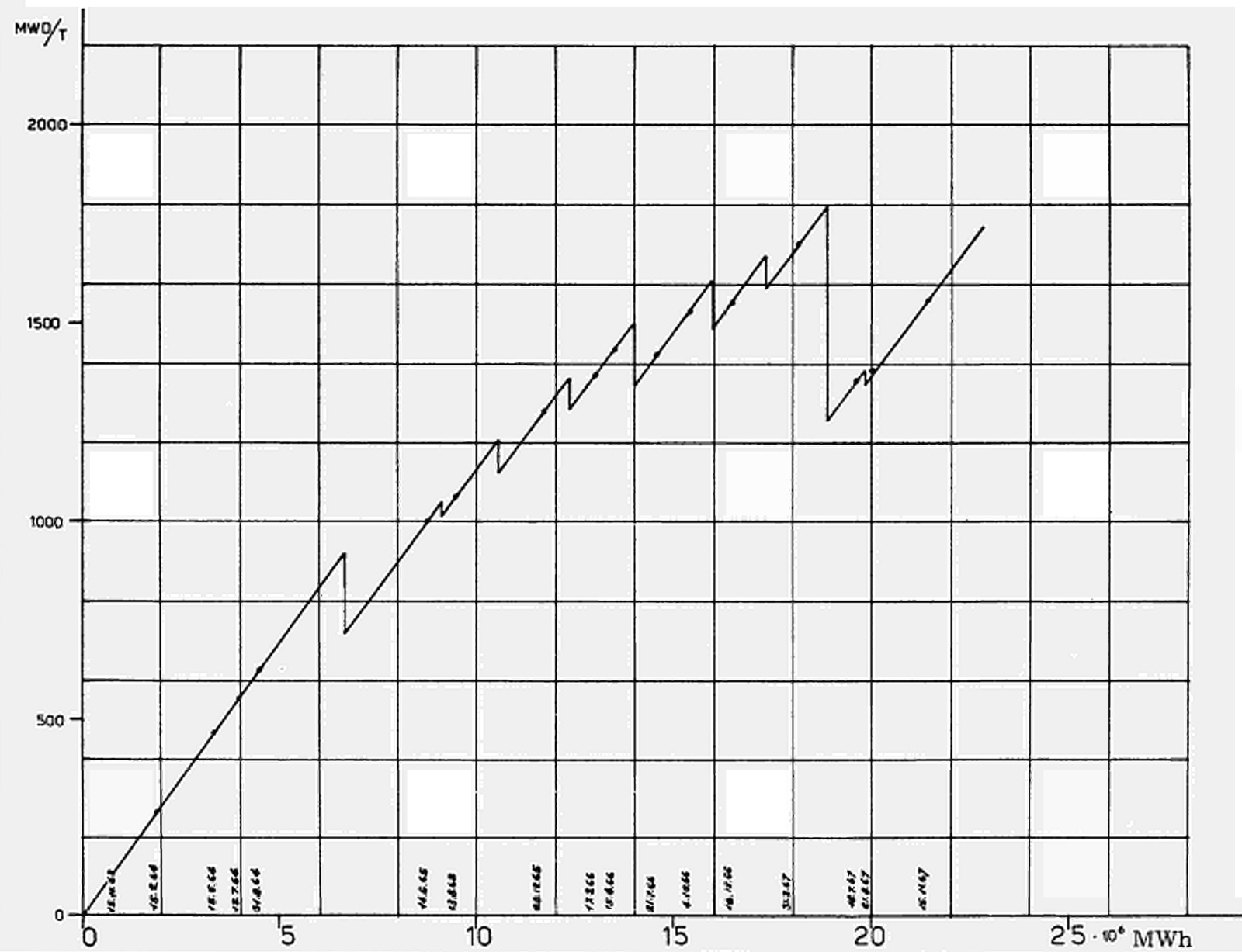


Fig. 2.2, VII Average irradiation of radial zone 6 as a function of the energy generated by the core.

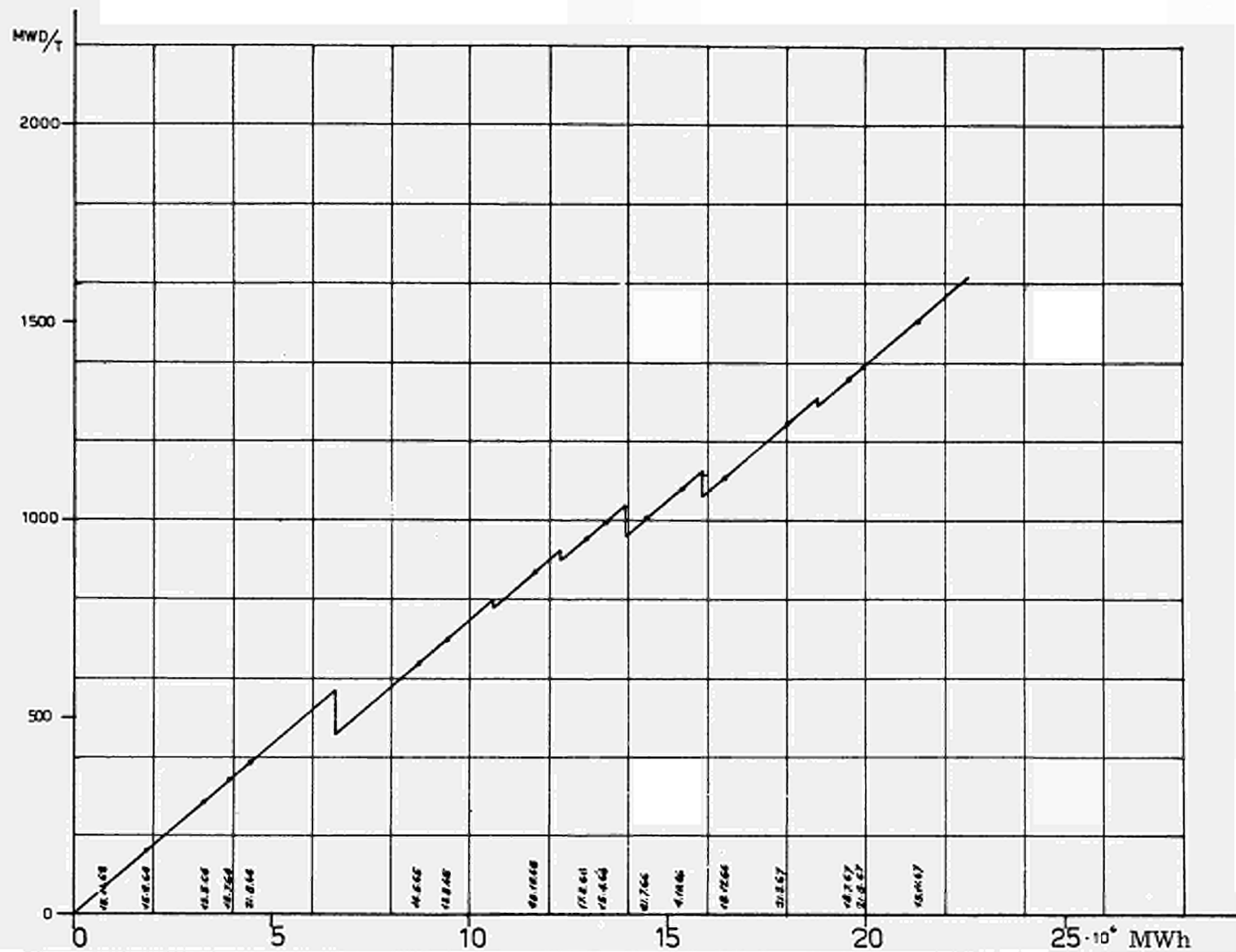


Fig. 2.2, VIII Average irradiation of radial zone 7 as a function of the energy generated by the core.

3.0 DETERMINATION OF ABSORBER WORTH

In the Latina reactor the long-term reactivity variations are compensated by varying the distribution and weight of apposite steel absorbers located in interstitial channels. Each absorber channel is constituted of a stack of eight basic absorbers, weighing 3.327 kg each, on which light (0.698 kg) or heavy (1.253 kg) rings can be placed, up to a maximum of ten rings per absorber.

Between May 1963 and December 1967, the absorber pattern was changed fourteen times, as shown in Figs. 3.0.I to XIV.

The reactivity absorbed by each pattern represents the most important term in the build-up curve, and was calculated by means of the PDQ 02, PIFFERO and FTD2 codes (See ref. 35). To ascertain the adequacy of these codes, two experimental calibrations of the absorbers were performed in order to check the calculated results against the experimental ones.

The following paragraphs 3.1 and 3.2 briefly describe the measurements and the comparisons with the calculated values (see ref. 15, 23, 30, 53). Paragraph 3.3 describes the calculations for the determination of the reactivity controlled by the fourteen different absorber patterns.

To assess the worth of intermediate absorber patterns, simplified interpolation methods were adopted for the purpose of performing the reactivity balances.

3.1 Experimental absorber calibrations

Since the experimental calibration of an absorber channel is a very delicate operation, the absorbers were calibrated after a prolonged reactor shutdowns so as to bring the core to the most stable condition possible from the standpoints of temperature, xenon decay, etc. The calibrations were performed by measuring the flux doubling times resulting from the removal of absorber channels of different weight from the core; from these doubling times was derived the corresponding reactivity on the basis of Nordheim's equation, and by correcting the results by a factor χ , which is a function of the general reactor irradiation conditions (see refs. 11, 53).

The results of the measurements taken at 1100 and 1500 MWD/T are summarized in tables 3.1.I, II, III. These results are also plotted in Figs. 3.1.I and 3.1.II.

3.2 Calculation of absorber-controlled reactivity

To determine the reactivity variation of the Latina reactor in time, it was necessary to prepare a calculation method which could provide with sufficient accuracy the information that cannot be obtained experimentally. The calculation method adopted (see refs. 53, 57, 58) is based on a synthesis of the two-dimension codes PDQ 02 and FTD2, so as to obtain the core reactivity as well as the flux and temperature distributions. In brief, the method permits the solution of the two-group diffusion equation in the

three dimension by means of the PDQ 02 and FTD2 codes, taking into account the singularities present in the core.

The basic criterion is to determine core reactivity, flux distributions at a certain level, and channel power by means of an FTD2 calculation in which a few parameters associated with the radial variation of the axial flux shape have been introduced. These parameters are the axial bucklings and axial flux integrals computed by means of the PDQ 02 code in R, Z geometry.

The nuclear lattice constants are computed by the method correlated with the experimental results of the British Industries Collaborative Experimental Programme (ref. 56).

A few modification were made to account for the experimental results obtained during the commissioning and initial operation of the Latina reactor.

The cells containing control rods and empty channels are represented in the FTD2 code by lattice parameters obtained by homogenizing the heterogeneous structure so as to maintain the cell boundary conditions.

In addition, the FTD2 has a particular option for the representation of the absorbers located in interstitial positions of the lattice, as occurs in the Latina reactor.

The singularities are dealt with differently in the PDQ 02 for reasons of cylindrical symmetry; the absorbers and control rods are homogenized within the respective areas of influence by the supercell technique.

The thermal extrapolation length of the gray rods is obtained by the diffusion theory, referred to the fine structure of the channel flux. The corresponding epithermal extrapolation length was assumed to be infinite.

The epithermal extrapolation length of the black rods is also obtained by means of the diffusion theory, whereas the thermal extrapolation length is obtained by Kushneriuk and MacKay's method.

The results of the calculations performed as described above are summarized in table 3.2.I which also lists, for comparison purposes, the experimental results obtained from the first set of measurements on the Latina reactor.

The calculated values of the absorber-controlled reactivity were obtained by difference between the eigenvalues resulting from the FTD2 calculations. These results are plotted in Fig. 3.2.I.

From an examination of table 3.2.I and Fig. 3.2.I it appears that, apart from the measurement relating to absorber B+8L+2H, the differences between the calculated and measured values are on the order of 4-6% for absorbers loaded with light rings, and 1% for the absorber loaded with three heavy rings.

It should be borne in mind that the results are greatly affected by the local value of the flux in the measured channel; a 2% error in the evaluation of the local flux produces an error of about 4% in the absorber-controlled reactivity.

Since the differences observed between the calculated and measured reactivities can be attributed partly to inaccuracy in the evaluation of the local flux in the measured channel, it was not deemed advisable to vary the extrapolation lengths used in the calculations.

3.3 Calculation of the reactivity controlled by the various absorber patterns

The calculation of the reactivity absorbed by the fourteen patterns considered (see refs. 38, 50) is based on the method described in paragraph 3.2. In practice, two calculations were performed, one with and one without the interstitial absorbers associated with the pattern being examined, and the controlled reactivity was obtained by difference.

Each time a slightly different reactor subdivision was used according to the position of the group B general control rods selected at the time of the calculation. Each zone was characterized by given values of irradiation, fuel temperature and moderator temperature derived from experimental data.

It should be noted that the sector rods were always considered fully withdrawn, because the quantity of interest is the sum of the reactivities controlled by the absorbers and rods respectively. On the other hand, the reactivity controlled by the sector rods is obtained from experimental calibration curves measured in the presence of absorbers and correlated on a theoretical basis to nominal operating conditions; therefore, these curves already take into account the variation in absorber-controlled reactivity as a result of sector rod withdrawal.

The group B general rods were not withdrawn in the same manner as the sector rods because they are normally just slightly inserted and at any rate distributed uniformly enough over the core and therefore the variation of absorber controlled reactivity owing to their withdrawal is negligible.

The results and all the information of interest are given in table 3.3.I.

TABLE 3.1.I: Measurements performed on channel 09 F 09 IZ (central zone) at 1100 MWD/T

T 1/2 (sec)	ξ_0 (p. c. m.)	ξ (p. c. m.)	Absolute weight (kg)	(p. c. m./kg)	Type of channel *
150	36.1	30.9	43.368	0.716	B+3L
228	26.5	22.7	26.618	0.853	B
114	45.7	39.1	60.118	0.651	B+6L
137	39.9	34.2	56.700	0.603	B+3H
75	64.6	55.3	91.338	0.605	B+8L+2H

where:

B, weight of a basic absorber element = 3.3273 kg
H, weight of a heavy ring = 1.2534 kg
L, weight of a light ring = 0.6979 kg

TABLE 3.1.II: Measurements performed on channel 09 F 09 IZ (central zone) at 1500 MWD/T

T 1/2 (sec)	ξ_0 (p. c. m.)	ξ (p. c. m.)	Weight (kg)	(p. c. m./kg)	Type of channel *
183	30.6	25.8	43.368	0.595	B+3L
219	26.9	22.7	36.646	0.619	B+H
151	35.9	30.3	56.700	0.534	B+3H
113	46.1	38.9	76.754	0.509	B+5H

TABLE 3.1.III: Measurements performed on channel 13 F 07 IZ (peripheral zone) at 1500 MWD/T

T 1/2 (sec)	ξ_0 (p. c. m.)	ξ (p. c. m.)	Weight (kg)	(p. c. m./kg)	Type of channel *
155	34.9	29.4	69.006	0.426	B+4L+2H
130	40.9	34.5	82.450	0.418	B+10L
206	28.2	23.8	56.700	0.420	B+3H
333	16.7	14.1	26.618	0.529	B

* Each channel comprises eight typical absorbers

TABLE 3.2.I: Comparison between the theoretical and experimental results relating to reactivity controlled by absorbers of different weights

Type of channel	Weight (kg)	Eigenvalue (FTD2)	(1) Calculated reactivity (p. c. m.)	(2) Calculated reactivity (p. c. m.)	$\frac{(1) - (2)}{(2)}$ (%)
Empty	--	1.000271	--	--	--
B	26.618	1.000484	21.3	22.8	-6.6
B+3L	43.368	1.000570	29.9	31.1	-3.8
B+6L	60.118	1.000645	37.4	39.3	-4.8
B+10L	82.450	1.000725	45.4	--	--
B+3H	56.700	1.000618	34.7	34.3	+1.1
B+6H	86.782	1.000727	45.6	--	--
B+10H	126.890	1.000825	55.4	--	--
B+8L+2H	91.338	1.000745	47.4	55.6	-14.7

TABLE 3.3.I: Reactivity controlled by the 14 absorber patterns in the first five years of Latina reactor operation.

Absorber patter No.	End of absorber discharge	Date of reactivity balance	kg of loaded steel			Fuel channel discharged	Average reactor irradiation (MWD/T)	Reactivity controlled by absorber pattern (p. c. m.)
			Flattened flux area	Unflattened flux area	TOTAL			
1		7. 7. 1963	559. 13	---	559. 13	--	53	659
2	18. 9. 1963	23. 11. 1963	997. 68	302. 34	1300. 02	--	120	1128
3	20. 1. 1964	31. 1. 1964	1697. 38	302. 38	1999. 76	--	251	1682
4	12. 3. 1964	26. 3. 1964	2361. 44	1101. 14	3462. 58	--	392	2326
5	13. 5. 1964	22. 5. 1964	2773. 23	1640. 99	4414. 22	--	520	2800
6	7. 8. 1964	3. 9. 1964	3293. 20	2176. 56	5469. 76	--	716	3056
7	18. 11. 1964	30. 11. 1964	3293. 20	2175. 59	5468. 79	206	870	2992
8	1. 2. 1965	18. 3. 1965	2962. 99	2244. 62	5207. 61	514	1039	2788
9	18. 6. 1965	13. 8. 1965	2505. 01	2125. 28	4630. 29	779	1148	2572
10	18. 12. 1965	28. 12. 1965	2119. 07	1942. 23	4051. 30	926	1419	2142
11	7. 4. 1966	15. 4. 1966	1950. 59	1566. 33	3516. 92	1135	1547	1976
12	4. 12. 1966	17. 12. 1966	1745. 41	1384. 31	3129. 72	1613	1584	1853
13	5. 7. 1967	18. 7. 1967	1933. 28	1475. 12	3408. 40	2417	1288	2080
14	7. 8. 1967	21. 8. 1967	2112. 82	1563. 26	3676. 08	2443	1338	2179

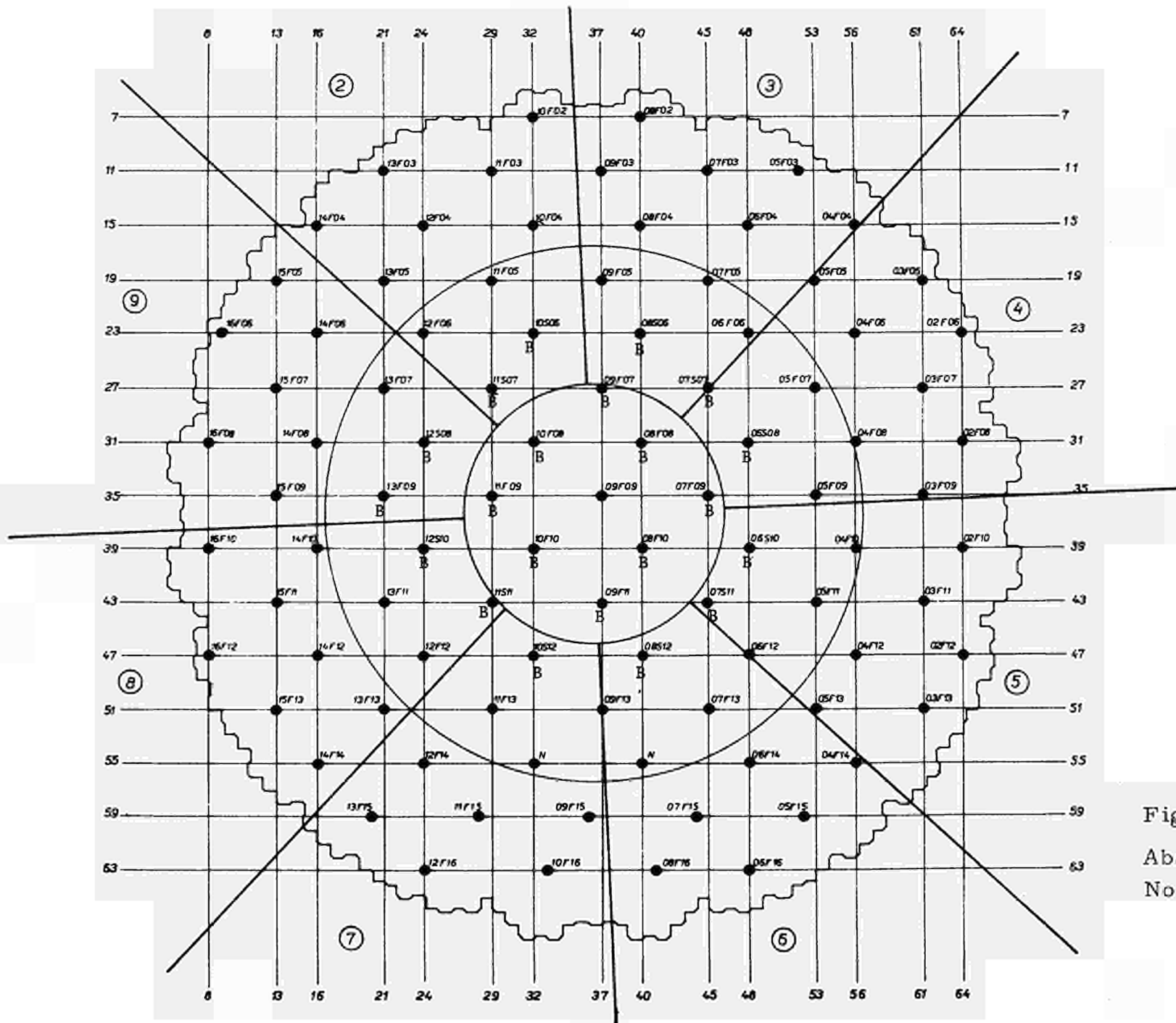


Fig. 3.0, I
Absorber pattern
No. 1

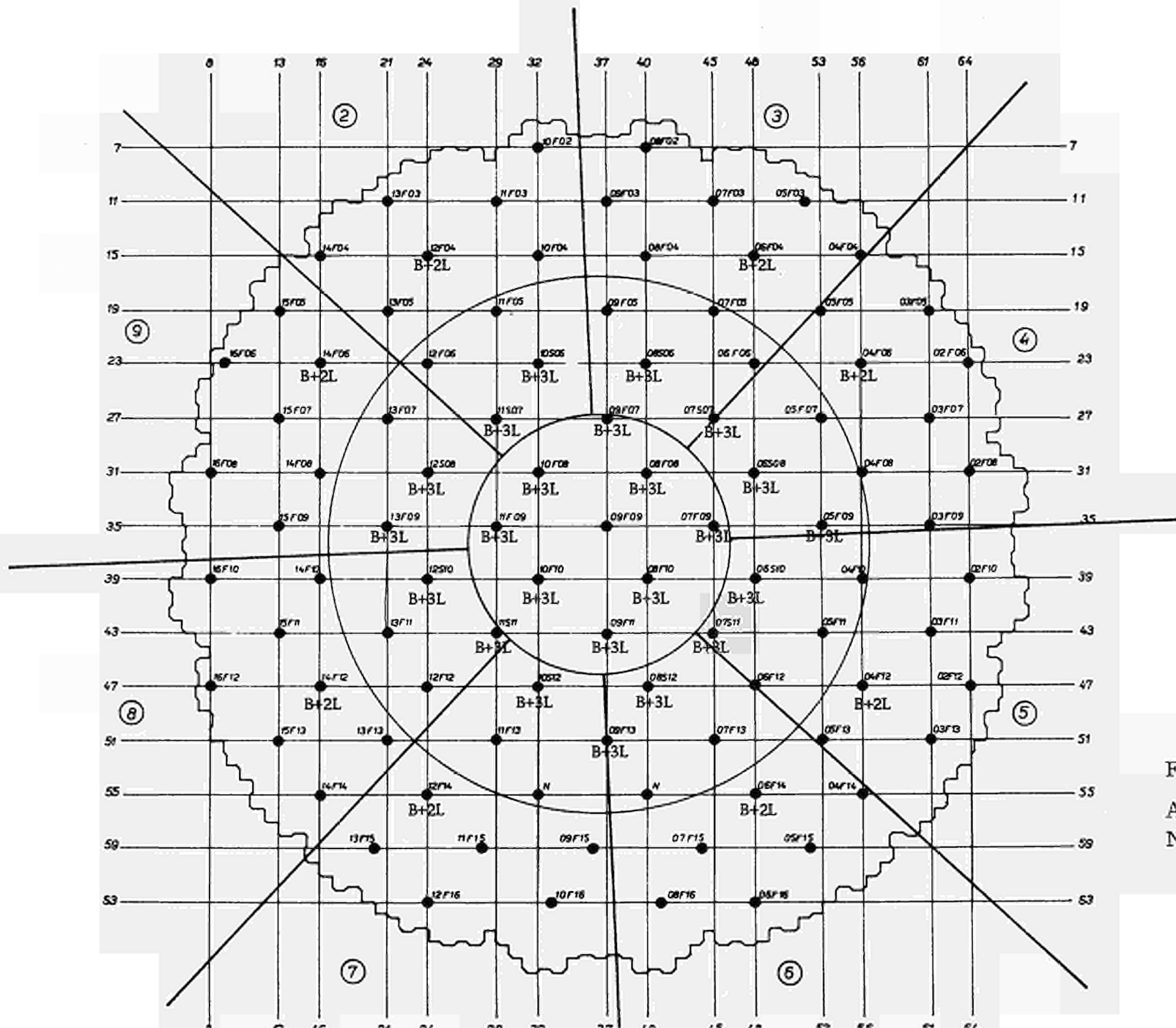


Fig. 3.0, II
Absorber pattern
No. 2

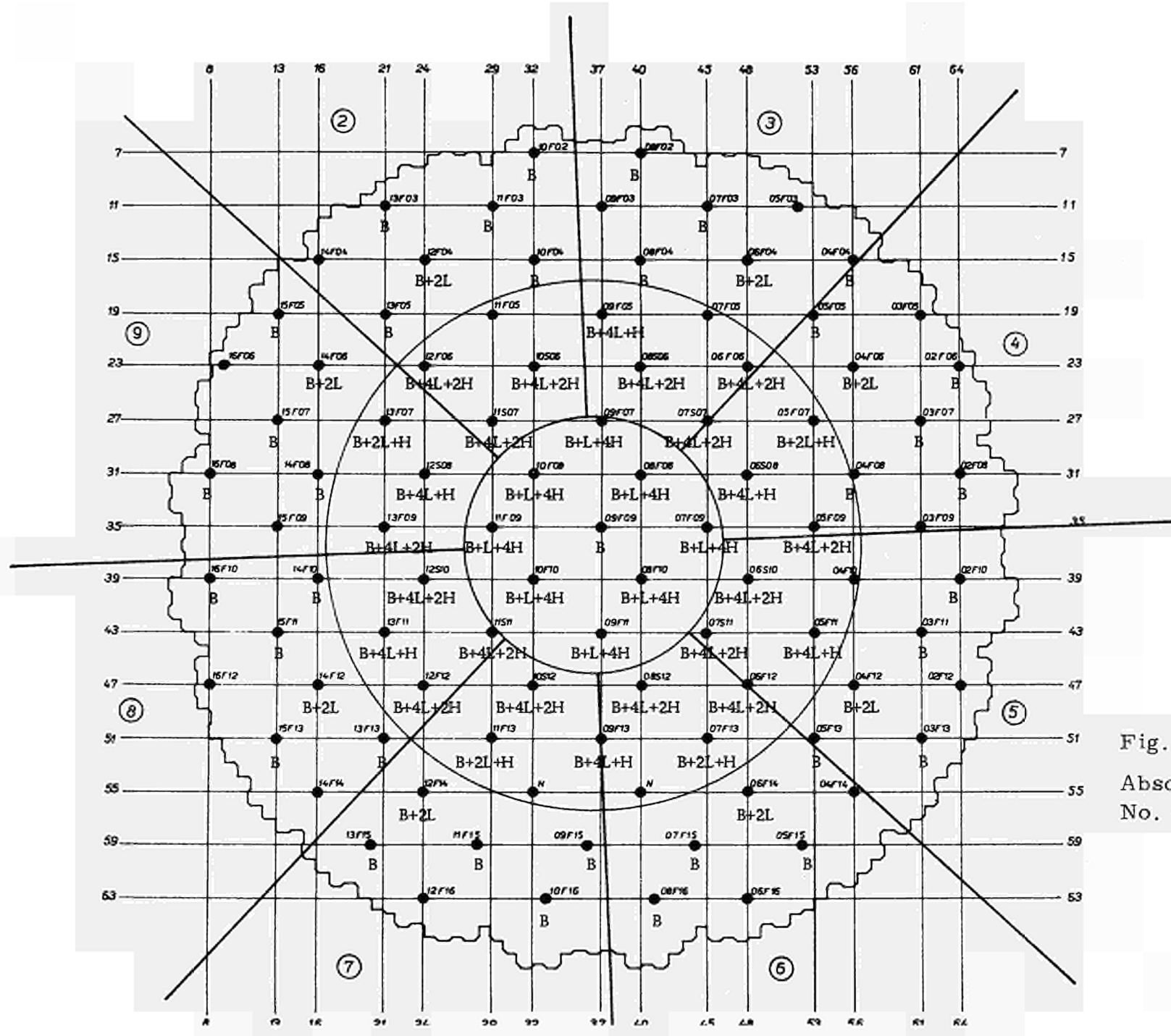


Fig. 3.0, IV
Absorber pattern
No. 4

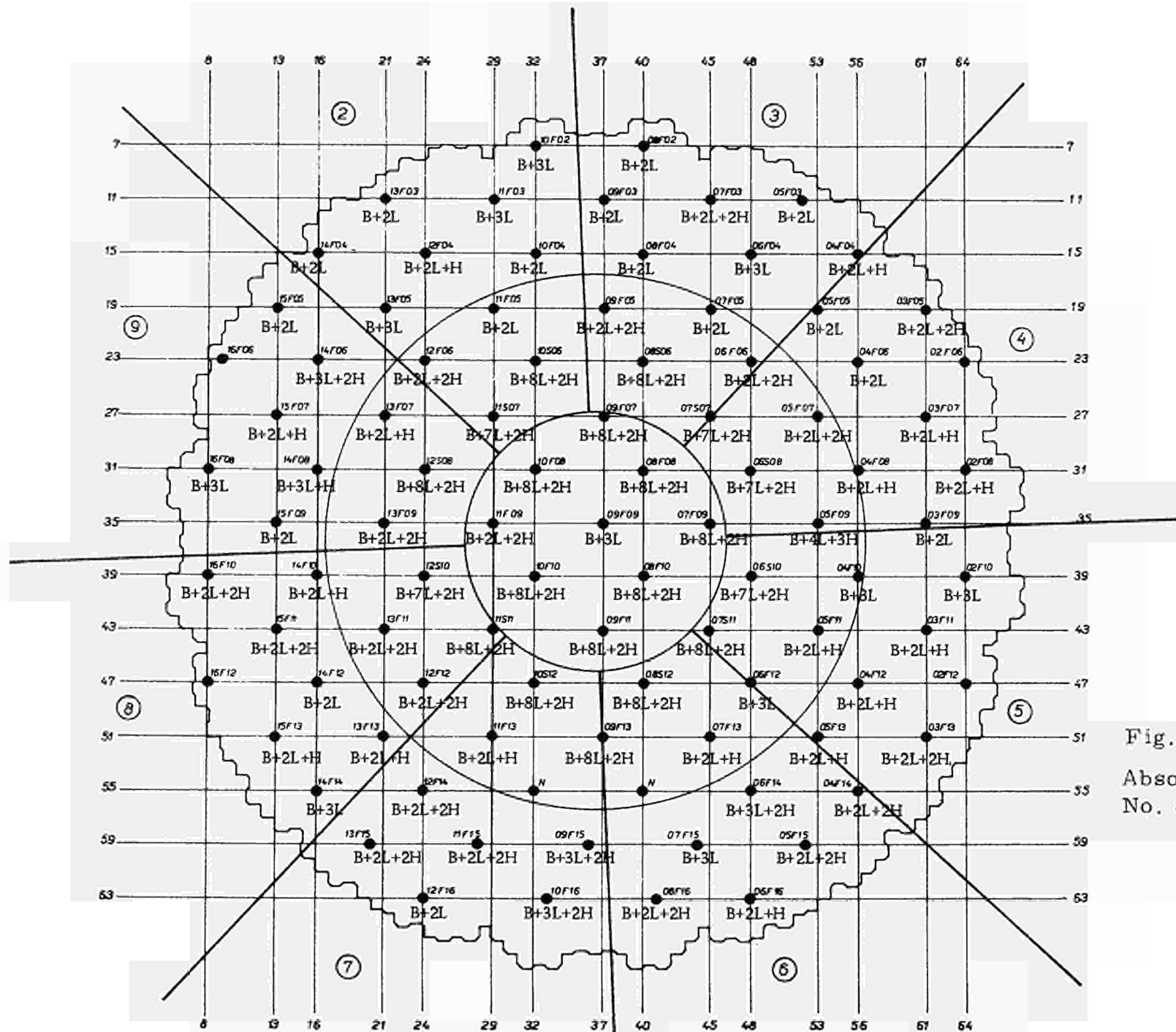


Fig. 3.0, VIII
Absorber pattern
No. 8

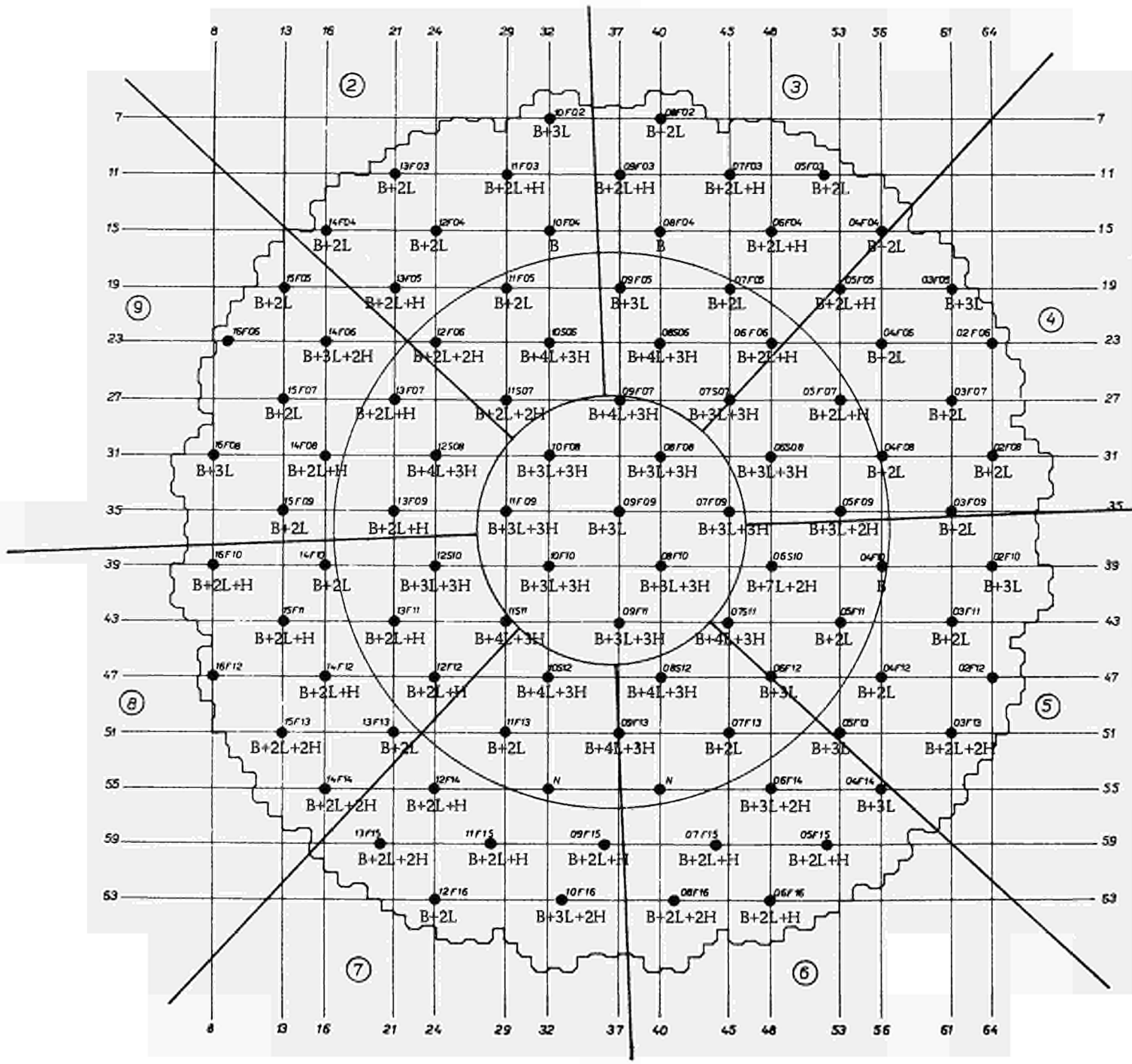


Fig. 3.0, IX
 Absorber pattern
 No. 9

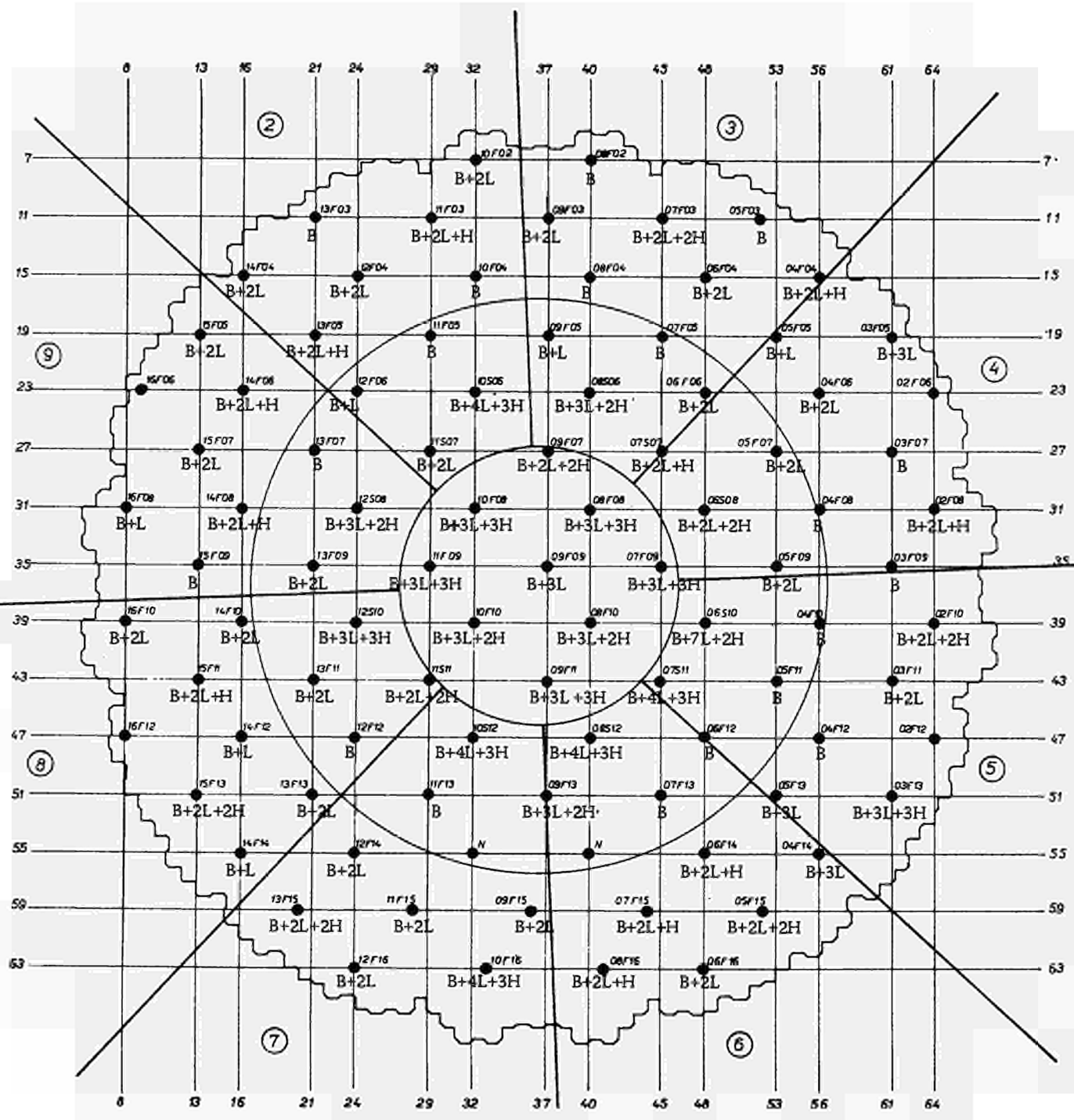


Fig. 3.0, X
Absorber pattern
No. 10

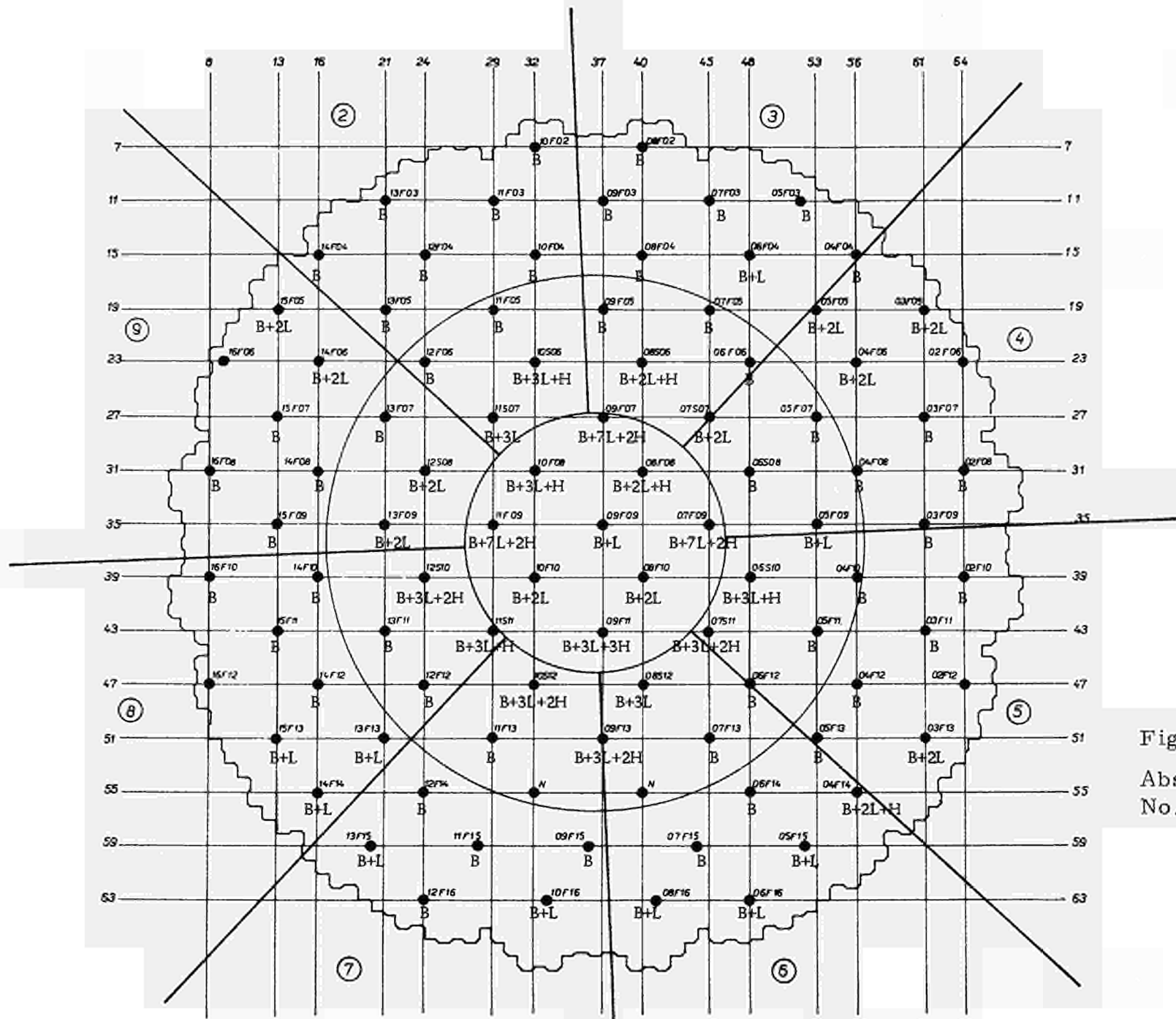


Fig. 3.0, XII
Absorber pattern
No. 12

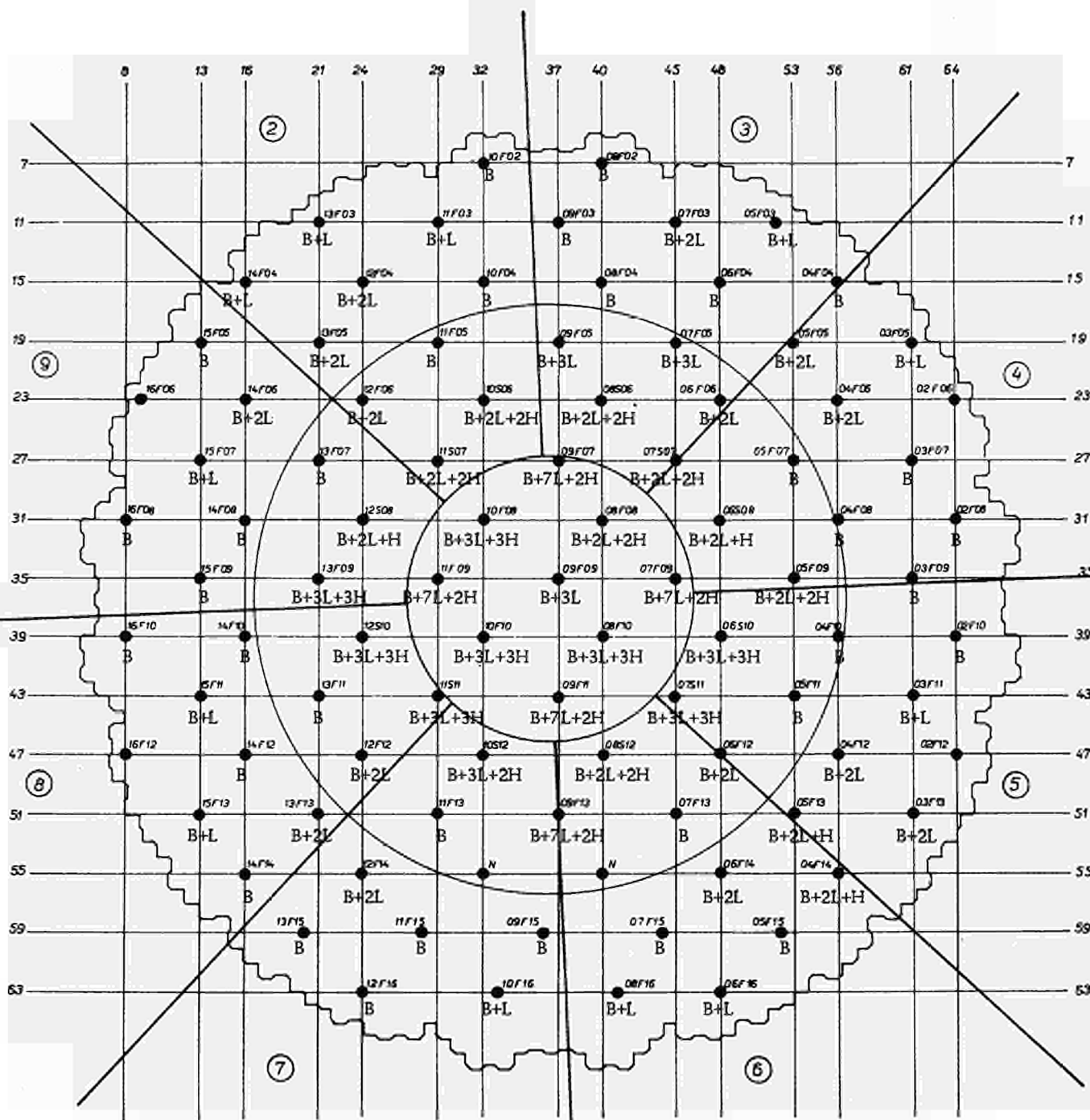


Fig. 3.0, XIV
Absorber pattern
No. 14

x Measurements performed on channel 09 F 09 IZ

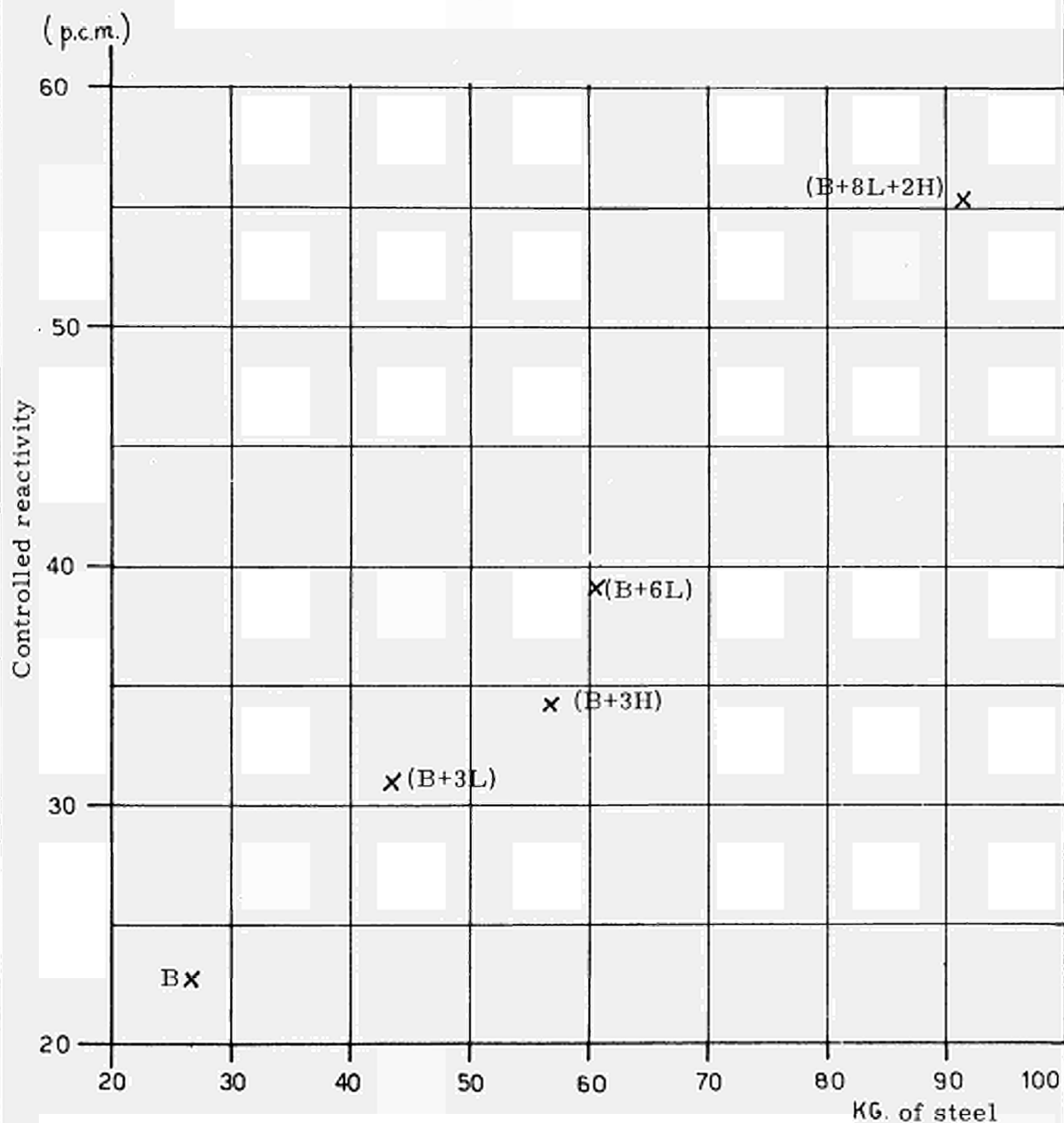


Fig. 3.1,1 Experimental results of absorber calibrations performed at 1100 MWD/T.

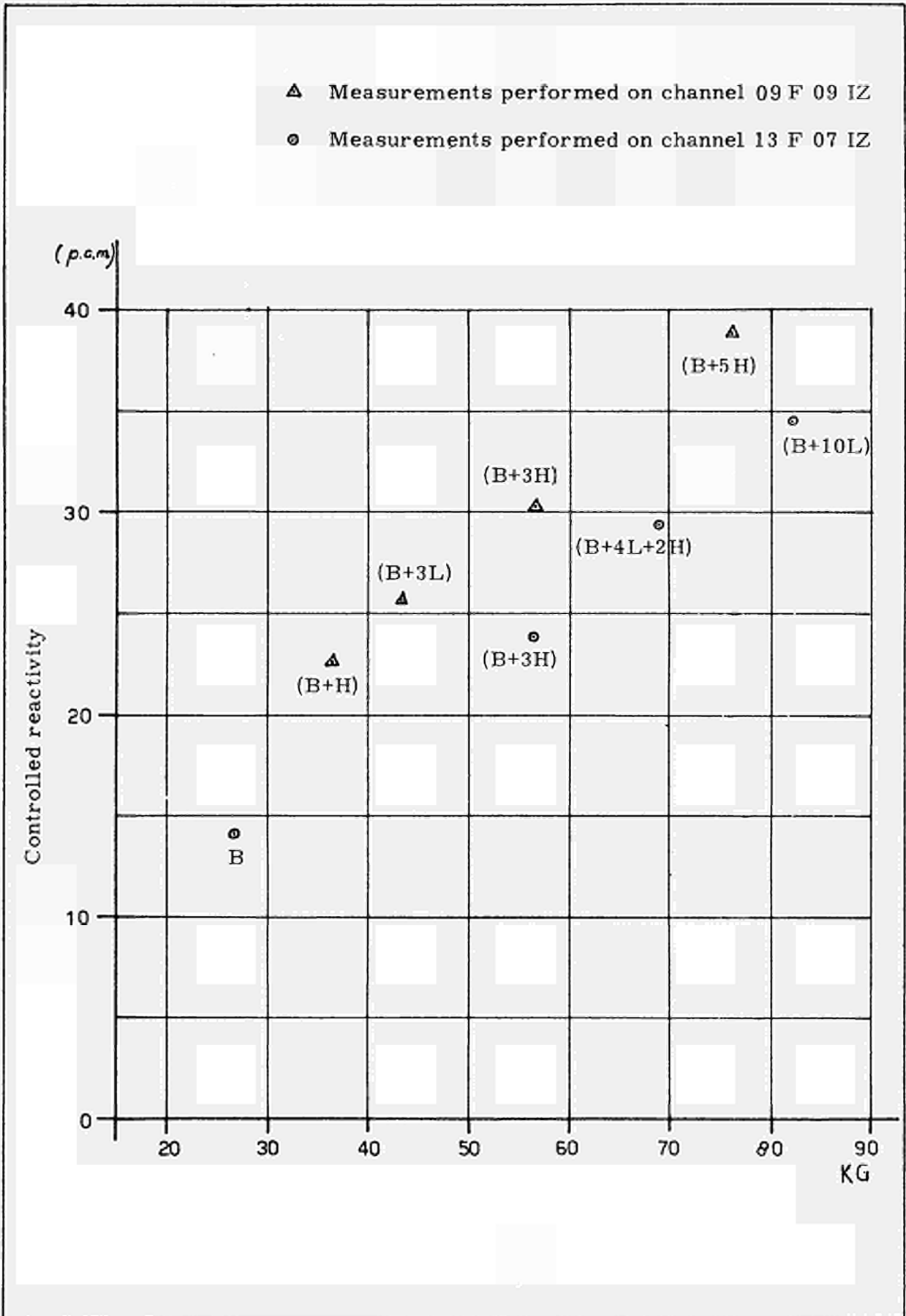


Fig. 3.1 II Experimental results of absorber calibrations at 1500 MWD/t.

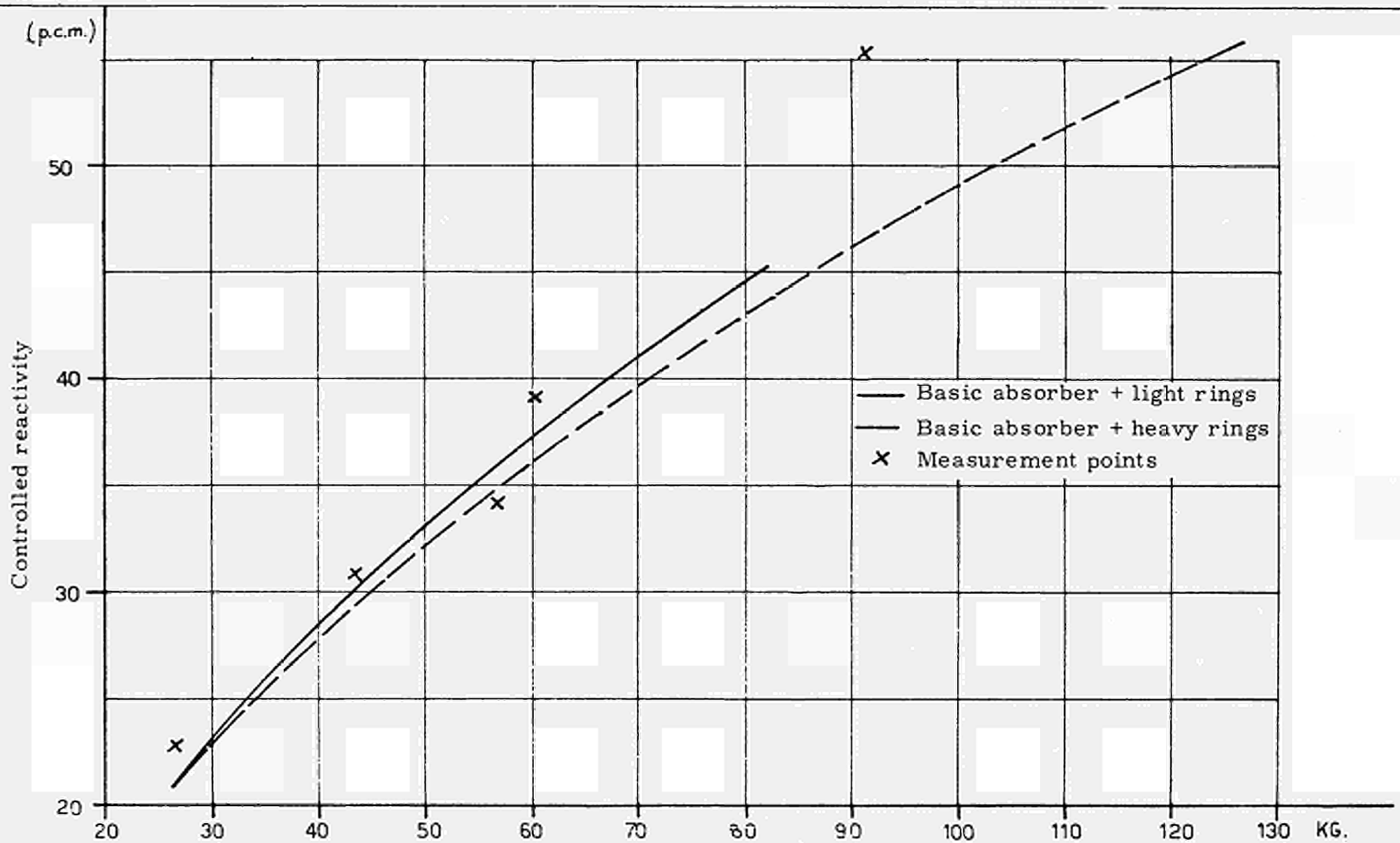


Fig. 3.2,1 Theoretical-experimental comparison of results of absorber calibration performed at 1100 MWD/T.

4.0 DESCRIPTION OF THE METHOD USED FOR ROD CALIBRATION UNDER REDUCED-TEMPERATURE ISOTHERMAL CONDITIONS

The method used to calibrate the control rods during operation utilizes the xenon-induced reactivity transient following a rapid power reduction from rated value to a few kW. After a power variation, the amount of reactivity absorbed by xenon first increases and then decreases slowly to zero.

During the first 8-10 hours after shutdown, the xenon effect combined with the temperature effect generally renders the reactor subcritical notwithstanding the complete withdrawal of all the control rods.

Subsequently, as xenon decays, the reactor becomes critical again; from this moment onwards, the reactivity gradually released as a result of xenon decay is balanced by insertion of the rods to be calibrated (see. Fig. 4.0.1). If, during this balancing stage, the rods are periodically withdrawn for a few minutes from the height corresponding to z withdrawal cycles to the height of $z + \Delta z$ cycles thus permitting the reactor to diverge temporarily, then from the measurement of the doubling time we may derive (through a, appropriate correlation formula) the reactivity $\Delta \rho$ released as a result of rod withdrawal by Δz cycles from height z . After every measurement of the doubling time, the reactor is balanced again by means of the rods.

These measurements, repeated at different values of z , provide the incremental ratios $(\Delta \rho / \Delta z)_z$. Then the calibration curve, that is, the rod-controlled reactivity versus withdrawal cycles, is obtained by integrating the above-mentioned function. It should be noted that the measurement is performed in isothermal conditions, but at a lower temperature than the operating temperature, so that it is necessary to extrapolate the results to the nominal reactor conditions.

4.0.1 Processing of experimental data

Processing of the experimental data is based essentially on the correlation between doubling times and reactivity so that it is necessary to do some preliminary work to determine such correlation with reference to the irradiation conditions existing in the core at the time of the measurement. On the basis of these preliminary data it is then possible to proceed with the determination of the control rod calibration curves.

The following three paragraphs describe the method adopted to determine the correlation between reactivity and doubling times, and the data processing performed to obtain the rod calibration curve and the evaluation of the xenon transient.

4.0.2 Correlation between doubling times and reactivity

It is known that this correlation is computed on a theoretical basis on a fresh core, with due consideration being given to the various groups of delayed neutrons originated by fission. As irradiation increases, the composition of fissile isotopes in the fuel changes, with a gradual depletion of U-235 and enrichment in Pu-239 and Pu-241. Since the groups of delayed

neutrons produced by the fission of these last two isotopes differ from one another and from those produced by U-235 both in magnitude and in the decay constant, the correlation between reactivity and doubling time changes as fuel irradiation increases.

It has been demonstrated theoretically (see ref. 53, para.1) that it is possible to calculate a corrective factor γ of the correlation between doubling time and reactivity for a fresh core; this factor is very nearly the same, for a given irradiation level, over the whole range of doubling times of interest for the measurement.

To compute the factor γ which is representative of the whole reactor, we proceed as follows:

- a. The reactor is subdivided ideally in "n" zones in cylindrical symmetry, and for each zone the fissile isotope contents of the various species are calculated and the value of γ_{RZ} is determined according to the procedure described in ref. 53.
- b. Since the flux levels are always extremely low during the measurements and it is thus not possible to find out the flux shape with the normal instrumentation, the flux shapes are derived by means of the theoretical calculation methods described in paragraph 4 of ref. 53.
- c. These flux shapes can then be used to weigh the zone factors γ_{RZ} with respect to the square of the flux, and thus to obtain the γ factor representative of the reactor as a whole.
- d. By special studies it was then demonstrated that the variation of the flux shape, which follows a rod movement during calibration and the decay of xenon, determines a variation in the γ factor by about 1% at the most.
- e. Ref. 53 (pages 12 and 47) provides a comparison between the values of the γ factor obtained from models having a different number of zones. From the study conducted in the above-mentioned report it appears that a point model of the reactor with an irradiation equal to the average core irradiation -- that is, not weighted with respect to the square of the flux -- provides a reactor factor γ which differs by only 1.6% from the corresponding value obtained with a 112-zone model. Therefore, it appears reasonable to consider the γ factor referred to the average core irradiation accurate enough for the processing of the experimental data.

4.0.3 Determination of the calibration curves

The experimental data are processed as described below.

- a. Each doubling-time measurement is preceded and followed by a certain number of balancing points measured experimentally. For each measurement, a series of statistical interpolations is performed between the preceding and following balancing points. Starting from the

interpolation performed between the point immediately preceding and the point immediately following each individual measurement, the interpolations are then extended, wherever possible, to include the balancing points related to other preceding and following measurements. These interpolations are performed by means of polynomials of different orders between the 1st and the 9th.

For each point of doubling-time measurement it is thus possible to determine (by means of the statistically more reliable polynomial) the position that the rods would have assumed to balance the reactor if they had always exactly compensated the xenon transient.

- b. Knowing the position $(z + \Delta z) = z^*$ (see Fig. 4.0.I) which the rods occupied at the time of the doubling-time measurement and the position to which they would move to keep the reactor balanced if they had compensated the xenon transient exactly, we can determine the control rod capacity coefficient defined as

$$\alpha(z) = \left[\frac{\Delta \rho}{\Delta z} \right]_z$$

where:

$\Delta \rho$ = reactivity corresponding to the measured doubling time;
 Δz = movement of the rods from the balancing position z .

- c. Since the measurement of the doubling time takes several minutes during which the rods, if they had continually compensated the xenon transient, would have moved from position z' to position z'' , in consideration of the narrowness of the interval $(z'' - z')$, it is believed sufficiently approximate to identify the control rod capacity coefficient with the derivative of the calibration curve at the point $(z'' + z')/2 = z$.
- d. The curves of the capacity coefficients $\alpha(z)$ related to the calibrated rods are then plotted by statistical interpolation of the measurement points.
- e. The rod calibration curve is then determined by integration of the function $\alpha(z)$.

4.1 Experimental measurements

The 100 control rods in the reactor (see Fig. 4.1.I) are subdivided into the following groups:

1. 20 sector rods, automatically controlled, having the function of maintaining the average gas temperature at the channel outlets constant in each of the nine sectors into which the core is subdivided.

2. 22 group B general rods used to follow reactivity transients that are not compensated or that can be compensated in practice by the sector rods and absorbers.
3. 46 group A general rods, normally all out.
4. 12 safety rods, for added protection, which are normally withdrawn even during reactor shutdown.

4.1.1 Results of the experimental measurements

a) Calibration at 128 MWD/T

During commissioning, the group B general rods were calibrated by means of the air-poisoning technique, with the sector rods positioned at 286 withdrawal cycles.

To demonstrate the validity of the xenon technique as a means to calibrate the control rods during operation, the group B general rods were calibrated between 155 and 228 withdrawal cycles with the sectors rods completely withdrawn.

A comparison of the results obtained with the two techniques would have been more meaningful if the average reactor irradiation and the position of the sector rods had been the same in both cases. This was not possible for operating reasons but, nonetheless, the good agreement between the results obtained in the two cases (see Fig. 4.1.1.I) sufficiently confirms the validity of the rod calibration method based on the xenon-decay transient.

b) Calibration at 1100 MWD/T

The initial purpose of this measurement was to calibrate the sector rods between 435 (complete withdrawal) and 200 cycles, and then the B rods between 200 and 286 cycles (see Table 4.1.III).

Fig. 4.1.1.II shows the curve of partial sector-rod calibration with the B rods withdrawn. With regard to the group B rods we note that, since they were calibrated in the range between 200 and 286 withdrawal cycles, in order to determine the related absolute calibration curve, it has been necessary to evaluate the reactivity controlled by this group of rods in correspondence of the first point, that is, at 286 cycles. For this purpose, after having obtained the two curves representing the variations in reactivity absorbed respectively by the sector rods and by the B rods as a function of the withdrawal cycles, we plotted the values as a function of the time lapse from the beginning of the calibration and geometrically joined the two resulting curves, thus obtaining the absolute value of reactivity absorbed by xenon (see Fig. 4.1.1.VI).

The difference between the reactivity absorbed (absolute value) by xenon at the time of criticality with all the rods out and at the time when the B rods were at 286 cycles (and the sector rods at 276 cycles) gives the absolute value of reactivity absorbed by the two groups of rods in those positions. Hence, the curve in Fig. 4.1.1.III was plotted; then, assuming that the sector rods at 276 cycles absorb about the same amount of reactivity both when the B rods are all out and when they are at 286 cycles, we obtained by subtraction the absolute value of reactivity absorbed by the B rods alone at 286 withdrawal cycles. The whole curve was then normalized on this point (see. Fig. 4.1.1.IV).

With regard to the corrective factor χ for the correlation between doubling time and reactivity, we simply used the factor corresponding to the average reactor irradiations, that is, 0.857, instead of the factor obtained as an average of the zone χ_{RZ} 's weighted over the square of the flux because, as stated in paragraph 4.0.2, the difference between the χ values obtained with the two methods is practically negligible.

c) Calibration at 1425 MWD/T

Fig. 4.1.1.II shows the new calibration curve for the sector rods between 435 and 272 withdrawal cycles, with the B rods withdrawn.

Fig. 4.1.1.III gives the sum of the reactivities controlled by the B rods (between 435 and 200 cycles) and by the sector rods positioned at mid height.

Fig. 4.1.1.IV shows the reactivity controlled by the B rods alone in the assumption, as a first approximation, that the semi-inserted sector rods always absorb the same amount of reactivity (695 p.c.m.), whatever the position of the B rods.

Fig. 4.1.1.V represents the sum of reactivities controlled by the sector rods (between 272 and 249 cycles) and by the B rods stationary at 200 cycles. Also in this case, in order to evaluate the absolute value of the calibration curve, it was necessary to calculate the reactivity absorbed at the first point, that is, at 249 withdrawal cycles. The procedure was similar to the one described in the preceding paragraph.

4.2 Description of the method followed for the theoretical calibration of the sector rods and related results

Since it was not possible, for various reasons, to calibrate the control rods experimentally with the reactor in nominal conditions, the variation in reactivity absorbed by the rods at different irradiation levels was evaluated on a theoretical basis by passing from the experimental calibration conditions (isothermal reactor at 180°C) to normal operating conditions (average weighted graphite temperature at 310°C).

For each of the theoretical calibrations, we assessed the characteristic parameters of the zones into which the core was ideally subdivided for

the purpose of the calculations (see Fig. 4.2.I), namely, the average irradiation, average temperature, average specific power of the zone, absorber pattern, etc. These parameters, appropriately processed, were used as input data for the system of computer programs.

For each situation of interest two FATE (a synthesis of the PDQ02, PIF- FERO and FTD2 programs as mentioned in the preceding paragraph 3.2) runs were performed, one with the sector rods inserted at about mid height, and the other with the rods all out. The difference between the eigenvalues obtained by the FTD2 code for the two cases represents the reactivity absorbed by the semi-inserted sector rods.

These calculations were repeated for various irradiation levels and absorber patterns, both with the reactor isothermal at zero power and reduced temperature, and with the reactor in nominal operating conditions, as shown synthetically in tables 4.2.I, II and III.

4.3 Comparison of calculated and experimental results in isothermal conditions

For the purpose of comparing the calculated results with the experimental ones, the values of the sector rod capacity at mid height are tabulated in table 4.3.I, referred to the cases dealt with on a theoretical basis and experimentally. As will be noted from this table, notwithstanding some difference between the absolute calculated and experimental values, there is an agreement in the trend of the rod capacity variation as a function of irradiation. In particular, it may be noted that:

1. The calculated values are constantly overrated by about 19% with respect to the experimental values.
2. The percent reduction in rod capacity from a fresh core to an irradiated core is practically the same, both in the theoretical and in the experimental analyses, in every case considered, namely -27.3% versus -27.7% at 1100 MWD/T, and -9.8% versus -9.6% at 1525 MWD/T.
3. The results justify the use in hot conditions -- with appropriate adjustments -- of the calculation method adopted in cold conditions for the determination of the sector rod worth. It is known that there are no experimental calibration curves for the Latina core evaluated under nominal operating conditions.

With regard to the variation in rod worth with irradiation, we may comment as follows:

1. The reduction in sector rod worth in cold condition which occurred between the first and second calibration can be explained qualitatively if allowance is made for the greater hardness of the spectrum (owing to the increased irradiation, the increased absorber weight and the effects of the positive moderator temperature coefficient. Indeed, the modera-

tor temperature coefficient is a monotonic function which increases with irradiation so that, at the time of the second calibration, the central zone containing the sector rods was characterized by a higher positive temperature coefficient than that of the peripheral region. In going from nominal hot conditions to cold calibration conditions, this circumstance determined a relative reduction in the neutron flux in the zone containing the sector rods.

This is possibly the reason for the variation in B-rod worth between the first and second calibrations.

2. The increase in sector rod worth which occurred between the second and third calibrations can be explained qualitatively if allowance is made for the lighter absorber weight in the whole reactor and the reduced irradiation in the zone affected by the sector rods (from 1341 to 1208 MWD/T) owing to accelerated fuel discharge only in the central flattened area where the sector rods are located.

With reference to the preceding remarks concerning the calibration of group B rods, it may be noted that the average local irradiation in the areas surrounding the rods themselves increases from 1116 to 1532 MWD/T between the second and third calibrations, whereas the twenty absorbers nearest the B rods are lighter by more than 53 kg of steel rings.

These conflicting effects may explain the fact that the B-rod worth remained practically constant between the second and third calibrations.

4.4 Criterion followed to obtain semi-empirical calibration curves under nominal operating conditions

Tables 4.2.I and II and Fig. 4.4.1 give the results of the calculations for the reactivity absorbed by the sector rods at 302 withdrawal cycles at zero power and at nominal power.

The ratios of the reactivity absorbed at nominal power to that absorbed at zero power give the theoretical factors for conversion from cold to hot conditions as a function of irradiation.

TABLE 4.1.I : Reactor conditions at the time of power reduction, related to the three calibrations

DATE	11. 1. 1964	14. 5. 1965	31. 3. 1967
- Average core irradiation, MWD/T	128	1100	1425
- Thermal power, MWt	440	750	730
- Max fuel temperature, C	430	444	462
- Average inlet gas temperature, C	175	180	185
- Average outlet gas temperature, C	371	385	391
- Coolant pressure, kg/cm ²	11. 3	13. 2	12. 4
- Blower speed, rpm	1550	2250	2250
- Average sector rod position, meters	4. 00	4. 25	3. 92
cycles	282	292. 28	272
- Average irradiation in sector rod area, MWD/T	250	1341	1208
- Group "A" general rod position	All out	All out	All out
- Group "B" general rod position, withdrawal meters	4. 43	6. 80	6. 70
cycles	303. 1	392	385
- Average irradiation in rod "B" area, MWD/T	126	1116	1532
- Safety rod position	All out	All out	All out
- Absorber pattern	No. 2-3	No. 8	No. 12
- Time of beginning of power reduction	22. 30	22. 45	22. 25

TABLE 4.1.II: Reactor conditions at the beginning of measurements relating to the three calibrations

- Thermal power	50	10	10	kWt
- Max fuel temperature	150	218	229	°C
- Average fuel temperature	150	212	222	°C
- Max graphite temperature	150	209	219	°C
- Average graphite temperature	150	197	208	°C
- Average inlet gas temperature	150	190	200	°C
- Average outlet gas temperature	150	202	214	°C
- Coolant pressure	-	10.5	10.5	kg/cm ²
- Blower speed	500	500	500	rpm
- Position of all rod groups	All out	All out	All out	-
- Time of beginning of 1st measurement	15.05	13.46	9.00 (1.4.67)	-

TABLE 4.1.III : Sequence of doubling-time measurements

I = 128 MWD/T				I = 1100 MWD/T				I = 1425 MWD/T			
Sector rod withdrawal cycles	Rod "B" withdrawal cycles	No. of doubling time measurements	Time required	Sector rod withdrawal cycles	Rod "B" withdrawal cycles	No. of doubling time measurements	Time required	Sector rod withdrawal cycles	Rod "B" withdrawal cycles	No. of doubling time measurements	Time required
All out	228 + 155	7	8	435 + 200	All out	14	15	435 + 276	All out	7	11
				276	300 + 200	30	47	276	435 + 200	17	25
								272 + 249	200	7	13

TABLE 4.2.I : Isotherm reactor at 180°C - Zero power

Sector rods at 302 withdrawal cycles = 4.75 meters' withdrawal

Absorber patter No.	kg of loaded steel			Medium fuel irradiation MWD/T		DATE	No. of un- loaded fuel channel	Sector rod controlled reactivity (p. c. m.)
	Flattened flux area	Unflattened flux area	TOTAL	Sector rod con- trolled area (PDQ02)	Reactor			
2	997.68	302.34	1300.02	113	120	23.11.63	-	666
8	2962.99	2244.62	5207.61	1077	1039	18.3.65	206	535
10	2119.07	1942.23	4061.30	1463	1418	28.12.65	926	586
12	1745.41	1384.31	3129.72	1027	1425	31.3.67	2059	664

TABLE 4.2.II : Reactor at nominal operating power , temperature 310°C

Sector rods at 302 withdrawal cycles = 4.75 meters' withdrawal

Absorber patter No.	kg of loaded steel			Medium fuel irradiation MWD/T		DATE	No. of un- loaded fuel channel	Sector rod controlled reactivity (p. c. m.)
	Falttened flux area	Unflattened flux area	TOTAL	Sector rod con- trolled area (PDQ02)	Reactor			
2	997.68	302.34	1300.02	113	120	23.11.63	-	694
5	2773.23	1604.99	4414.22	523	516	19.5.64	-	737
7	3293.20	2175.59	5468.79	851	870	18.11.64	206	712
8	2962.99	2244.62	5207.61	1077	1039	18.3.65	514	723
9	2505.01	2125.28	4630.29	1203	1150	13.8.65	779	752
10	2119.07	1942.23	4061.30	1463	1418	28.12.65	926	799
12	1745.41	1384.31	3129.72	1027	1425	31.3.67	2059	788

TABLE 4.3.I

Reactor Irradiation (MWD/T)	0	1110	1425
Theoretical result (p.c.m. absorbed)	736 *	535	664
Variation from corresponding value for I = 0		-201	-72
Percentage of said variation from the corresponding value for I = 0		-27.3%	-9.8%
Experimental result (p.c.m. absorbed)	595	430	538
Variation from corresponding value for I = 0		-165	-57
Percentage of said variation from the corresponding value for I = 0		-27.7%	-9.6%
Absolute difference between theoretical and experimental results (p.c.m.)	141	105	126
Percentage of said difference as compared with the theoretical result	19.2%	19.6%	19.0%

* Value obtained by extrapolation, with a second-order curve, of the calculated values for 128 MWD/T (666 p.c.m.), 1100 MWD/T (535 p.c.m.) and for 1425 MWD/T (664 p.c.m.).

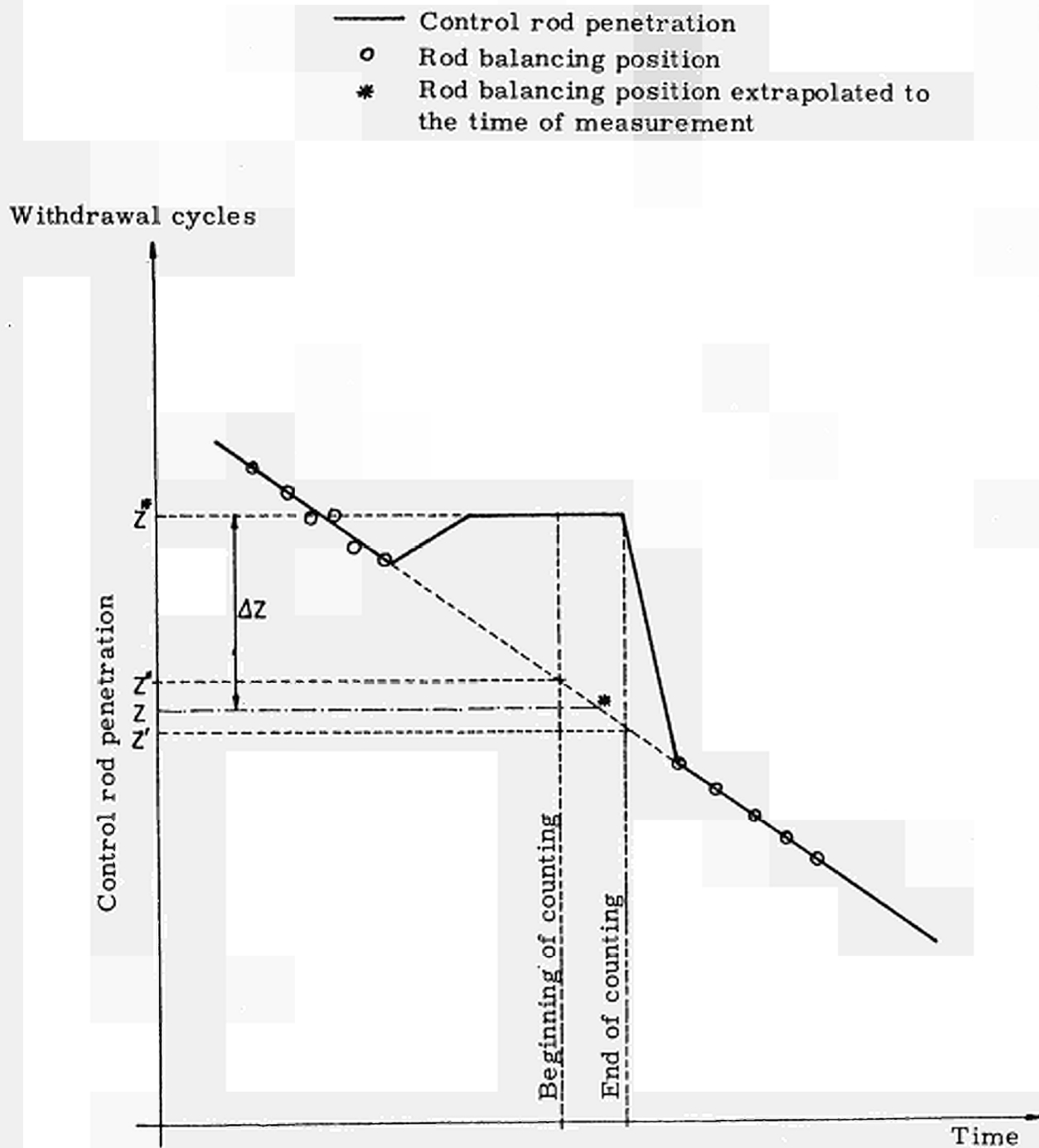


Fig. 4.0, 1 Reactor balancing scheme during calibration by Xe technique.

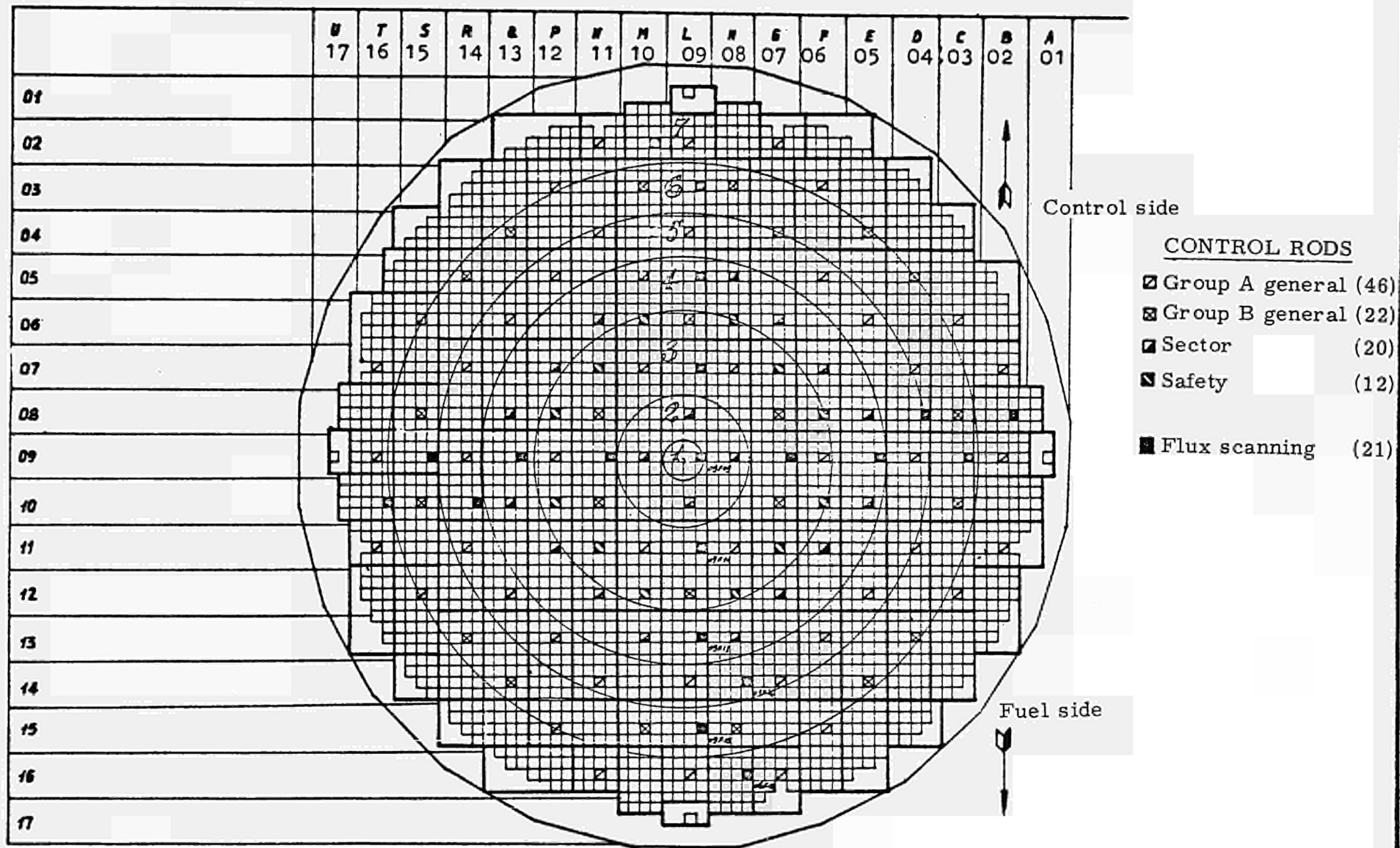


FIG. 4.1,I - Position of various control rod groups

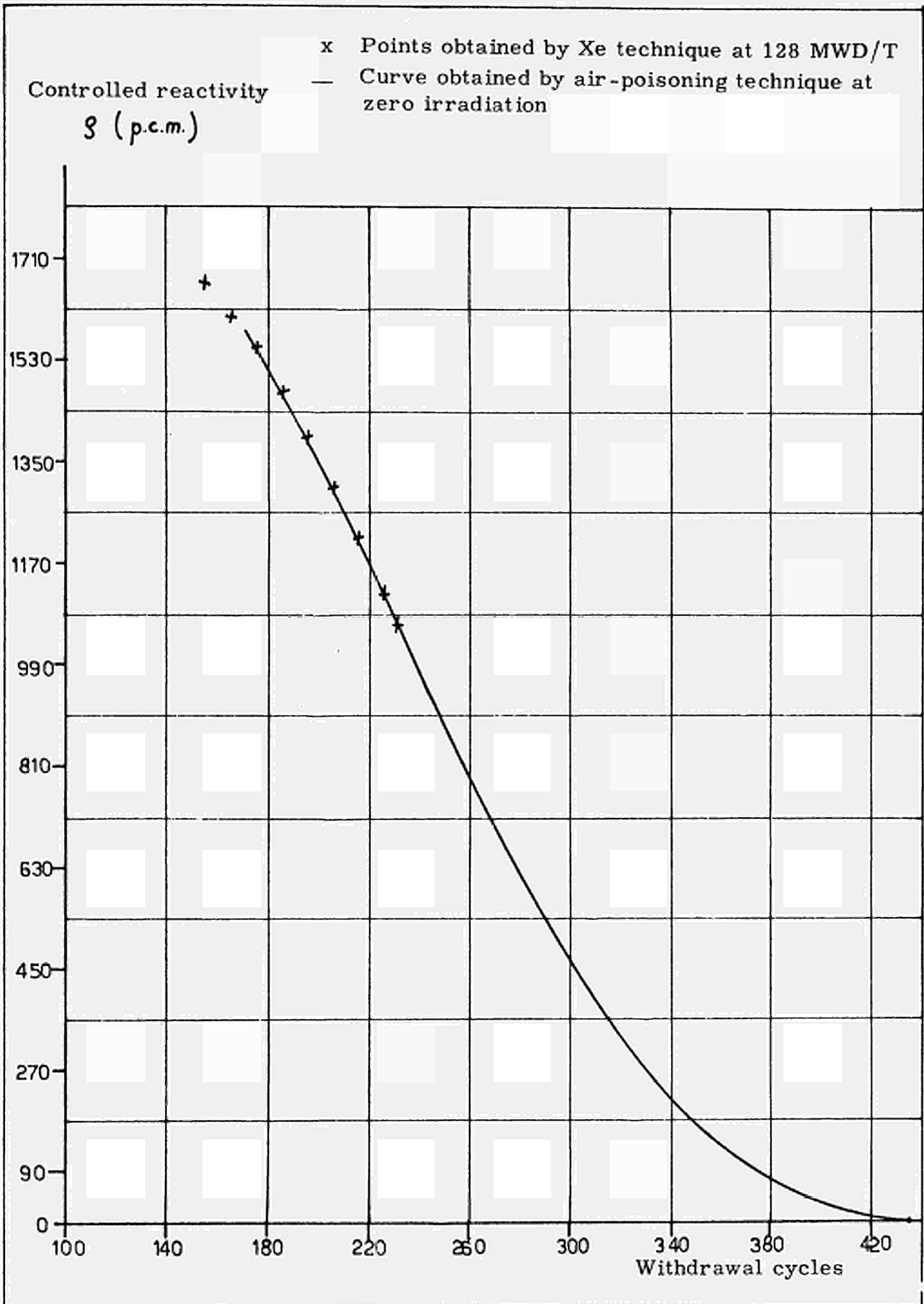


Fig.4.1.1,1 Comparison between group B rod calibration curves measured at zero irradiation (air-poisoning technique) and at 128 MWD/T (xenon technique).

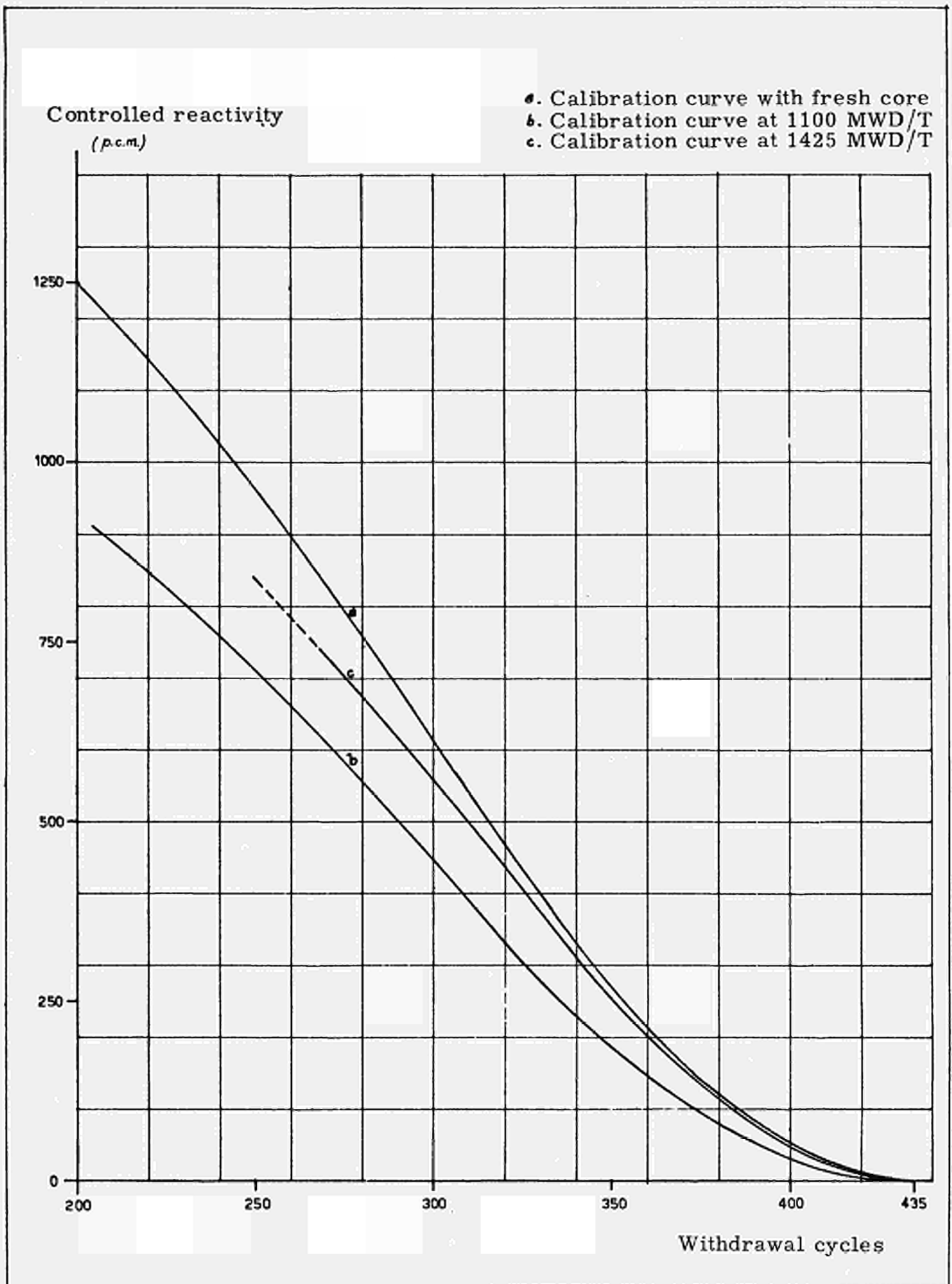


Fig.4.1.1,II Experimental calibration curves of the sector rods with the group B general rods all out.

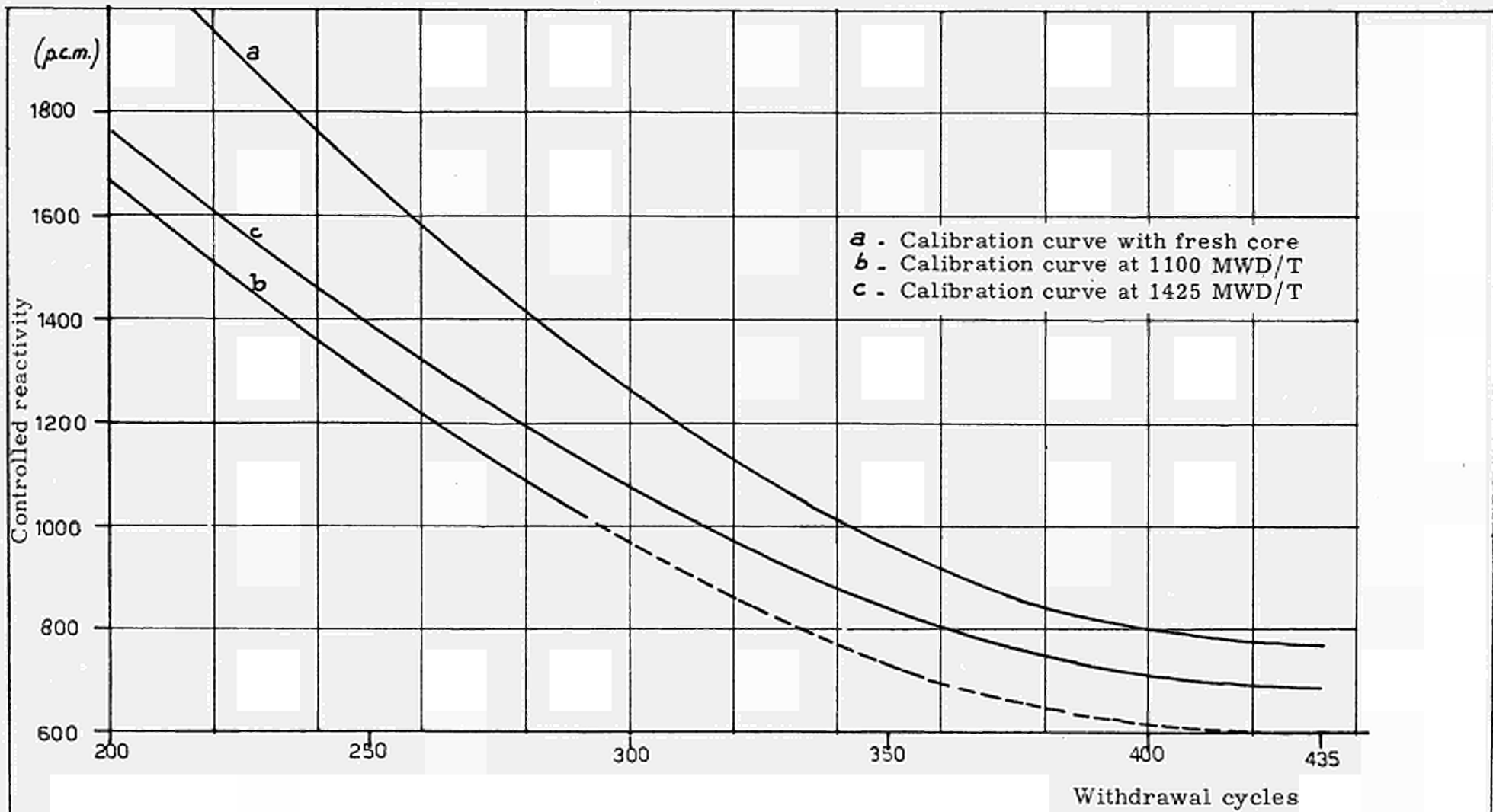


Fig.4.1.1, III Group B general rod calibration curve with the sector rods at mid height.

Controlled reactivity

1500 - (p.c.m.)

- a - Calibration curve for fresh core
- b. Calibration curve at 1100 MWD/T
- c. Calibration curve at 1425 MWD/T

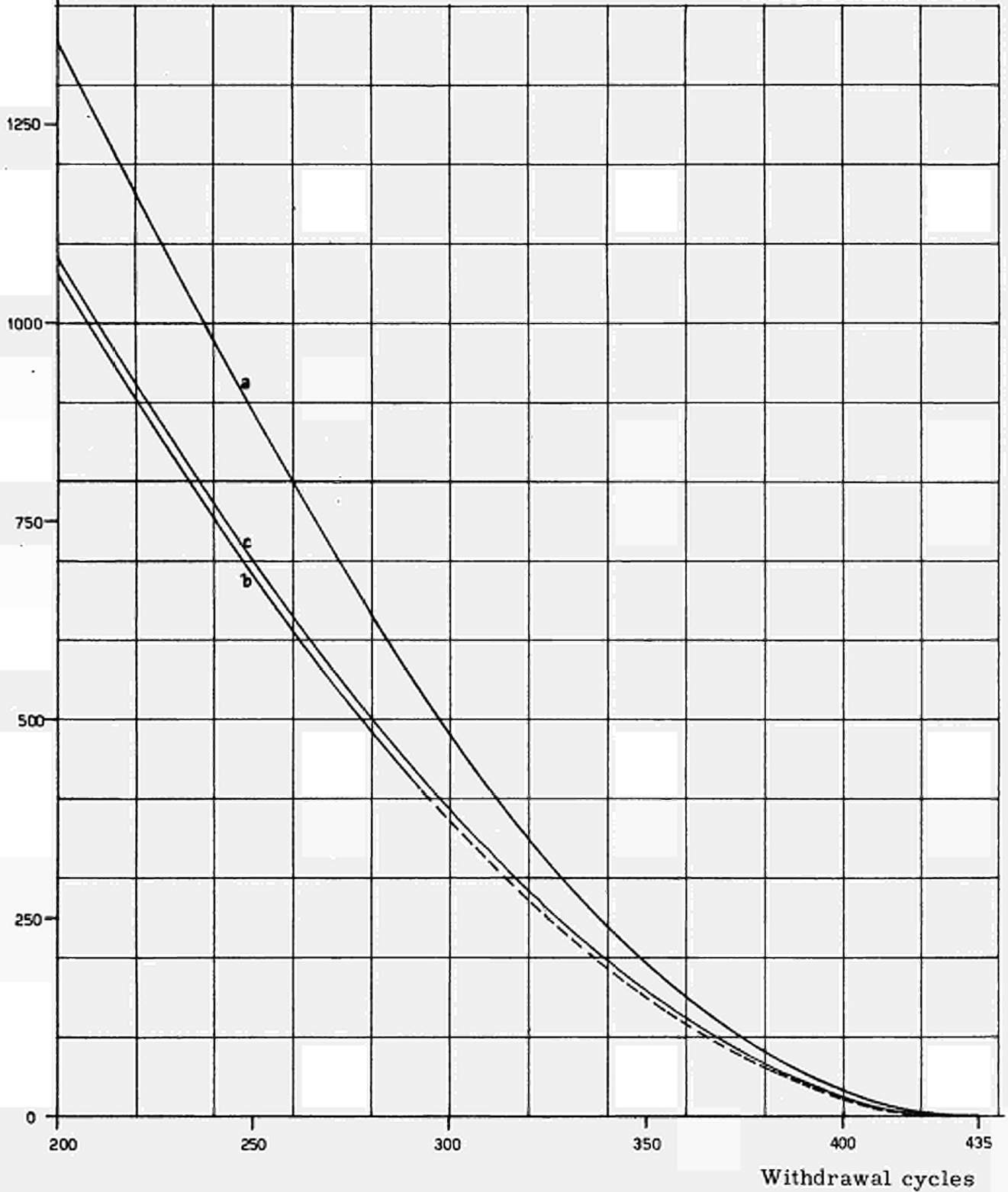


Fig.4.1.1,IV Group B general rod calibration curve net of reactivity controlled by sector rods at mid height.

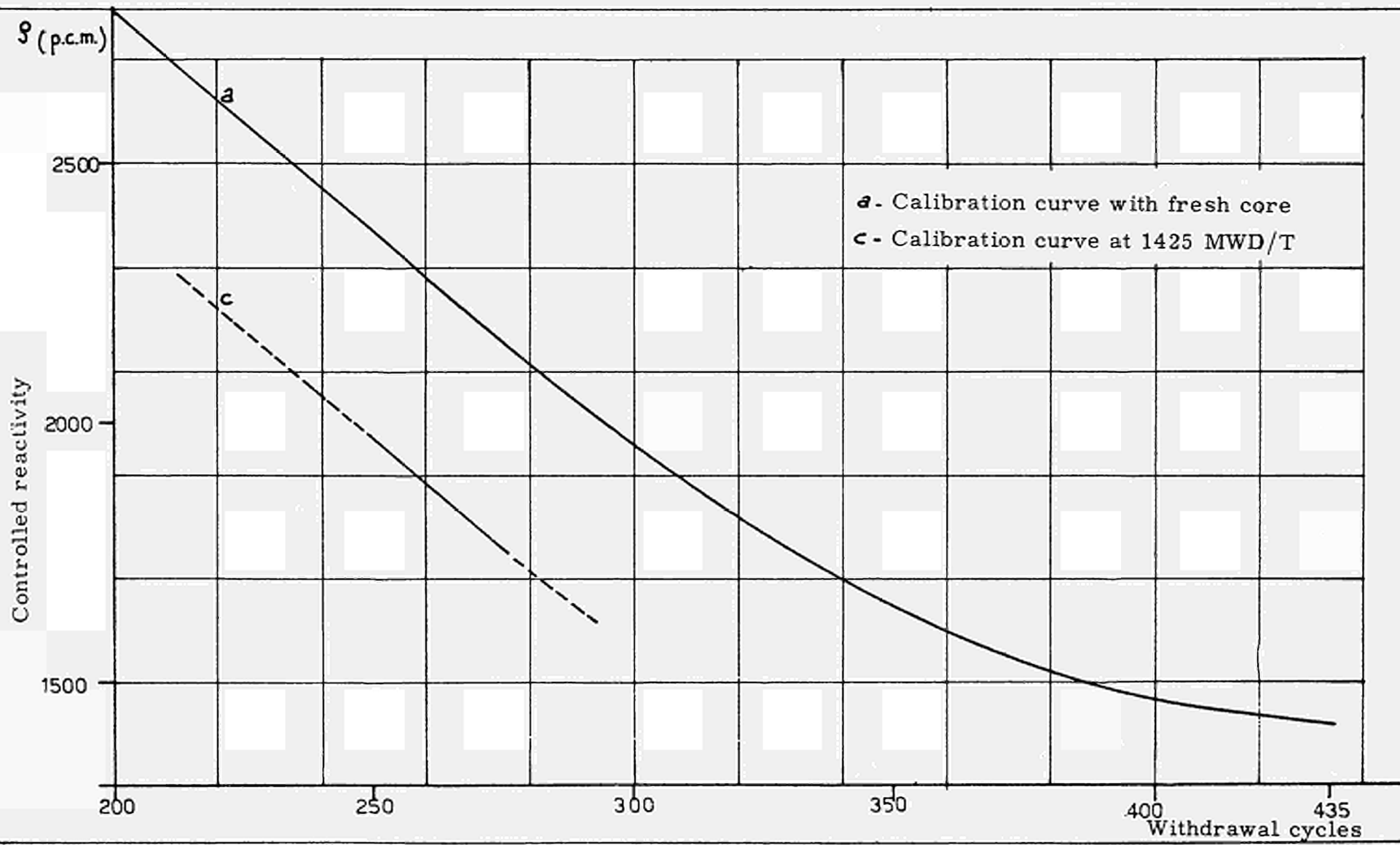


Fig.4.1.1, V Sector rod calibration curves with the group B rods at 200 withdrawal cycles.

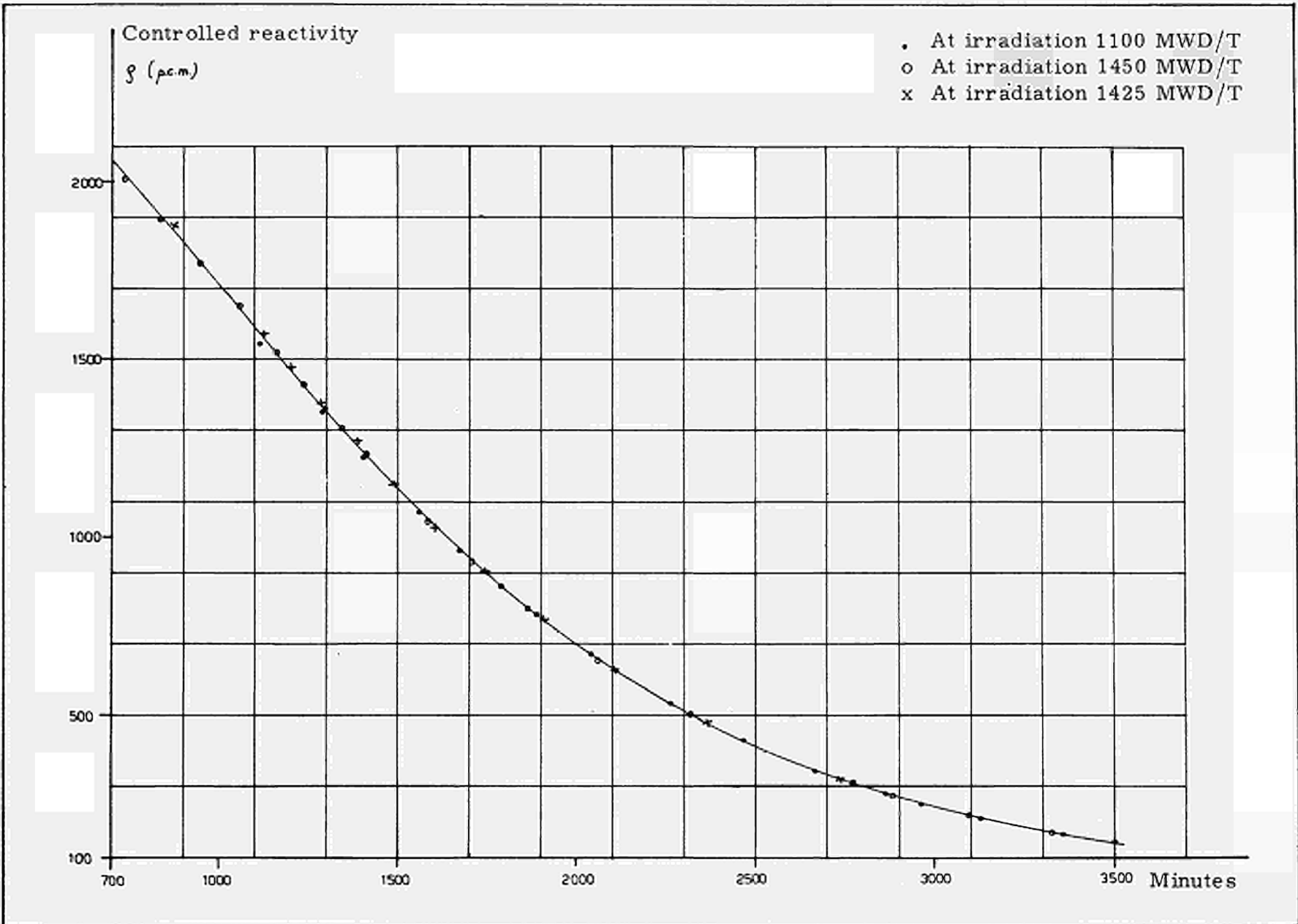


Fig.4.1.1 , VI Xenon-controlled reactivity as a function of time from reactor shutdown.

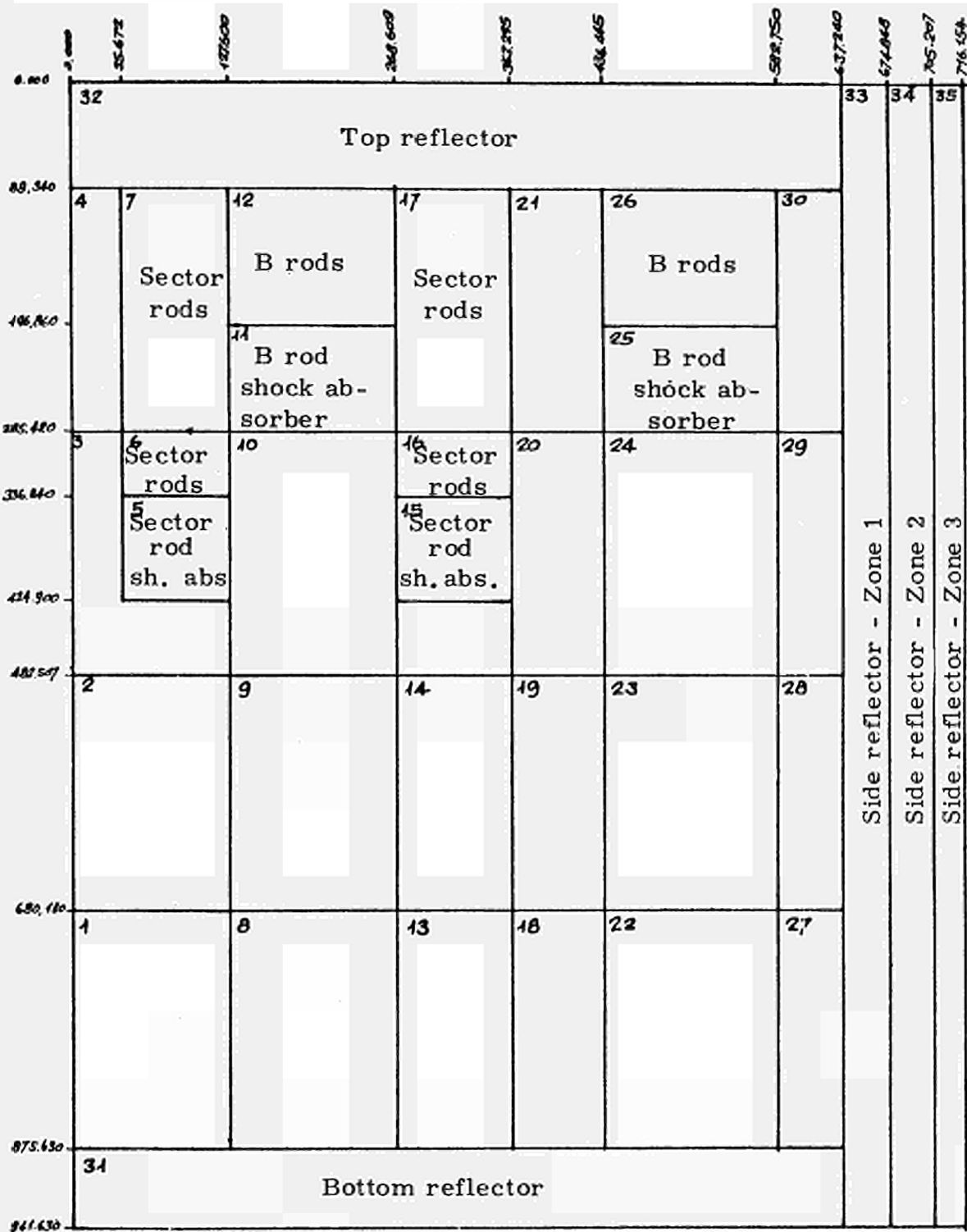


Fig. 4.2.1 Core zone subdivision assumed for the calculations

Controlled reactivity

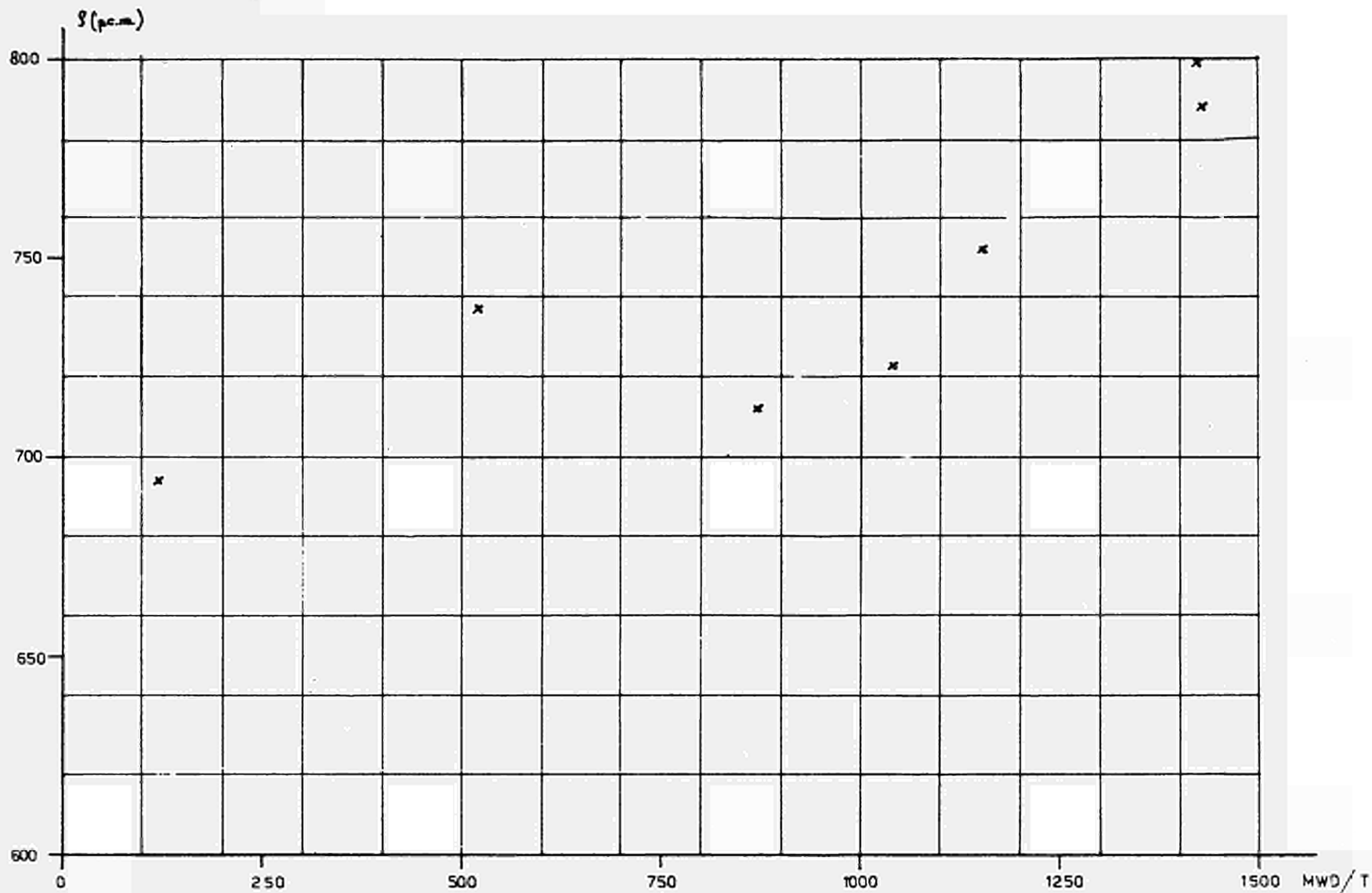


Fig. 4.4,1 Sector-rod-controlled reactivity at 302 withdrawal cycles under normal operating conditions versus irradiation

5.0 DETERMINATION OF REACTIVITY ASSOCIATED WITH TEMPERATURE VARIATIONS

The general reactor conditions at the time when the reactivity balances are performed normally differ from reference conditions. The temperature effects are taken into account by multiplying the average weighted fuel and moderator temperature deviations from reference conditions by the respective temperature coefficients; the contributions thus obtained are then summed algebraically with the other terms of the heat balance.

While there are no uncertainties about the definition of the temperature coefficients for a zero-dimension model, it is difficult to find a sufficiently practical definition of these coefficients for a heterogenous power reactor in the technical literature. The definition adopted here for the Latina reactor can easily be used to bring back to the reference temperatures the experimental data measured for the execution of the heat balances called for in this research program. (*)

Once the reactor irradiation and temperature conditions are fixed, the fuel temperature coefficient around the temperature of interest is defined as:

$$\alpha_u = \frac{\Delta \rho_u}{\int_v \Delta T_u \phi^2 dV / \int_v \phi^2 dV} \quad (1)$$

where $\Delta \rho_u$ represents the overall reactivity variation associated with the fuel temperature variation, and the fraction in the denominator represents the fuel temperature variation averaged by the statistical weight method.

The moderator temperature coefficient is similarly defined, to wit,

$$\alpha_g = \frac{\Delta \rho_g}{\int_v \Delta T_g \phi^2 dV / \int_v \phi^2 dV} \quad (2)$$

Finally, it should be pointed out that, strictly speaking the flux ϕ differs in equations (1) and (2) as it refers respectively to the fuel and to the moderator. In practice, from the macroscopic point of view it is sufficiently accurate to assume that the flux distribution in the core and moderator is the same all over the core.

(*) It is known, at any rate, that there is no strictly univocal correlation between an average weighted temperature variation around the nominal values and the consequent reactivity variation; the latter also depends on the temperature transient induced in the individual reactor zones. However, in consideration of the characteristics of the Latina reactor and the temperature coefficient measurement procedures, the definitions given here are approximate enough, both from the operational point of view and for the temperature corrections to be made in the reactivity balances.

Instead, for the combined temperature coefficient, used is made of the ratio between the intrinsic reactivity variation and the temperature variation (approximately the same for both the fuel and the moderator) which produced it. Thus, this coefficient also includes the moderate temperature effects caused by xenon.

5.1 Description of the method used for the measurement of the combined temperature coefficient

The method selected for the measurements of the combined temperature coefficient, as explained later on, is based on the reactivity transient resulting from a decrease in coolant temperature at the core inlet.

The procedure for this measurement can be summarized as follows:

- a. The reactor is kept at a constant power level long enough to reach xenon equilibrium.
- b. Reactor operation is shifted from automatic to manual, while the power level is kept constant until the end of the measurement by slight movements of the sector rod bank.
- c. With the reactor at equilibrium, a preliminary measurement of all the parameters of interest is taken.
- d. Feedwater heating in the heat exchangers is reduced so as to lower the coolant temperature at the core inlet by about 8°C.
- e. When equilibrium of the new core temperatures is reached, the parameters of interest are monitored for two hours in order to detect any small xenon transients caused by slight fluctuations in the power level.
- f. A final measurement is taken of all the parameters of interest.

This method lends itself well for application to gas-graphite power reactors, both because of its simplicity and because of the reliability of the results which are obtained from relatively simple processing of the experimental data.

The essential data to be processed for this measurement are:

- (a) fuel and moderator temperatures;
- (b) control rod positions during the measurement.

The parameters to be determined for the calculation of α_c are:

- (a) rod-controlled reactivity variation, $\Delta \rho_{\text{tot}}$, during the temperature transient;
- (b) temperature variation, $\Delta \overline{T}_R$, representative of the core as a whole.

Once these two parameters are known, the temperature coefficient is given by the formula:

$$\alpha_c = \frac{\Delta \rho_{\text{tot}}}{\Delta \overline{T}_R}$$

In this formula $\Delta \rho_{\text{tot}}$ can be determined from the rod movement curve by means of the calibration curve corrected to allow for the difference between the reference conditions and those in which the calibration was performed. On the contrary, in consideration of the particular type of transient occurring during the measurement, $\Delta \overline{T}_R$ for the initial and final equilibrium conditions can be assumed, with a good degree of approximation, to be the same for the graphite and for the fuel, so that the corresponding temperature variations weighted over the square of the flux are also equal. As a result, to determine $\Delta \overline{T}_R$, it will suffice to determine the graphite temperature variation weighted over the square of the flux.

5.2 Description of the method used for the measurement of the separate temperature coefficients

The methods for the measurement of the temperature coefficients separately are generally based on the analysis of rapid transients, but some of these methods -- though used successfully on other reactors -- proved difficult to apply to the Latina reactor. This is owing to the difficulty of interpreting the core temperature transients correctly without resorting to overly complicated and time-consuming calculation models.

The main cause of the difficulties encountered is to be attributed to the location of the thermocouples which indicate the moderator temperature in the various zones into which the reactor is ideally subdivided. In fact, the thermocouples are located near the corners of the graphite blocks and thus away from the fuel channels. In our reactor, this circumstance, combined with the presence of small gas leaks from the channels, results in temperature readings, during transients, which are not representative of the graphite as a whole. To bypass this difficulty, efforts were made to develop a suitable method to determine the separate temperature coefficients starting from equilibrium conditions.

This method is based essentially on the analysis of two successive transients, the first being obtained by a rapid reduction in power and the second by a rapid reduction in the coolant flow rate. Each transient is prolonged until thermal equilibrium is reached and the xenon transient is measured. In this manner, three different conditions of thermal equilibrium and corresponding reactivity variations are established in the core so that, by determining the fuel and moderator temperature variations at equilibrium as compared with the initial conditions, and the corresponding reactivity variations net of xenon effects, we may write a two-equation system in the unknowns α_u and α_g to determine the separate temperature coefficients.

It should be noted that the two equations of the system are independent as they refer to two equilibrium conditions which differ in power level and coolant flow rate. However, after the reduction relating to the first transient, the power level is maintained rigorously constant in order to simplify the evaluation of the xenon transient.

To process the experimental data relating to the two equilibrium conditions reached during the measurement, we may write for each condition a balance equation, referred to the initial condition, in which the reactivity variations $\Delta \rho$, net of the xenon effects, appear as the sum of the reactivity variations attributed to changes in fuel temperature and moderator temperature, respectively. Analytically, we have:

$$\Delta \rho_1 = \alpha_u \Delta T_{u_1} + \alpha_g \Delta T_{g_1}$$

$$\Delta \rho_2 = \alpha_u \Delta T_{u_2} + \alpha_g \Delta T_{g_2}$$

By solving this system of two equations we find the values of the unknowns α_u and α_g which respectively represent the temperature coefficients of uranium and graphite.

5.3 Experimental results

The experimental results are summarized in tables 5.3.I and II and are plotted in Figs. 5.3.I and II. These results were used to account for the deviations from the reference temperature during the performance of the individual reactivity balances.

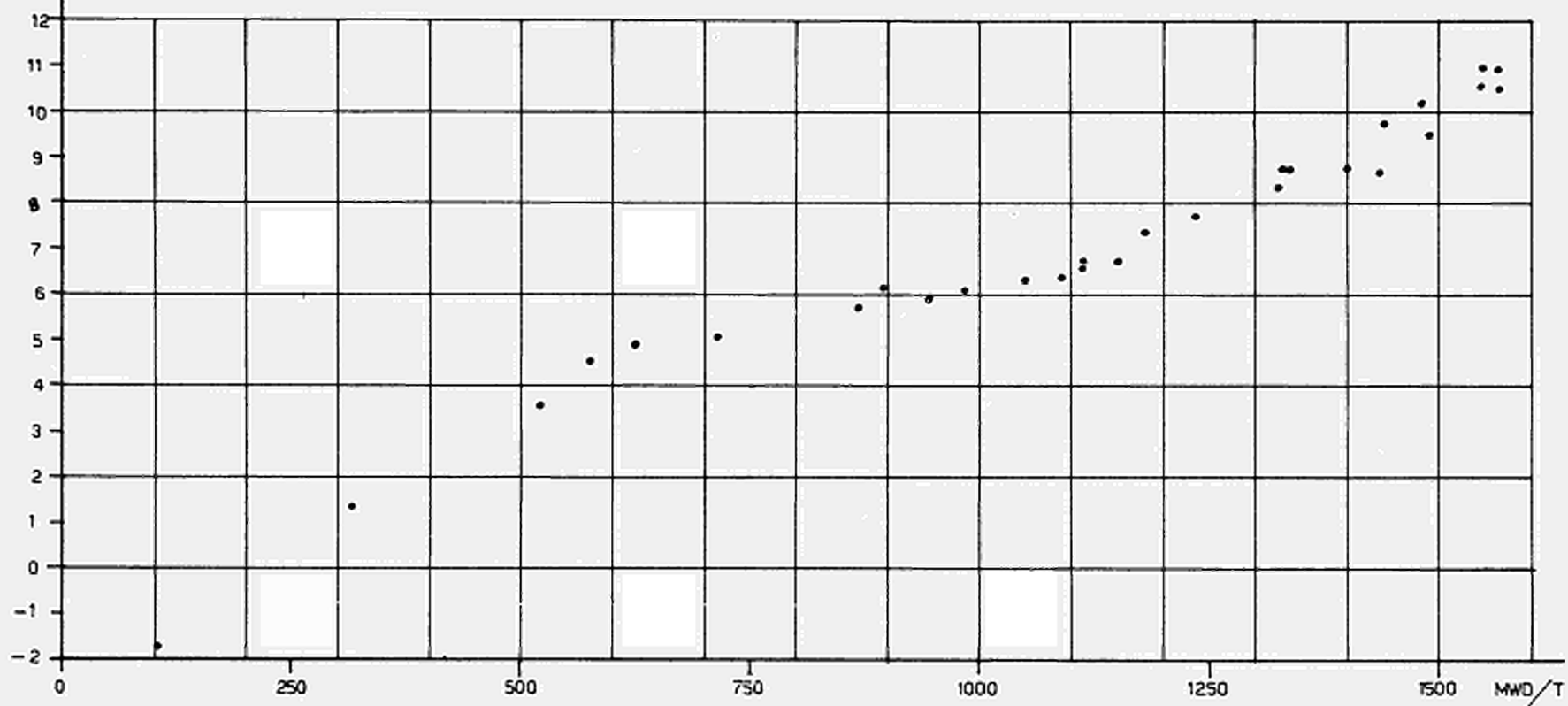
TABLE 5.3.I.

Irrad'n MWD/T	α_c (p.c.m)/°C	Irrad'n MWD/T	α_c (p.c.m)/°C	Irrad'n MWD/T	α_c (p.c.m)/°C
102	-1.73	1049	6.30	1547	10.97
314	1.35	1090	6.36	1545	10.53
520	3.54	1113	6.58	1482	10.24
575	4.52	1114	6.73	1566	10.49
625	4.89	1148	6.69	1563	10.92
716	5.03	1180	7.33	1440	9.74
870	5.70	1233	7.70	1325	8.35
895	6.06	1329	8.73	1338	8.73
944	5.89	1489	9.50	1396	8.74
983	6.05	1479	10.24	1435	8.69

TABLE 5.3.II

Irrad'n MWD/T	α_g (p.c.m)/°C	α_u (p.c.m)/°C
819	7.34	-1.16
1019	7.85	-0.97
1149	7.62	-0.54
1384	11.36	-1.44
1507	12.42	-1.16
1302	9.29	-1.23
1525	10.92	-1.24

α_c ($\mu\text{cm.}$)



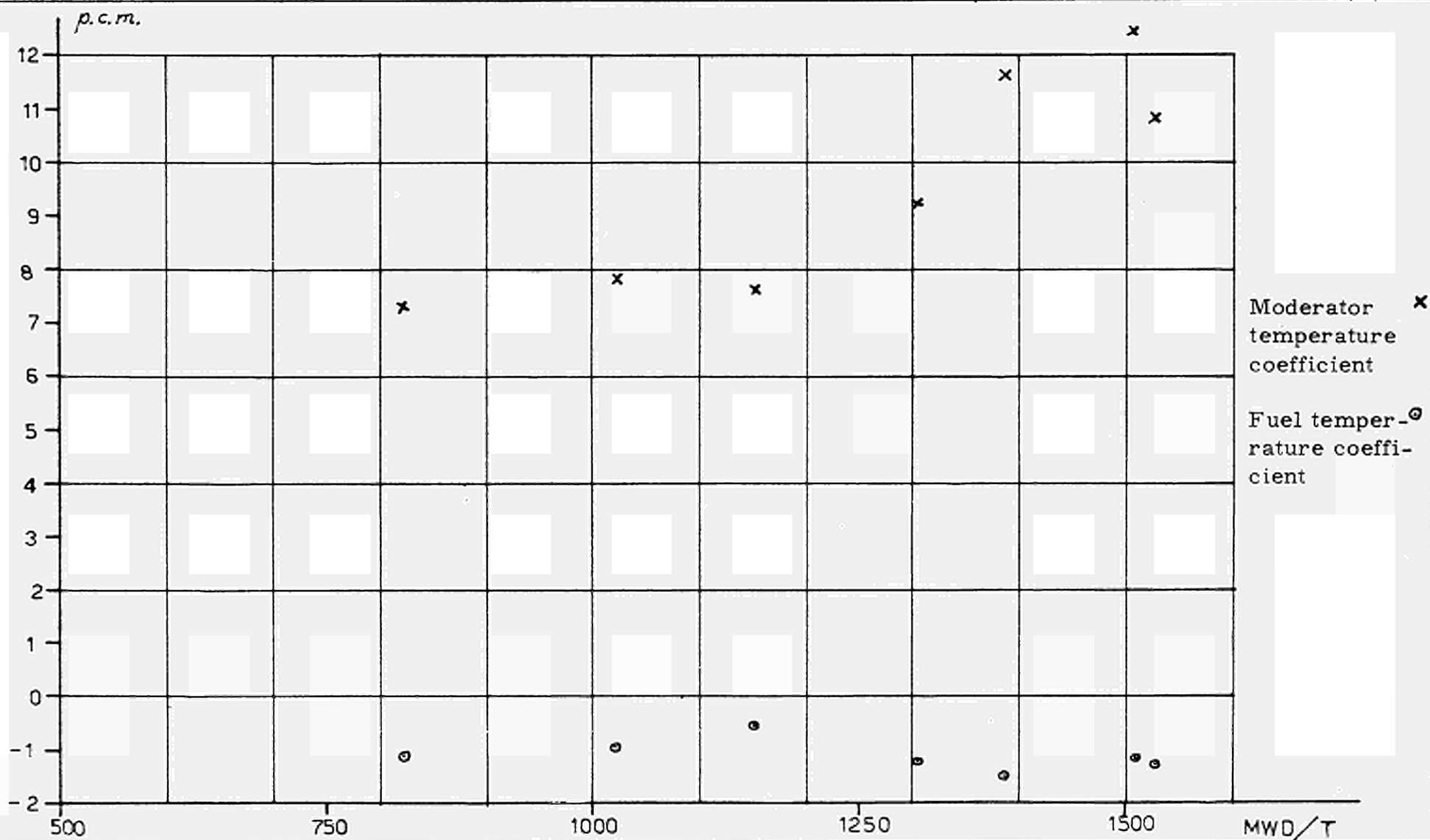


Fig. 5.3, II Separate temperature coefficients as a function of average core irradiation.

6.0 DETERMINATION OF XENON-CONTROLLED REACTIVITY

The reactivity controlled by xenon at equilibrium is a function of the number of fissions and of the type of fissile isotopes and neutron spectrum. In order to evaluate the variation in xenon-controlled reactivity as a function of irradiation, calculations were performed with the ALTHAEA code referred to a channel typical of the whole core.

The results demonstrate that between 0 and 1600 MWD/T the xenon-controlled reactivity varies only by a few tens of p.c.m. The partial transients in xenon-controlled reactivity measured during rod calibration and following reactor scrams also support the calculations. Indeed, if the experimental transients are extrapolated to the time of reactor scram, the xenon-controlled reactivity values differ slightly from the initial value corresponding to the fresh core.

For this reason it was not considered worthwhile to deal with the xenon-controlled reactivity variation at equilibrium separately, and it was therefore included in the overall core reactivity variation.

7.0 DETERMINATION OF BORON-CONTROLLED REACTIVITY

Among the impurities contained in the unirradiated graphite of the Latina reactor core, boron is present in about 0.08 ppm. The parasitic absorption of reactivity by boron decreased with graphite irradiation because of the gradual reduction of boron resulting from the nuclear transformations induced by exposure to the neutron flux.

The results of the calculations to evaluate this effect are shown in Fig. 7.0.I.

Since the variation in boron-controlled reactivity constitutes a phenomenon which is conceptually separated from the variation of the intrinsic core reactivity as normally defined, the boron effect was deducted from the latter.

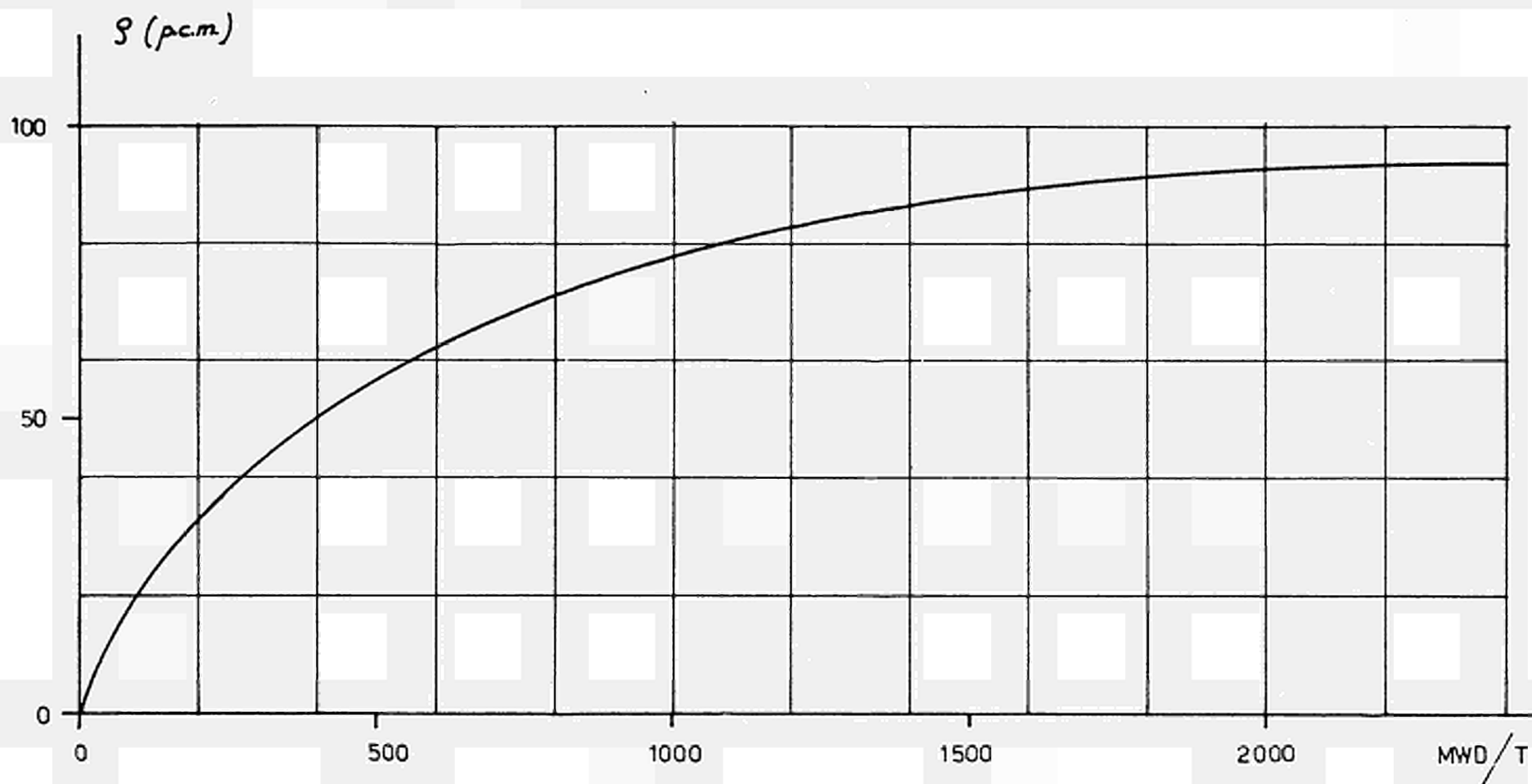


Fig. 7.0, I Reactivity released after gradual destruction of boron impurities in the graphite

8.0 REACTIVITY BALANCES

Chapter 1 described the terms of the balance equation in detail, whereas Chapters 2 to 7 summarize the results of the calculations and measurements for the determination of the parameters required for the practical performance of the reactivity balances.

In particular, Chapter 7 discusses the variation in the reactivity controlled by the boron impurities present in the graphite, which impurities decrease with irradiation. Since the effect of the impurities can be regarded as an independent phenomenon, the boron-controlled reactivity was calculated simply as a function of irradiation and then deducted from the final reactivity balances.

Tables 8.0.I to 8.0.X summarize the values of the terms of the reactivity balances performed.

The reactivity variations, that is, the results of the balances performed from time to time, were calculated by difference in respect of the initial reference condition. This condition contemplated the reactor at nominal power, zero irradiation and in xenon equilibrium.

With reference to tables 8.0.I to X, the terms in the reactivity balance contained in the various columns can be defined as follows:

- (1) Date = Date to which the reactivity balance is referred
- (2) I = Average reactor irradiation corresponding to the balance conditions (MWD/T)
- (3) E_{th} = Thermal energy produced from the beginning of reactor operation (MWh)
- (4) P_{th} = Thermal power generated under the balance conditions (MW)
- (5) Pattern number = Number of the absorber pattern in effect at the time of balance execution
- (6) ρ_{rods} = Reactivity absorbed by the control rods in p.c.m. This value is derived from the cold calibration curves at different irradiations, corrected by factors representing the ratio between the theoretical values of rod-controlled reactivity respectively under cold and operating conditions.
- (7) $\Delta\rho_{rods}$ = Variation in rod-controlled reactivity as a function of temperature and irradiation as compared with the initial reference conditions (p.c.m.)
- (8) ρ_{abs} = Absorber-controlled reactivity under reference conditions (p.c.m.)
- (9) $\Delta\rho_{abs}$ = Variation in absorber-controlled reactivity with respect to the initial absorber pattern (p.c.m.)

- (10) ΔT_g = Deviation of average weighted moderator temperature from reference conditions (300° C)
- (11) $\Delta \rho_g$ = Reactivity variation associated with deviation of average weighted moderator temperature from reference conditions (p. c. m.)
- (12) ΔT_u = Deviation of average weighted fuel temperature from reference conditions (450° C)
- (13) $\Delta \rho_u$ = Reactivity variation associated with deviation of average weighted fuel temperature from reference conditions (p. c. m.)
- (14) ρ_{Xe} = Xenon-controlled reactivity under balance conditions (p. c. m.)
- (15) $\Delta \rho_{Xe}$ = Reactivity variation associated with power deviation from reference (720 MW)
- (16) $\Delta \rho_{boron}$ = Variation in boron-controlled reactivity from initial value (p.c.m.)
- (17) $\Delta \rho_{tot}$ = Reactivity variation with respect to initial reference balance at irradiation zero (p. c. m.)

The results tabulated in Tables 8.0.I to X are represented graphically in Fig. 8.0.I. The results relating to the subsequent operating period are not included in this figure as the average core irradiation remained practically constant from the eleventh absorber patten onwards.

DATE	i	E _{th}	P _{th}	Pattern number	ρ_{rods}	$\Delta\rho_{\text{rods}}$	ρ_{abs}	$\Delta\rho_{\text{abs}}$	ΔT_g	$\Delta\rho_g$	ΔT_u	$\Delta\rho_u$	ρ_{Xe}	$\Delta\rho_{\text{Xe}}$	$\Delta\rho_{\text{boron}}$	$\Delta\rho_{\text{tbt}}$
	0	0	720	1	510	0	659	0	0	0	0	0	2040	0	0	0
31.5.63	10	45.000	319	1	1020	510	659	0	-9	-27	-65	-98	1368	-672	-3	-290
10.6.63	18	103.000	313	1	1050	540	659	0	-20	-55	-82	-124	1352	-688	-4	-331
29.6.63	38	225.000	523	1	755	245	659	0	-8	-19	-37	-55	1779	-261	-6	-96
5.7.63	48	270.000	558	1	744	234	659	0	-9	-18	-34	-50	1831	-209	-11	-53
9.7.63	57	300.000	569	1	759	249	659	0	-7	-14	-31	-46	1850	-190	-13	-14
16.11.63	112	685.000	226	2	1421	911	1128	469	-3	-2	-73	-106	1103	-937	-22	313
21.11.63	118	725.000	459	2	896	386	1128	469	+5	+2	-25	-36	1669	-371	-24	426
23.11.63	120	745.000	461	2	912	402	1128	469	+6	+2	-23	-35	1670	-370	-24	444
26.11.63	126	795.000	453	2	942	432	1128	469	+6	+1	-24	-35	1660	-380	-25	462
9.12.63	131	840.000	223	2	1554	1044	1128	469	-4	0	-82	-119	1090	-950	-25	419
25.12.63	165	1.045.000	460	2-3	949	439	1362	703	+4	-3	-36	-53	1670	-370	-31	685
29.12.63	171	1.109.000	448	2-3	936	426	1362	703	+4	-4	-37	-54	1650	-390	-30	651
17.1.64	215	1.390.000	682	2-3	837	326	1585	926	+9	-17	+3	+4	1994	-46	-35	1159
24.1.64	232	1.500.000	698	3	765	255	1682	1023	+11	-27	+7	+10	2007	-33	-36	1192
31.1.64	251	1.616.266	708	3	838	328	1682	1023	+11	-32	+10	+14	2028	-12	-38	1283
14.2.64	292	1.860.000	701	3-4	737	227	2054	1395	+11	-44	+7	+10	2018	-22	-42	1524
20.2.64	304	1.965.000	712	3-4	663	153	2140	1481	+13	-54	+11	+16	2031	-9	-43	1544

TABLE 8.0, II

DATE	I	E _{th}	P _{th}	Pattern number	ρ_{rods}	$\Delta\rho_{\text{rods}}$	ρ_{abs}	$\Delta\rho_{\text{abs}}$	ΔT_g	$\Delta\rho_g$	ΔT_u	$\Delta\rho_u$	ρ_{Xe}	$\Delta\rho_{\text{Xe}}$	$\Delta\rho_{\text{boron}}$	$\Delta\rho_{\text{tot}}$
22. 2. 64	314	2. 000. 000	706	3-4	629	119	2140	1481	11	-50	8	12	2026	-14	-43	1505
25. 2. 64	322	2. 045. 000	697	3-4	681	171	2140	1481	11	-50	6	9	2007	-33	-44	1534
10. 3. 64	348	2. 255. 000	695	3-4	727	217	2286	1627	11	-57	6	8	2006	-34	-47	1715
17. 3. 64	367	2. 365. 000	700	4	731	221	2326	1667	11	-60	7	10	2017	-23	-48	1767
23. 3. 64	384	2. 470. 000	694	4	772	262	2326	1667	11	-65	6	8	2005	-35	-49	1788
26. 3. 64	392	2. 520. 000	710	4	768	258	2326	1667	11	-70	9	12	2029	-11	-49	1807
9. 4. 64	429	2. 760. 000	708	4-5	777	267	2460	1801	11	-82	4	6	2028	-12	-51	1929
20. 4. 64	459	2. 950. 000	716	4-5	765	255	2596	1937	12	-94	6	9	2035	-5	-55	2047
28. 4. 64	474	3. 045. 000	674	4-5	851	341	2621	1962	6	-49	-7	-10	1987	-53	-56	2155
13. 5. 64	503	3. 270. 000	470	5	1062	552	2008	2141	1	-13	-26	-36	1690	-350	-57	2237
22. 5. 64	520	3. 345. 000	479	5	1024	514	2008	2141	2	-22	-24	-33	1703	-337	-58	2205
26. 5. 64	525	3. 380. 000	476	5	1060	550	2008	2141	2	-27	-24	-33	1701	-339	-58	2234
30. 5. 64	532	3. 424. 283	477	5	1074	564	2008	2141	2	-23	-24	-33	1702	-338	-58	2253
6. 6. 64	545	3. 490. 000	479	5	1084	574	2008	2141	4	-46	-25	-34	1703	-337	-59	2239
12. 6. 64	557	3. 560. 000	477	5-6	1079	569	2822	2163	4	-46	-26	-34	1702	-338	-60	2254
25. 6. 64	575	3. 690. 000	488	5-6	974	464	2932	2273	6	-70	-22	-28	1715	-325	-61	2253
6. 7. 64	598	3. 830. 000	492	5-6	891	381	3035	2376	5	-62	-19	-26	1728	-312	-62	2295
15. 7. 64	610	3. 860. 000	470	6	888	486	3056	2307	4	-53	-22	-30	1703	-337	-62	2241

DATE	I	E _{th}	P _{th}	Pattern number	ρ_{rods}	$\Delta\rho_{\text{rods}}$	ρ_{abs}	Δf_{abs}	ΔT_g	$\Delta\rho_g$	ΔT_u	$\Delta\rho_u$	ρ_{Xe}	$\Delta\rho_{\text{Xe}}$	$\Delta\rho_{\text{boron}}$	$\Delta\rho_{\text{tot}}$
20.7.64	625	3.995.000	483	6	932	422	3056	2397	4	-51	-22	-29	1712	-328	-64	2347
27.7.64	635	4.080.000	480	6	947	437	3056	2397	5	-60	-22	-28	1705	-335	-64	2347
3.9.64	715	4.500.000	701	6	682	172	3056	2397	9	-110	0	0	2018	-22	-67	2370
16.9.64	738	4.706.120	699	6	638	128	3056	2397	10	-118	1	1	2017	-23	-69	2315
29.9.64	761	4.910.000	714	6	625	115	3056	2397	10	-117	2	3	2031	-9	-70	2319
6.10.64	776	5.035.000	718	6-7	628	118	3048	2389	14	-171	9	12	2038	-2	-71	2275
22.10.64	801	5.275.000	719	6-7	606	96	3029	2370	14	-176	2	14	2038	-2	-72	2230
30.10.64	822	5.435.948	731	6-7	621	111	3029	2370	15	-184	6	20	2050	10	-72	2255
6.11.64	834	5.535.000	721	6-7	626	116	3029	2370	14	-170	7	8	2040	0	-73	2251
27.11.64	865	5.870.000	720	7	577	67	2992	2333	11	-144	3	4	2039	-1	-74	2186
30.11.64	869	5.926.563	733	7	584	74	2992	2333	13	-162	7	8	2051	11	-74	2190
7.12.64	878	6.045.000	728	7	553	43	2992	2333	10	-132	6	7	2048	8	-75	2184
18.12.64	895	6.240.000	728	7	543	33	2992	2333	10	-124	5	6	2048	8	-76	2179
23.12.64	906	6.320.000	728	7-8	545	35	2922	2263	9	-113	4	6	2048	8	-77	2122
29.12.64	917	6.465.727	729	7-8	577	67	2896	2237	9	-119	5	6	2049	9	-78	2121
4.1.65	932	6.537.214	725	7-8	557	47	2896	2237	12	-153	8	10	2045	5	-79	2067
11.1.65	944	6.661.443	728	7-8	555	45	2896	2237	12	-152	8	10	2048	8	-79	2069
22.1.65	956	6.851.286	727	7-8	508	-2	2896	2237	12	-153	8	9	2047	7	-80	2018

TABLE 8.0, IV

DATE	I	E_{th}	P_{th}	Pattern number	ρ_{rods}	$\Delta\rho_{rods}$	ρ_{abs}	$\Delta\rho_{abs}$	ΔT_g	$\Delta\rho_g$	ΔT_u	$\Delta\rho_u$	ρ_{Xe}	$\Delta\rho_{Xe}$	$\Delta\rho_{boron}$	$\Delta\rho_{tot}$
26. 1. 65	962	6. 922. 586	726	7-8	505	-5	2896	2237	12	-156	8	10	2047	7	-80	2013
29. 1. 65	968	6. 976. 071	728	7-8	506	-4	2902	2243	12	-154	8	10	2048	8	-80	2023
8. 2. 65	982	7. 149. 993	727	8	593	83	2788	2129	11	-141	5	6	2047	7	-81	2003
10. 2. 65	985	7. 185. 056	727	8	549	39	2788	2129	11	-148	6	7	2047	7	-81	1953
15. 2. 65	992	7. 269. 248	665	8	633	123	2788	2129	3	-42	-22	8	1978	-62	-81	2075
24. 2. 65	1013	7. 422. 908	722	8	583	73	2788	2129	10	-141	4	5	2040	0	-82	1984
28. 2. 65	1022	7. 493. 379	721	8	557	47	2788	2129	10	-136	3	4	2039	-1	-82	1961
6. 3. 65	1031	7. 598. 135	724	8	577	67	2788	2129	11	-149	9	10	2045	5	-83	1979
15. 3. 65	1037	7. 713. 542	723	8	604	94	2788	2129	11	-149	8	10	2044	4	-83	2005
18. 3. 65	1039	7. 766. 144	727	8	587	77	2788	2129	11	-154	11	12	2047	7	-83	1987
28. 3. 65	1045	7. 932. 023	726	8	576	66	2788	2129	12	-159	10	12	2047	7	-84	1971
9. 4. 65	1069	8. 136. 835	723	8	537	27	2788	2129	10	-134	6	7	2044	4	-84	1949
13. 4. 65	1080	8. 207. 053	739	8	561	51	2788	2129	12	-132	12	14	2059	19	-84	1997
21. 4. 65	1091	8. 345. 436	729	8	537	27	2788	2129	11	-155	9	10	2049	19	-85	1945
26. 4. 65	1096	8. 425. 820	733	8	554	44	2788	2129	12	-163	10	12	2051	11	-85	1948
3. 5. 65	1108	8. 529. 885	592	8	618	108	2788	2129	-5	79	-40	-46	1882	-158	-86	2026
5. 8. 65	1145	9. 268. 465	723	9	691	181	2572	1913	13	-184	8	9	2042	2	-87	1834
13. 8. 65	1148	9. 402. 236	723	9	624	114	2572	1913	14	-191	8	9	2042	2	-87	1760

TABLE 9.0, v

DATE	I	E _{th}	P _{th}	Pattern number	ρ_{rods}	$\Delta\rho_{\text{rods}}$	ρ_{abs}	$\Delta\rho_{\text{abs}}$	ΔT_g	$\Delta\rho_g$	ΔT_u	$\Delta\rho_u$	ρ_{Xe}	$\Delta\rho_{\text{Xe}}$	$\Delta\rho_{\text{boron}}$	$\Delta\rho_{\text{tot}}$
17. 8. 65	1150	9. 472. 541	732	9	604	94	2572	1913	12	-177	9	10	2050	10	-88	1762
28. 8. 65	1157	9. 655. 321	733	9	583	73	2572	1913	12	-168	8	9	2050	10	-88	1749
17. 9. 65	1191	9. 972. 011	739	9	566	56	2572	1913	13	-182	9	10	2059	19	-89	1727
8. 10. 65	1205	10. 292. 019	739	9	559	49	2572	1913	10	-147	9	10	2059	19	-90	1754
19. 10. 65	1234	10. 477. 661	723	9	570	60	2572	1913	9	-139	5	6	2042	2	-90	1752
28. 10. 65	1258	10. 623. 969	727	9-10	590	80	2569	1910	7	-110	5	5	2045	5	-90	1800
31. 10. 65	1264	10. 677. 993	743	9-10	568	58	2569	1910	10	-150	9	10	2062	22	-90	1760
2. 11. 65	1269	10. 713. 064	740	9-10	563	53	2569	1910	12	-175	7	8	2061	21	-90	1727
7. 11. 65	1283	10. 800. 686	735	9-10	594	84	2569	1910	11	-163	6	6	2051	11	-91	1757
16. 11. 65	1307	10. 951. 256	730	9-10	595	85	2569	1910	11	-175	5	5	2047	7	-91	1741
24. 11. 65	1328	11. 086. 861	743	9-10	602	92	2569	1910	12	-176	8	8	2062	22	-91	1765
13. 12. 65	1378	11. 404. 010	741	9-10	755	245	2262	1603	13	-195	10	10	2061	21	-91	1593
14. 12. 65	1381	11. 421. 514	737	9-10	775	265	2241	1582	12	-184	8	8	2058	18	-91	1588
28. 12. 65	1418	11. 636. 193	737	10	887	377	2142	1483	12	-190	8	9	2058	18	-92	1605
3. 1. 66	1428	11. 741. 471	747	10	890	380	2142	1483	10	-162	12	12	2069	29	-92	1650
22. 1. 66	1456	12. 040. 012	747	10	827	317	2142	1483	10	-157	12	12	2069	29	-92	1592
25. 1. 66	1458	12. 092. 857	752	10	810	300	2142	1483	10	-158	13	13	2072	32	-92	1578
10. 2. 66	1489	12. 355. 822	757	10	820	310	2142	1483	12	-192	13	13	2075	35	-93	1556

TABLE 8.0, VI

DATE	I	E _{th}	P _{th}	Pattern number	ρ_{rods}	$\Delta\rho_{\text{rods}}$	ρ_{abs}	$\Delta\rho_{\text{abs}}$	ΔT_g	$\Delta\rho_g$	ΔT_u	$\Delta\rho_u$	ρ_{Xe}	$\Delta\rho_{\text{Xe}}$	$\Delta\rho_{\text{boron}}$	$\Delta\rho_{\text{tot}}$
14. 2. 66	1500	12. 425. 813	740	10	813	303	2142	1483	13	-208	12	12	2061	21	-93	1518
25. 2. 66	1508	12. 616. 211	732	10	784	274	2142	1483	14	-220	11	11	2050	10	-93	1465
28. 2. 66	1507	12. 668. 090	743	10	777	267	2142	1483	13	-209	12	12	2062	22	-93	1482
4. 3. 66	1507	12. 737. 878	738	10	751	241	2142	1483	16	-253	16	16	2058	18	-93	1412
17. 3. 66	1495	12. 935. 276	725	10	738	228	2142	1483	15	-233	13	13	2043	3	-93	1402
22. 3. 66	1509	13. 018. 671	743	10	710	200	2142	1483	14	-226	15	15	2062	22	-93	1401
28. 3. 66	1494	13. 122. 696	747	10-11	762	252	2060	1401	14	-217	16	16	2069	29	-93	1388
8. 4. 66	1519	13. 313. 711	748	11	881	371	1976	1317	14	-223	12	12	2070	30	-93	1414
15. 4. 66	1547	13. 432. 188	749	11	834	324	1976	1317	13	-212	12	12	2071	31	-93	1379
19. 4. 66	1556	13. 502. 504	756	11	838	328	1976	1317	13	-218	13	13	2080	40	-94	1386
13. 5. 66	1537	13. 869. 482	721	11	784	274	1976	1317	14	-227	5	5	2042	2	-94	1277
17. 5. 66	1541	13. 939. 977	722	11	751	241	1976	1317	14	-222	5	5	2043	3	-94	1250
31. 5. 66	1529	14. 107. 818	478	11	1075	551	1976	1317	9	-146	-29	-29	1700	-340	-94	1263
8. 6. 66	1515	14. 196. 707	484	11	1087	577	1976	1317	6	-104	-29	-29	1726	-314	-94	1353
16. 6. 66	1506	14. 290. 141	481	11	1069	559	1976	1317	7	-117	-28	-28	1721	-319	-94	1318
23. 6. 66	1491	14. 371. 417	504	11	1063	553	1976	1317	7	-113	-24	-24	1746	-294	-94	1345
30. 6. 66	1479	14. 453. 562	480	11	1040	530	1976	1317	7	-123	-28	-28	1705	-335	-94	1390
11. 8. 66	1446	14. 570. 546	675	11	806	296	1976	1317	5	-91	-11	-11	1988	-52	-94	1365

DATE	I	F_{th}	P_{th}	Pattern number	ρ_{rods}	$\Delta\rho_{rods}$	ρ_{abs}	$\Delta\rho_{abs}$	ΔT_g	$\Delta\rho_g$	ΔT_u	$\Delta\rho_u$	ρ_{Xe}	$\Delta\rho_{Xe}$	$\Delta\rho_{baron}$	$\Delta\rho_{tot}$
16. 8. 66	1459	14. 654. 459	701	11	674	164	1976	1317	9	-157	-2	-2	2019	-21	-94	1207
26. 8. 66	1481	14. 795. 365	719	11	705	195	1976	1317	9	-142	0	0	2039	-1	-94	1275
31. 8. 66	1494	14. 880. 850	709	11	696	186	1976	1317	9	-152	0	0	2027	-13	-94	1244
5. 9. 66	1506	14. 958. 747	619	11	870	360	1976	1317	1	-22	-26	-26	1920	-120	-94	1455
9. 9. 66	1516	15. 023. 798	703	11	691	181	1976	1317	12	-187	0	0	2021	-19	-94	1198
14. 9. 66	1529	15. 106. 545	716	11	664	154	1976	1317	12	-202	2	2	2032	-8	-94	1169
19. 9. 66	1535	15. 185. 988	711	11	672	162	1976	1317	13	-219	2	3	2028	-12	-94	1157
29. 9. 66	1548	15. 301. 457	695	11	700	190	1976	1317	13	-213	0	0	2010	-30	-94	1170
4. 10. 66	1551	15. 385. 641	715	11	655	145	1976	1317	16	-259	6	7	2030	-10	-94	1106
10. 10. 66	1559	15. 488. 116	711	11	673	163	1976	1317	16	-259	6	7	2028	-12	-94	1122
21. 10. 66	1549	15. 532. 833	694	11	660	150	1976	1317	14	-235	1	2	2009	-31	-94	1110
25. 10. 66	1549	15. 648. 419	707	11	666	156	1976	1317	15	-247	4	4	2024	-16	-94	1120
11. 11. 66	1538	15. 879. 304	697	11-12	679	169	1981	1322	12	-196	-2	-2	2011	-29	-94	1170
21. 11. 66	1553	15. 999. 622	711	11-12	741	231	1936	1277	14	-225	2	2	2028	-12	-94	1179
23. 11. 66	1558	16. 034. 966	720	11-12	735	225	1928	1269	14	-226	3	3	2038	-2	-94	1175
25. 11. 66	1562	16. 070. 206	712	11-12	719	209	1919	1260	13	-206	0	0	2028	-12	-94	1157
10. 12. 66	1579	16. 271. 439	717	12	862	352	1853	1194	10	-171	-1	-1	2033	-7	-94	1273
17. 12. 66	1584	16. 389. 383	670	12	936	426	1853	1194	6	-103	-20	-30	1980	-60	-94	1333

TABLE 8.0, VIII

DATE	I	F _{th}	P _{th}	Pattern number	f _{rods}	Δf _{rods}	f _{abs}	Δf _{abs}	ΔT _g	Δf _g	ΔT _u	Δf _u	f _{Xe}	Δf _{Xe}	Δf _{boron}	Δf _{tot}
23.12.66	1575	16.493.247	711	12	802	292	1853	1194	11	-176	-1	-2	2028	-12	-94	1202
30.12.66	1567	16.613.888	716	12	809	299	1853	1194	12	-191	0	0	2032	-8	-94	1200
4.1.67	1569	16.701.006	721	12	832	322	1853	1194	10	-167	0	0	2035	-5	-94	1250
9.1.67	1555	16.788.083	719	12	827	317	1853	1194	10	-164	0	0	2034	-6	-94	1247
13.1.67	1557	16.857.421	714	12	842	332	1853	1194	10	-161	-1	0	2031	-9	-94	1262
20.1.67	1564	16.978.899	717	12	831	321	1853	1194	10	-163	0	0	2033	-7	-94	1251
7.2.67	1521	17.207.189	716	12	906	396	1853	1194	14	-220	4	4	2032	-8	-94	1272
13.2.67	1499	17.311.581	725	12	901	391	1853	1194	14	-231	6	7	2042	2	-94	1269
16.2.67	1485	17.363.922	728	12	893	383	1853	1194	14	-231	6	7	2048	8	-94	1267
3.3.67	1439	17.600.691	717	12	922	411	1853	1194	12	-184	1	2	2033	-7	-94	1323
10.3.67	1424	17.719.889	721	12	929	419	1853	1194	12	-195	3	3	2038	-2	-94	1325
16.3.67	1435	17.822.630	722	12	933	423	1853	1194	13	-199	2	3	2038	-2	-94	1325
30.3.67	1423	18.036.979	725	12	972	462	1853	1194	13	-198	4	5	2042	2	-94	1371
12.5.67	1350	18.540.087	716	12	1045	535	1853	1194	9	-138	0	0	2032	-8	-94	1489
24.5.67	1300	18.730.766	715	12	1076	566	1853	1194	12	-174	2	3	2030	-10	-94	1485
16.6.67	1336	19.051.644	707	13	998	488	2080	1421	11	-166	0	-1	2024	-16	-94	1632
19.6.67	1328	19.101.342	714	13	993	483	2080	1421	11	-166	0	1	2030	-10	-94	1635

DATE	I	E _{th}	P _{th}	Pattern number	f_{rods}	Δf_{rods}	f_{abs}	Δf_{abs}	ΔT_g	Δf_g	ΔT_u	Δf_u	f_{Xe}	Δf_{Xe}	Δf_{boron}	Δf_{tot}
23.6.67	1320	19.167.337	704	13	992	482	2080	1421	11	-163	-1	-2	2020	-20	-94	1624
11.7.67	1296	19.438.589	720	13	981	471	2080	1421	12	-174	0	1	2039	-1	-94	1624
14.7.67	1294	19.489.940	728	13	942	432	2080	1421	12	-173	2	2	2048	8	-94	1596
18.7.67	1286	19.558.515	720	13	949	439	2080	1421	12	-174	0	1	2039	-1	-94	1592
21.7.67	1296	19.609.315	715	13	951	441	2080	1421	11	-165	-1	-1	2030	-10	-94	1592
27.7.67	1300	19.707.583	719	13	953	443	2080	1421	11	-170	0	0	2037	-3	-94	1597
21.8.67	1338	19.999.907	719	14	954	444	2179	1520	11	-168	1	2	2037	-3	-94	1701
3.9.67	1366	20.165.564	628	14	1061	551	2179	1520	0	6	-32	-34	1930	-110	-94	1839
7.9.67	1376	20.233.419	722	14	985	475	2179	1520	13	-197	5	6	2036	-4	-94	1706
14.9.67	1393	20.354.280	722	14	1014	504	2179	1520	13	-198	5	6	2036	-4	-94	1734
18.9.67	1403	20.423.522	721	14	980	470	2179	1520	13	-199	5	6	2035	-5	-94	1698
28.9.67	1430	20.597.956	723	14	992	482	2179	1520	13	-199	6	7	2038	-2	-94	1714
6.10.67	1451	20.733.359	728	14	1025	515	2179	1520	13	-208	7	7	2048	8	-94	1746
20.10.67	1486	20.957.635	727	14	1028	518	2179	1520	13	-210	7	7	2046	6	-94	1747
25.10.67	1499	21.040.759	726	14	922	412	2179	1520	13	-204	6	7	2045	5	-94	1646
10.11.67	1520	21.286.992	729	15	805	295	2428	1769	14	-221	8	8	2050	10	-94	1767
17.11.67	1535	21.408.508	735	15	765	255	2428	1769	13	-219	9	9	2053	13	-94	1733
22.11.67	1525	21.497.083	732	15	768	258	2428	1769	13	-209	7	7	2051	11	-94	1742

TABLE 8. O, X

DATE	I	F _{th}	P _{th}	Pattem number	ρ_{rods}	$\Delta\rho_{\text{rods}}$	ρ_{abs}	$\Delta\rho_{\text{abs}}$	ΔT_g	$\Delta\rho_g$	ΔT_u	$\Delta\rho_u$	ρ_{Xe}	$\Delta\rho_{\text{Xe}}$	$\Delta\rho_{\text{boron}}$	$\Delta\rho_{\text{tot}}$
29. 11. 67	1527	21. 617. 310	734	15	748	238	2428	1769	13	-209	7	8	2052	12	-94	1724
5. 12. 67	1528	21. 698. 449	470	15	1180	670	2428	1769	7	-116	-30	-31	1688	-352	-94	1846
13. 12. 67	1528	21. 816. 602	740	15	815	305	2428	1769	14	-226	9	10	2061	21	-94	1785
22. 12. 67	1525	21. 935. 122	727	15	810	300	2428	1769	14	-227	7	7	2046	6	-94	1761
27. 12. 67	1524	22. 022. 682	733	15	777	267	2428	1769	14	-232	9	9	2052	12	-94	1732

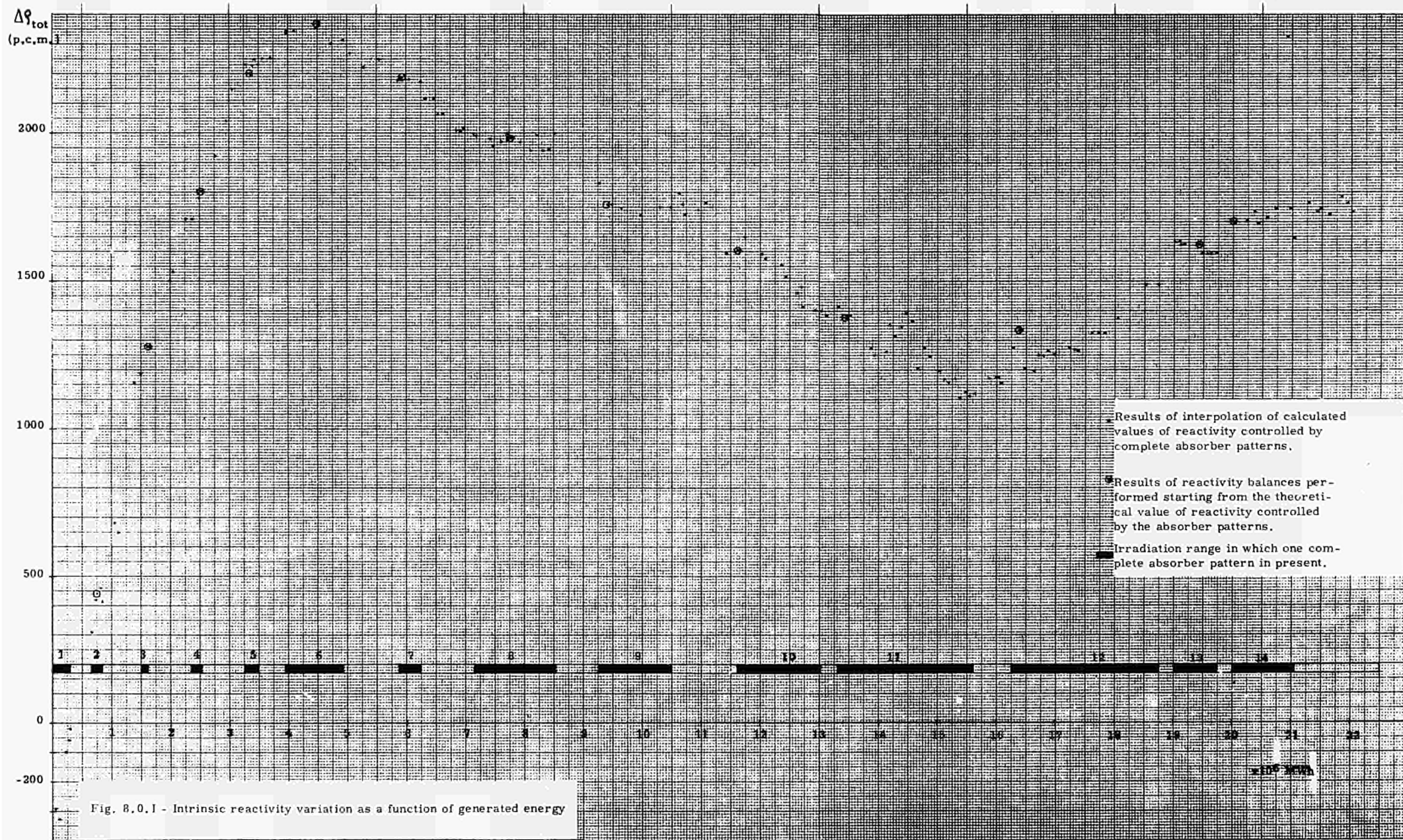


Fig. 8.0.1 - Intrinsic reactivity variation as a function of generated energy

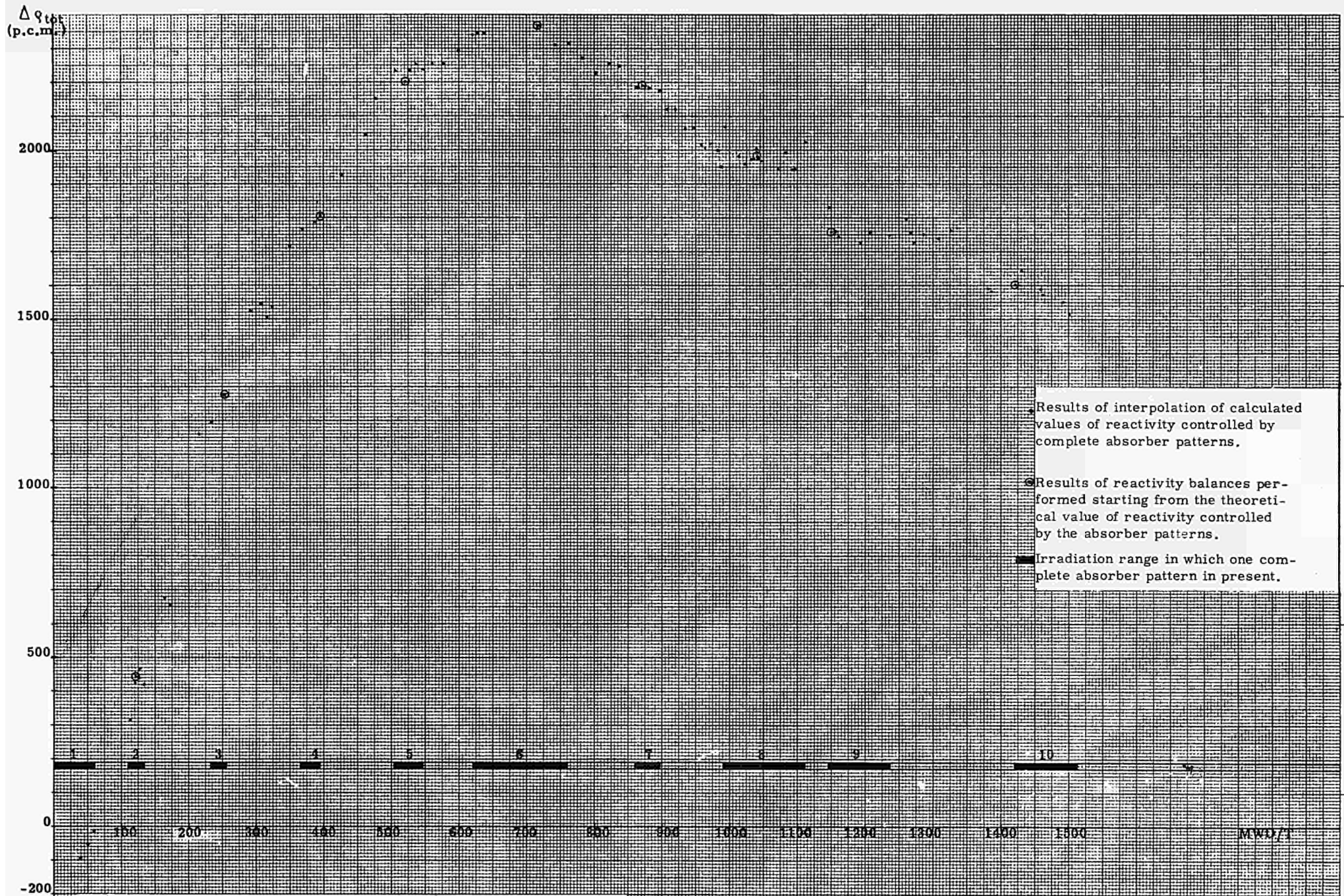


Fig. 8.0.II - Intrinsic reactivity variation as a function of fuel irradiation

9.0 CONCLUSIONS

The measurements and calculations performed under the ENEL-EURATOM research program 050.65.1 - TEG I permitted the determination of the variation of intrinsic reactivity in the Latina reactor over the whole time interval corresponding to an energy production of about 21×10^9 kWh (Figs 8.0.I, II).

Examination of the data and procedures used for the reactivity balances indicates that the uncertainty in the results is lower than $\pm 10\%$.

The variation of the intrinsic core reactivity towards the end of the curve reflects both the delay in the beginning of the fuel cycle and the irregular refuelling pattern. Indeed, the tables summarizing the heat balances indicate that the average reactor irradiation increases monotonically up to about 13.5×10^9 kWh and then remains constant up to about 16.5×10^9 kWh. Subsequently, up to about 19.5×10^9 kWh, irradiation decreases and then rises again to almost 1500 MWD/T at about 21×10^9 kWh.

The accelerated discharge rate between 16.1×10^9 kWh and 19.0×10^9 kWh involved exclusively channels in the flattened region with an average irradiation over 3200 MWD/T. Together with the particular type of fuel cycle adopted (with a semi-repeated initial delay), the foregoing circumstance explains the trend of the intrinsic reactivity variation at the end of the curve.

On the basis of a comparison between the results of calculations and/or measurements on the Latina or similar reactors, the following remarks can be made:

1. The reactivity buildup in Calder Hall reactor No. 3 (ref. 60) measured at 947 MWD/T was 2090 ± 100 p.c.m. versus a corresponding value of 2030 ± 200 p.c.m. for the Latina reactor. If the other value given in ref. 60 is used, we find that at 1650 MWD/T the reactivity buildup in the Calder Hall reactor is 1175 ± 100 p.c.m. versus 1202 ± 120 p.c.m. at 1584 MWD/T for the Latina reactor. This excellent agreement should possibly be verified critically by taking into account the different refuelling schemes and the different characteristics of the two cores.
2. The report under ref. 61 gives the results of the calculations relating to the reactivity controlled by the sixth absorber configuration in the Latina reactor. The result obtained by reference to a simplified radial flux shape is 3097 p.c.m., whereas the same result, corrected to allow for the actual flux shape, is 3062 p.c.m.; the corresponding value in table 3.3.I of this report is equal to 3056 p.c.m.

The good agreement observed indicates that the results of the reactivity balances carried out under this contract are sufficiently accurate and can therefore be used for a cross-check of the calculation methods. To facilitate this cross-check, this report contains a list of documents issued to EURATOM which provides a fairly accurate history of the irradiation of the various zones into which the Latina core was ideally subdivided and the operating data of interest for the calculations.

In addition, the above-mentioned documents contain the detailed results of the measurements for the determination of absorber-controlled and rod-controlled reactivity under special conditions. These results permit the verification of the adequacy of the calculation methods to represent both the absorbers and the control rods under various irradiation conditions.

10.0 REFERENCES

- 1) DOC. 824.211.811/1
"Research program on the reactor of the Latina Nuclear Power Station".
- 2) DOC. 824.211.811/2
"Programma dei lavori e previsioni di spesa relativi al quadrimestre 1° gennaio - 30 aprile 1965".
- 3) DOC. 824.211.811/3
"Taratura delle barre di controllo col metodo dello Xenon: rendiconto della prima misura effettuata".
- 4) DOC. 824.211.811/4
"Relazione tecnica e consuntivo di spesa relativi al periodo 1° gennaio-30 aprile 1965.
Programma dei lavori e previsioni di spesa relativi al periodo 1° maggio - 31 agosto 1965".
- 5) DOC. 824.211.811/5
"Raccolta dei dati concernenti le distribuzioni assiali del flusso neutronico misurate dall'inizio dell'esercizio al 3.7.1965".
- 6) DOC. 824.211.811/6
"Impostazione del metodo di calcolo da impiegare per l'esecuzione dei bilanci di reattività".
- 7) DOC. 824.211.811/7
"Impostazione generale del problema relativo alla misura dei coefficienti di temperatura della reattività e rendiconto delle misure elaborate durante i primi due quadrimestri di esecuzione del contratto".
- 8) DOC. 824.211.811/8
"Raccolta dei dati concernenti la potenza termica, la potenza elettrica e la posizione delle barre settoriali e generali relativi al periodo 1° ottobre 1964 - 31 luglio 1965".
- 9) DOC. 824.211.811/9
"Relazione tecnica e consuntivo di spesa relativi al periodo 1° maggio - 31 agosto 1965".
Programma di lavoro e previsioni di spesa relativi al periodo 1° settembre - 31 dicembre 1965".

- 10) DOC. 824.211.811/10
"Impostazione del calcolo dei transitori di Xenon del reattore di Latina su di un elaboratore di dati".
- 11) DOC. 824.211.811/11
"Impostazione del metodo di calcolo relativo alla correlazione tempi di raddoppio/reattività a nocciolo irraggiato e resoconto dei risultati ottenuti".
- 12) DOC. 824.211.811/12
"Raccolta dei dati concernenti la potenza termica, la potenza elettrica e la posizione delle barre settoriali e generali gruppo B relativi al periodo 1° gennaio - 30 settembre 1964".
- 13) DOC. 824.211.811/13
"Metodo di calcolo della distribuzione tridimensionale del flusso adottato ad integrazione delle misure sperimentali e sue applicazioni".
- 14) DOC. 824.211.811/14
"Relazione tecnica e consuntivo di spesa relativi al periodo 1° settembre - 31 dicembre 1965.
Programma di lavoro e previsioni di spesa relativi al periodo 1° gennaio - 30 aprile 1965".
- 15) DOC. 824.211.811/15
"Taratura degli assorbitori a nocciolo irraggiato: rendiconto delle prime cinque misure effettuate".
- 16) DOC. 824.211.811/16
"Rapporto annuale concernente il lavoro svolto nel 1965".
- 17) DOC. 824.211.811/17
"Calcolo degli irraggiamenti di zona del combustibile relativi al biennio maggio 1963 - maggio 1965".
- 18) DOC. 824.211.811/18
"Raccolta dei dati concernenti la potenza termica, la potenza elettrica e la posizione delle barre settoriali e generali gruppo B relativi al periodo 1° agosto 1965 - 28 febbraio 1966".
- 19) DOC. 824.211.811/19
"Specifiche dei programmi per il calcolatore numerico della Centrale di Latina".

- 20) DOC. 824.211.811/20
"Relazione tecnica e consuntivo di spesa relativi al periodo 1° gennaio - 30 aprile 1966.
Programma di lavoro e previsioni di spesa relativi al periodo 1° maggio - 31 agosto 1966".
- 21) DOC. 824.211.811/21
"Utilizzazione di un codice di evoluzione di reattività per reticoli a grafite-gas".
- 22) DOC. 824.211.811/22
"Raccolta dei dati concernenti le distribuzioni assiali del flusso neutronico misurate dal 6.8.65 al 3.4.66".
- 23) DOC. 824.211.811/23
"Analisi teorica delle misure sugli assorbitori effettuate a Latina il 17.6.1965".
- 24) DOC. 824.211.811/24
"Relazione tecnica particolare sull'esame delle caratteristiche tecniche delle offerte presentate per l'elaboratore da impiegare per il contratto di ricerche ENEL-EURATOM 050.65.1 - TEG I".
- 25) DOC. 824.211.811/25
"Raccolta dei dati concernenti la potenza termica, la potenza elettrica e la posizione delle barre settoriali e generali gruppo B relativi al periodo 1° marzo - 30 giugno 1966".
- 26) DOC. 824.211.811/26
"Relazione tecnica e consuntivo di spesa relativi al periodo 1° maggio - 31 agosto 1966.
Programma di lavoro e previsioni di spesa relativi al periodo 1° settembre - 31 dicembre 1966".
- 27) DOC. 824.211.811/27
"Rendiconto delle misure dei coefficienti di temperatura elaborate durante il terzo, quarto e quinto quadrimestre di esecuzione del contratto".
- 28) DOC. 824.211.811/28
"Taratura delle barre di controllo a 1100 MWD/T".
- 29) DOC. 824.211.811/29
"Relazione tecnica e consuntivo di spesa relativi al periodo 1° settembre - 31 dicembre 1966.
Programma dei lavori e previsioni di spesa relativi al periodo 1° gennaio - 30 aprile 1967".

- 30) DOC. 824.211.811/30
"Taratura degli assorbitori a nocciolo irraggiato; rendiconto delle misure effettuate a Latina nel luglio 1966".
- 31) DOC. 824.211.811/31
"Raccolta dei dati concernenti la potenza termica, la potenza elettrica e la posizione delle barre settoriali generali gruppo B relativi al periodo 1.7.66 - 31.12.66".
- 32) DOC. 824.211.811/32
"Metodo per il calcolo degli irraggiamenti di zona del combustibile della centrale di Latina".
- 33) DOC. 824.211.811/33
"Raccolta dei dati concernenti le distribuzioni assiali del flusso neutronico, misurate dal 14.5.66 al 31.12.66".
- 34) DOC. 824.211.811/34
"Rapporto annuale del lavoro svolto nel 1966".
- 35) DOC. 824.211.811/35
"L'efficacia degli assorbitori nel reattore di Latina".
- 36) DOC. 824.211.811/36
"Relazione tecnica e consuntivo di spesa relativi al periodo 1° gennaio - 30 aprile 1967.
Programma di lavoro e previsioni di spesa relativi al periodo 1° maggio - 31 agosto 1967".
- 37) DOC. 824.211.811/37
"Raccolta dei dati concernenti la potenza termica, la potenza elettrica e la posizione delle barre settoriali e generali gruppo B relativi al periodo 1° gennaio - 30 aprile 67".
- 38) DOC. 824.211.811/38
"Reattività controllata dalle prime dodici configurazioni di assorbitori".
- 39) DOC. 824.211.811/39
"Raccolta dei dati concernenti le distribuzioni del flusso neutronico misurate dal 19.1 al 24.8.1967".
- 40) DOC. 824.211.811/40
"Raccolta dei dati concernenti la potenza termica, la potenza elettrica e la posizione delle barre settoriali e generali gruppo B relativi al periodo 1° maggio - 31 agosto 1967".

- 41) DOC. 824.211.811/41
"Taratura delle barre di controllo a 1425 MWD/T eseguita sul reattore di Latina dall'1 al 3 aprile 1967".
- 42) DOC. 824.211.811/42
"Taratura delle barre di controllo del reattore di Latina a nocciolo irraggiato".
- 43) DOC. 824.211.811/43
"Relazione tecnica e consuntivo di spesa relativo al periodo 1° maggio - 31 agosto 1967.
Programma di lavoro e previsioni di spesa relativi al periodo 1° settembre - 31 dicembre 1967".
- 44) DOC. 824.211.811/44
"Sistema di elaborazione dei dati della Centrale di Latina".
- 45) DOC. 824.211.811/45
"Raccolta dei dati concernenti la potenza termica, la potenza elettrica e la posizione delle barre settoriali e generali gruppo B relativi al periodo 1° settembre - 31 dicembre 1967".
- 46) DOC. 824.211.811/46
"Rendiconto delle misure dei coefficienti di temperatura elaborate durante il 6°, 7° ed 8° quadrimestre di esecuzione del contratto".
- 47) DOC. 824.211.811/47
"Raccolta dei dati concernenti le distribuzioni assiali del flusso misurate dall'agosto 1967 al febbraio 1968".
- 48) DOC. 824.211.811/48
"Calcolo degli irraggiamenti medi del reattore e di zona del combustibile, relativi al periodo maggio 1963 - dicembre 1967".
- 49) DOC. 824.211.811/49
"Relazione tecnica e consuntivo di spesa relativi al periodo 1° settembre - 31 dicembre 1967.
Programma relativo alla finalizzazione dei lavori in corso".
- 50) DOC. 824.211.811/50
"Reattività controllata dalla 13^ e 14^ configurazione di assorbitori".

- 51) DOC. 824.211.811/51
"Rendiconto delle misure dei coefficienti di temperatura elaborate durante il 9° quadrimestre di esecuzione del contratto".
- 52) "Programma di ricerche sulla Centrale di Latina". Report submitted to the EURATOM information meeting on research programs relating to proven-type gas-graphite reactors - Brussels, February 1965.
- 53) EUR 3487/i
"L'efficacia degli assorbitori nel reattore di Latina".
- 54) "Determination experimentale de l'evolution de la reactivité en fonction de l'irradiation du combustible". Reunion d'information technique sur les réacteurs de puissance a Bruxelles (13 et 14 Avril, 1967).
- 55) "Experimental determination of core reactivity build-up with irradiation in the Latina Nuclear Power Plant". ENEA seminar on Physics Measurements in Operating Reactors. (Rome, May 1966).
- 56) "British industries collaboration exponential programme". AEE W - R235 (Part I, III), Winfrith, AEE (1963).
- 57) EUR 3487/i
"Determinazione della reattività e delle distribuzioni del flusso nel reattore di Latina: confronto con i risultati sperimentali di commissioning". Convegno di Fisica del Reattore, Milano, Società Lombarda di Fisica (Novembre 1963).
- 58) "A method for the calculation of three dimensional flux and temperature distribution in a magnox reactor. Comparison with experimental measurements taken at Latina Power Station". A/Conf. 28.9.552 (1964).
- 59) DOC. 824.211.250/1
"Specificazione tecnica elaboratore di dati per la Centrale Elettro-nucleare di Latina".
"Disegni e tabelle degli allegati".
"Technical specification; data processing system for the Latina Nuclear Station".
"Attachments".
"Drawing and tables".

- 60) "An investigation of long term reactivity changes in magnox reactors". J.M. Butterfield et al. Joint International Conference on the Physics Problems in Thermal Reactor Design - London, June 1967.
- 61) "Calcul tridimensionnel des densités de puissance et de températures dans un reacteur graphite-gaz". G.A.A.A. Report 100-66-9 TEGF.

APPENDIX I

Description of the data processor installed at the Latina Station and summary list of programs used to perform the reactivity balances.

The computer installed at Latina is a GEPAC 4050 unit, provided entirely with silicon semi-conductors.

The computer uses parallel-type arithmetics with 24-bit words. The main memory constituted of ferrite cores contains 16,000 words which can be located individually. The auxiliary memory is a magnetic drum containing 131,000 words.

The computer is designed to permit parallel performance of different tasks and to render the calculation speed independent from the speed of the mechanical components, such as the printers or the selective relays for input-output signals.

The arithmetical operations can be performed with a fixed point or floating point. The fixed-point operations are performed by electronic circuits and the floating-point operations by special sub-programs. Fixed-point operations can be carried out on numbers up to 2^{23} , and the floating-point operations up to $2^{\pm 32}$.

The computer can be programmed in the symbolic language PAL, typical of GEPAC computers, or in a modified version of FORTRAN II.

Control of on-line program execution is entrusted to a supervisory program or "Monitor". Communications between the operator and the computer occur through a special typewriter and panel. Another panel is installed in the control room to provide information on demand to the station shift operators. In the control room the output data are printed out by two electric fixed-carriage IBM typewriters.

About one thousand values are sent to the computer from the plant, some of which arrive in the analog form and some in the digital form.

An automatic restart device has been provided to enable the computer to continue a program after a power supply failure which has not exceeded ten minutes.

The main functions assigned to the computer (ref. 19) are:

- Collection of station data
- Periodical calculation of the power generated by the reactor
- Periodical calculation of xenon poisoning
- Calculation of the average weighted temperatures of graphite and fuel, which are essential to obtain the reactivity coefficients
- Periodical calculation of channel powers and statistical weights
- Very-high-speed data collection during measurements
- Calculation of zone irradiations
- Calculation of the reactivity balance.

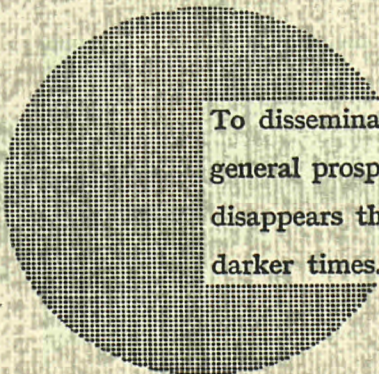
NOTICE TO THE READER

All Euratom reports are announced, as and when they are issued, in the monthly periodical **EURATOM INFORMATION**, edited by the Centre for Information and Documentation (CID). For subscription (1 year : US\$ 15, £ 6.5) or free specimen copies please write to :

Handelsblatt GmbH
"Euratom Information"
Postfach 1102
D-4 Düsseldorf (Germany)

or

**Centrale de vente des publications
des Communautés européennes**
37, rue Glesener
Luxembourg



To disseminate knowledge is to disseminate prosperity — I mean general prosperity and not individual riches — and with prosperity disappears the greater part of the evil which is our heritage from darker times.

Alfred Nobel

SALES OFFICES

All Euratom reports are on sale at the offices listed below, at the prices given on the back of the front cover (when ordering, specify clearly the EUR number and the title of the report, which are shown on the front cover).

CENTRALE DE VENTE DES PUBLICATIONS DES COMMUNAUTES EUROPEENNES

37, rue Glesener, Luxembourg (Compte chèque postal N° 191-90)

BELGIQUE — BELGIE

MONITEUR BELGE
40-42, rue de Louvain - Bruxelles
BELGISCH STAATSBAD
Leuvenseweg 40-42 - Brussel

LUXEMBOURG

CENTRALE DE VENTE
DES PUBLICATIONS DES
COMMUNAUTES EUROPEENNES
37, rue Glesener - Luxembourg

DEUTSCHLAND

BUNDESANZEIGER
Postfach - Köln 1

NEDERLAND

STAATSDRUKKERIJ
Christoffel Plantijnstraat - Den Haag

FRANCE

SERVICE DE VENTE EN FRANCE
DES PUBLICATIONS DES
COMMUNAUTES EUROPEENNES
26, rue Desaix - Paris 15°

ITALIA

LIBRERIA DELLO STATO
Piazza G. Verdi, 10 - Roma

UNITED KINGDOM

H. M. STATIONERY OFFICE
P.O. Box 569 - London S.E.1

EURATOM — C.I.D.
29, rue Aldringer
Luxembourg

CDNA04234ENC